Special Issue Foreword

Modern vehicles and transportation systems rely extensively on stand-alone and widely distributed control systems solutions. In fact, advanced transportation and vehicle systems simply would not exist in their recent forms without extensive use of electronic devices and sophisticated control algorithms; i.e., a combination of electronic sensors, data processors and smart actuators, which represent the "hidden intelligence" of these systems that govern their correct functioning. The ultimate goal is to improve traveler's safety and comfort, performance and energy efficiency of the transportation system as a whole through stand-alone control and interactions among vehicles and their immediate environment. The technology has the promise to provide solutions to some of our most intractable socio-economic problems – the high cost of traffic accidents and other losses originated in the transportation infrastructure.

The automotive industry has been a driving force for innovation and economic growth for one hundred years in the Győr industrial area in Hungary. Continuing this tradition, the Center for Automotive Research (JKK) hosted by the Széchenyi University of Győr, which is the biggest nonprofit institution of this category in the country, continues interdisciplinary research for intelligent vehicles and transportation systems.

This special issue contains 6 papers solicited from researchers working for the JKK in the past few months. They are all associated with the ongoing works related to the research and development of intelligent and future generation vehicles and transportation systems. Papers were sought to encompass the activity of the JKK briefly that is characterized by its highly interdisciplinary nature in this area. In particular, the articles reflect research spanning from the basic control theoretic approaches (linear and nonlinear approaches are equally weighted) to large-scale interdisciplinary views, which are designed to exploit information at multiple scales. This was done in an attempt to demonstrate how stand-alone control methods and solutions can be integrated in the analysis and synthesis of large-scale interconnected vehicle and transportation systems.

The paper Edelmayer et.al., for examples, introduces the novel idea of quasi consensus networks that can be used in the solution of a wide range of control and detection problems in cyber-physical systems including cooperative distributed and connected vehicle and traffic systems. The approach plays invaluable role in intrusion and malicious effect generated malfunction detection in security sensitive cyber-physical systems, such as in sensor networks.

The multivariable decoupling control solution of Bányász and Keviczky, which is based on Youla parametrization, suits to the robust controller design for 2 degrees-of-freedom (DoF) systems very frequently encountered in the synthesis of vehicle control.

In the scholarly article Keviczky and Bokor some fundamental issues of control design methods most frequently used in the recent industrial practice are discussed. More specifically, relationships between the classical pole-placement state feedback

designs, the Riccati-equation based LQ paradigm and the Kalman-frequency domain approaches are discussed.

Gáspár et.al. adopts the popular "plug-and-play" idea from information technology to the design of complex control systems with multiple functional building blocks applied to Electric Vehicle Systems (EVS) in the future.

Szabó et.al. treats the inherently nonlinear character of vehicle control problems in the framework of Linear Parameter Varying systems and relies on Linear Matrix Inequality when finding solutions to performance improvement of vehicle dynamics controllers. The approach presented facilitates solutions to specific control design tasks encountered in vehicle dynamics applications.

The paper Takarics et.al. and its wider 2 and 3 DoF approach in handling structural nonlinearities of the system provides a particularly interesting contribution in presenting stabilization solutions to the 3 DoF model of vehicle control problems.

We are pleased to submit this special issue to the engineering community and hope that it accomplishes our goal of highlighting recent advances in the combined and interdisciplinary fields of vehicle and traffic control achieved by the interdisciplinary research team of JKK at Széchenyi University, Győr.

Győr, December 2013.

Prof. József Bokor
Director of JKK
Member of
Hungarian Academy of Sciences

Prof. László Palkovics
Director of JKK
Member of
Hungarian Academy of Sciences

Mimo Decoupling Control Using a Youla-Parametrized Regulator

Cs. Bányász, L. Keviczky

Széchenyi István University, Győr
Computer and Automation Research Institute and Control Engineering Research Group
Hungarian Academy of Sciences
H-1111 Budapest, Kende u 13-17, HUNGARY
Phone: +361-466-5435
e-mail: banyasz@sztaki.hu; keviczky@sztaki.hu

Abstract: It is interesting to investigate how a decoupling controller can be designed. The YOULA-parametrization is a simple method to design controllers. The KB-parametrization is a successful extension of this method for two-degree-of-freedom (TDOF) systems. The paper extends this methodology for multivariable case after summarizing the classical TFM based methods. Interesting examples are also given including a decoupling lateral control application.

Keywords: MIMO processes, YOULA-parametrization, KB-parametrization, decoupling control

1. Introduction

The state equation of *Multiple Input Multiple Output* (shortly *MIMO),* i.e., multivariable linear dynamic systems has the form

$$\begin{aligned} \frac{\mathrm{d}x}{\mathrm{d}t} = \dot{x} &= \boldsymbol{Ax} + \boldsymbol{Bu} \\ y &= \boldsymbol{Cx} + \boldsymbol{Du} \end{aligned} \tag{1}$$

where $\boldsymbol{A}$, $\boldsymbol{B}$, $\boldsymbol{C}$ and $\boldsymbol{D}$ are (nxn), (nxp), (pxn) and (pxp) matrices, respectively. For the simplicity, let the number of the input and output variables be the same and denote by p (quadratic systems), so the input $\boldsymbol{u}$ and the output $\boldsymbol{y}$ are p-dimensional vectors. The (nxn)-dimensional *transfer function matrix* (*TFM*) of the *MIMO* process is

$$\boldsymbol{P}(s) = \mathbf{C}(s\mathbf{I} - \mathbf{A})^{-1}\mathbf{B} + \mathbf{D} = \mathbf{C}\boldsymbol{\Phi}(s)\mathbf{B} + \mathbf{D} = \frac{1}{\mathrm{A}(s)}\mathbf{B}(s) \tag{2}$$

where

$$\boldsymbol{\Phi}(s) = (s\mathbf{I} - \mathbf{A})^{-1} = \frac{1}{\mathrm{A}(s)}\boldsymbol{\Psi}(s) \qquad \boldsymbol{\Psi}(s) = \mathbf{adj}(s\mathbf{I} - \mathbf{A}) \tag{3}$$

The scalar denominator

$$\mathrm{A}(s)=\det(s\mathbf{I}-\mathbf{A}) \tag{4}$$

is the *n*-th-degree characteristic polynomial of the process. $\boldsymbol{\Phi}$ and $\boldsymbol{\Psi}$ are also (*n*x*n*)-dimensional. The form (2) means the simplest *MIMO* process model, though $\boldsymbol{P}(s)$ is not necessarily minimal, it might be reduced. The right side of (2) is usually also called the "naive" model of the *MIMO* process. (In this paper the parameter matrices of the state equation are denoted by bold plain fonts while the cursive bold fonts denote the *TFM*s.)

At the control design of the *SISO* processes the decomposition of the process into inverse stable and unstable factors was usually a requirement. The *TFM* $\boldsymbol{P}$ of a *MIMO* process can be decomposed in a similar way

$$\boldsymbol{P}=\boldsymbol{P}_{-}\boldsymbol{P}_{+}\neq\boldsymbol{P}_{+}\boldsymbol{P}_{-} \tag{5}$$

where $\boldsymbol{P}_{+}$ and $\boldsymbol{P}_{-}$ are the inverse stable (*IS*) and inverse unstable (*IU*) matrix operators (*TFM*), respectively. Obviously $\boldsymbol{P}$ can be always written in the equivalent form

$$\boldsymbol{P}=\bar{\boldsymbol{P}}_{+}\bar{\boldsymbol{P}}_{-}\neq\bar{\boldsymbol{P}}_{-}\bar{\boldsymbol{P}}_{+} \tag{6}$$

2. The YOULA-parametrized *MIMO* closed control loop

Formally it is very easy to extend the YOULA-parametrization to *MIMO* processes by introducing the *TFM*

$$\boldsymbol{Q}=\boldsymbol{C}(\mathbf{I}-\boldsymbol{P}\boldsymbol{C})^{-1}=(\mathbf{I}-\boldsymbol{C}\boldsymbol{P})^{-1}\boldsymbol{C} \tag{7}$$

which results in the following *YP MIMO* regulator [6], [7]

$$\boldsymbol{C}=(\mathbf{I}-\boldsymbol{Q}\boldsymbol{P})^{-1}\boldsymbol{Q}=\boldsymbol{Q}(\mathbf{I}-\boldsymbol{P}\boldsymbol{Q})^{-1} \tag{8}$$

Here $\boldsymbol{P}$ is assumed to be stable. It can be easily verified that the two sides of (7) and (8) are the same.

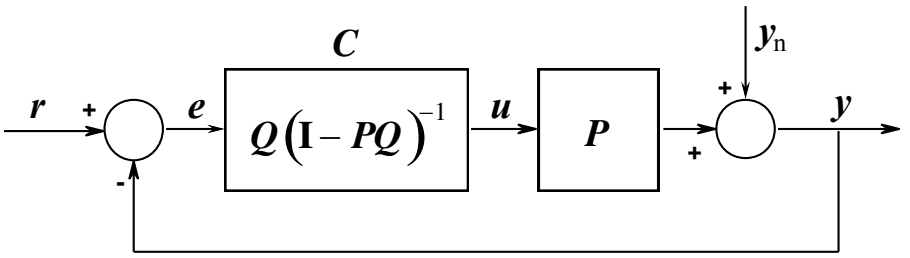

Figure 1. The generalization of the YOULA-parametrization for MIMO processes

The following identities have important role in the investigation of the *TFM* of the *MIMO* closed control loop

$$\begin{aligned}(\mathbf{I}+\boldsymbol{PC})^{-1}&=\left[\mathbf{I}+\boldsymbol{PQ}(\mathbf{I}-\boldsymbol{PQ})^{-1}\right]^{-1}=\mathbf{I}-\boldsymbol{PQ}\\(\mathbf{I}+\boldsymbol{CP})^{-1}&=\left[\mathbf{I}+(\mathbf{I}-\boldsymbol{QP})^{-1}\boldsymbol{QP}\right]^{-1}=\mathbf{I}-\boldsymbol{QP}\end{aligned} \tag{9}$$

$$\left[\mathbf{I}+(\mathbf{I}-\mathbf{A})^{-1}\mathbf{A}\right]^{-1}=\mathbf{I}-\mathbf{A} \qquad \left[\mathbf{I}+\mathbf{B}(\mathbf{I}-\mathbf{B})^{-1}\right]^{-1}=\mathbf{I}-\mathbf{B} \tag{10}$$

The overall transfer characteristics of the *YP* closed system shown in Fig. 1 can be obtained by simple calculations

$$\boldsymbol{y}=\boldsymbol{PQr}+(\mathbf{I}-\boldsymbol{PQ})\boldsymbol{y}_{\mathrm{n}} \tag{11}$$

but it has to be taken into account that the multiplication of the *TFM* is not commutative. Here the *KB*-parametrization introduced at *SISO* processes can also be applied, thus the multiplication by the pre-filter $\boldsymbol{Q}^{-1}$, what results in the *TDOF MIMO* closed system of Fig. 2, where the overall transfer characteristic is

$$\boldsymbol{y}=\boldsymbol{Pr}+(\mathbf{I}-\boldsymbol{PQ})\boldsymbol{y}_{\mathrm{n}} \tag{12}$$

what virtually opens the closed-loop. Note that the *KB*-parametrization can be applied for all closed control loops, not only for the *YP* loops and it always virtually opens the loop, thus it ensures the tracking properties $\boldsymbol{Pr}$. The noise rejection property $(\mathbf{I}-\boldsymbol{PQ})$, however, appears only in the case of *YP*.

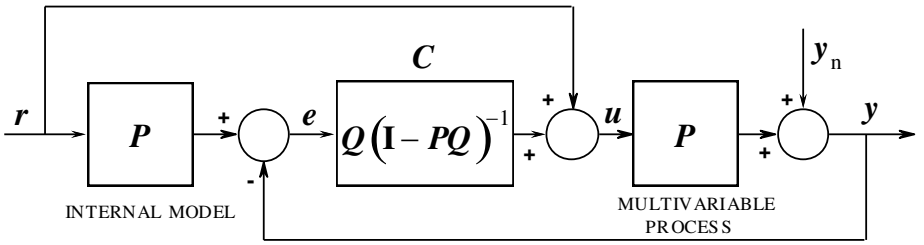

Figure 2. The KB-parametrized MIMO closed control loop

Extending the *generic TDOF* closed system from the *SISO* processes [6] to *MIMO* processes [7], we get the closed-loop shown in Fig. 3.

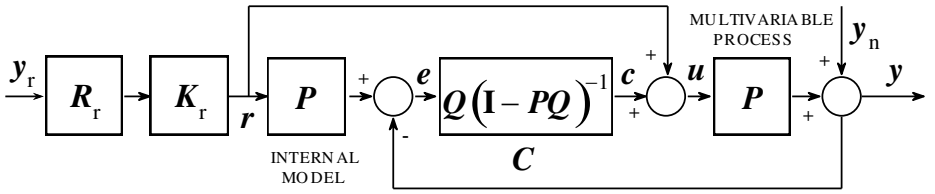

Figure 3. Generic TDOF closed-loop of MIMO processes

The overall characteristic of the generic closed system is

$$\boldsymbol{y} = \boldsymbol{P}\boldsymbol{Q}_{\mathrm{r}}\, \boldsymbol{y}_{\mathrm{r}} + \left(\boldsymbol{I} - \boldsymbol{P}\boldsymbol{Q}_{\mathrm{n}}\right)\boldsymbol{y}_{\mathrm{n}} = \boldsymbol{P}\boldsymbol{K}_{\mathrm{r}}\boldsymbol{R}_{\mathrm{r}}\, \boldsymbol{y}_{\mathrm{r}} + \left(\boldsymbol{I} - \boldsymbol{P}\boldsymbol{K}_{\mathrm{n}}\boldsymbol{R}_{\mathrm{n}}\right)\boldsymbol{y}_{\mathrm{n}} = \boldsymbol{y}_{\mathrm{t}} + \boldsymbol{y}_{\mathrm{d}} \tag{13}$$

Assume that the stable *MIMO* process $\boldsymbol{P}$ can be decomposed according to (5). Then the *MIMO* YOULA-parameters are

$$\boldsymbol{Q} = \boldsymbol{Q}_{\mathrm{n}} = \boldsymbol{K}_{\mathrm{n}}\boldsymbol{R}_{\mathrm{n}} = \boldsymbol{P}_{+}^{-1}\boldsymbol{G}_{\mathrm{n}}\boldsymbol{R}_{\mathrm{n}} \tag{14}$$

and

$$\boldsymbol{Q}_{\mathrm{r}} = \boldsymbol{K}_{\mathrm{r}}\boldsymbol{R}_{\mathrm{r}} = \boldsymbol{P}_{+}^{-1}\boldsymbol{G}_{\mathrm{r}}\boldsymbol{R}_{\mathrm{r}} \quad ; \quad \boldsymbol{K}_{\mathrm{n}} = \boldsymbol{P}_{+}^{-1}\boldsymbol{G}_{\mathrm{n}} \quad ; \quad \boldsymbol{K}_{\mathrm{r}} = \boldsymbol{P}_{+}^{-1}\boldsymbol{G}_{\mathrm{r}} \tag{15}$$

The YOULA-parametrized *MIMO* regulator is

$$\boldsymbol{C} = \boldsymbol{Q}\left(\mathbf{I} - \boldsymbol{P}\boldsymbol{Q}\right)^{-1} = \boldsymbol{K}_{\mathrm{n}}\boldsymbol{R}_{\mathrm{n}}\left(\mathbf{I} - \boldsymbol{P}\boldsymbol{K}_{\mathrm{n}}\boldsymbol{R}_{\mathrm{n}}\right)^{-1} = \boldsymbol{P}_{+}^{-1}\boldsymbol{G}_{\mathrm{n}}\boldsymbol{R}_{\mathrm{n}}\left(\mathbf{I} - \boldsymbol{P}_{-}\boldsymbol{G}_{\mathrm{n}}\boldsymbol{R}_{\mathrm{n}}\right)^{-1} \tag{16}$$

Using the expressions (14)-(16), the obtained closed system has the form

$$\boldsymbol{y} = \boldsymbol{P}_{-}\boldsymbol{G}_{\mathrm{r}}\boldsymbol{R}_{\mathrm{r}}\, \boldsymbol{y}_{\mathrm{r}} + \left(\mathbf{I} - \boldsymbol{P}_{-}\boldsymbol{G}_{\mathrm{n}}\boldsymbol{R}_{\mathrm{n}}\right)\boldsymbol{y}_{\mathrm{n}} = \boldsymbol{y}_{\mathrm{t}} + \boldsymbol{y}_{\mathrm{d}} \tag{17}$$

where, similarly to the *SISO* case, $\boldsymbol{y}_{\mathrm{t}}$ and $\boldsymbol{y}_{\mathrm{d}}$ mean the tracking and disturbance rejection properties, respectively. Here $\boldsymbol{K}_{\mathrm{r}}$ and $\boldsymbol{K}_{\mathrm{n}}$ contain the inverse $\boldsymbol{P}_{+}^{-1}$ of the invertible part $\boldsymbol{P}_{+}$ of $\boldsymbol{P}$, furthermore $\boldsymbol{G}_{\mathrm{r}}$ and $\boldsymbol{G}_{\mathrm{n}}$ attenuate the effect of the invariant factor $\boldsymbol{P}_{-}$.

If the process $\boldsymbol{P}$ is decomposed according to (6), then we get the YOULA-parametrized *MIMO* regulator as

$$\bar{\boldsymbol{C}} = \left(\mathbf{I} - \bar{\boldsymbol{Q}}\bar{\boldsymbol{P}}\right)^{-1}\bar{\boldsymbol{Q}} = \left(\mathbf{I} - \boldsymbol{R}_{\mathrm{n}}\bar{\boldsymbol{K}}_{\mathrm{n}}\bar{\boldsymbol{P}}\right)^{-1}\boldsymbol{R}_{\mathrm{n}}\bar{\boldsymbol{K}}_{\mathrm{n}} = \left(\mathbf{I} - \boldsymbol{R}_{\mathrm{n}}\bar{\boldsymbol{G}}_{\mathrm{n}}\bar{\boldsymbol{P}}_{-}\right)^{-1}\boldsymbol{R}_{\mathrm{n}}\bar{\boldsymbol{G}}_{\mathrm{n}}\bar{\boldsymbol{P}}_{+}^{-1} \tag{18}$$

where

$$\bar{\boldsymbol{K}}_{\mathrm{n}} = \bar{\boldsymbol{G}}_{\mathrm{n}}\,\bar{\boldsymbol{P}}_{+}^{-1} \tag{19}$$

Now the equation of the closed system becomes

$$\boldsymbol{y} = \boldsymbol{P}_{-}\boldsymbol{G}_{\mathrm{r}}\boldsymbol{R}_{\mathrm{r}}\,\boldsymbol{y}_{\mathrm{r}} + \left(\mathbf{I} - \boldsymbol{R}_{\mathrm{n}}\bar{\boldsymbol{G}}_{\mathrm{n}}\bar{\boldsymbol{P}}_{-}\right)\boldsymbol{y}_{\mathrm{n}} = \boldsymbol{y}_{\mathrm{t}} + \bar{\boldsymbol{y}}_{\mathrm{d}} \tag{20}$$

It is well seen that the tracking property $\boldsymbol{y}_{\mathrm{t}}$ is the same for the two-type of the decomposition, the noise rejection properties $\boldsymbol{y}_{\mathrm{d}}$ and $\bar{\boldsymbol{y}}_{\mathrm{d}}$, however, may be different.

Note that while, for the *SISO* case, the realizability of the YOULA-parametrized regulator can be simply ensured by the reasonable choice of the pole access of the reference models R_{r} and R_{n}, the same cannot be stated for the *MIMO* case. It is true that in many cases, raising the pole access of the elements in the main diagonal of $\boldsymbol{R}_{\mathrm{r}}$ and $\boldsymbol{R}_{\mathrm{n}}$ helps the realizability, if they are given in *TFM* form. The general condition, however, always needs further, thorough investigation. Consider next some special cases.

2.1. The YOULA-parametrized MIMO regulator for the "naive" process model

The derivation of the regulators (16) and (18) requires complex operations between the *TFM*s. This computation demand can be slightly decreased by using the "naive" model given in (2). In this case the decomposition (5) has the form

$$\boldsymbol{P}(s) = \boldsymbol{P}_{-}\boldsymbol{P}_{+} = \frac{1}{\mathrm{A}(s)}\mathbf{B}(s) = \frac{1}{\mathrm{A}(s)}\mathbf{B}_{-}(s)\mathbf{B}_{+}(s) \tag{21}$$

The advantage of this model is that the designated operation with the polynomial $\mathrm{A}(s)$ in the denominator can be exchanged by any matrix polynomial. Futher simplification can be reached for inverse stable processes, when the model (2) is

$$\boldsymbol{P} = \frac{1}{\mathrm{A}(s)}\mathbf{B}_{+}(s) \qquad \mathbf{B}_{+} = \mathbf{B} \qquad \mathbf{B}_{-} = \mathbf{I} \tag{22}$$

Let the reference models be given in the "naive" form, i.e.,

$$\boldsymbol{R}_{\mathrm{r}} = \frac{1}{\mathrm{A}_{\mathrm{r}}(s)}\mathbf{B}_{\mathrm{r}}(s) \qquad \boldsymbol{R}_{\mathrm{n}} = \frac{1}{\mathrm{A}_{\mathrm{n}}(s)}\mathbf{B}_{\mathrm{n}}(s) \tag{23}$$

If $\mathbf{B}_{-} = \mathbf{I}$ and $\mathbf{B}_{+} = \mathbf{B}$, then further optimization is impossible, thus it is reasonable to choose $\boldsymbol{G}_{\mathrm{r}} = \boldsymbol{G}_{\mathrm{n}} = \mathbf{I}$. In this case the *MIMO* YOULA-parameter is

$$\boldsymbol{Q} = \boldsymbol{Q}_{\mathrm{n}} = \mathrm{A}(s)\mathbf{B}^{-1}(s)\boldsymbol{R}_{\mathrm{n}} = \frac{\mathrm{A}(s)}{\mathrm{A}_{\mathrm{n}}(s)}\mathbf{B}^{-1}(s)\mathbf{B}_{\mathrm{n}}(s) \tag{24}$$

and the YOULA-parametrized *MIMO* regulator becomes

$$\boldsymbol{C}(s) = \mathrm{A}(s)\mathbf{B}^{-1}(s)\boldsymbol{R}_{\mathrm{n}}(s)\left[\mathbf{I} - \boldsymbol{R}_{\mathrm{n}}(s)\right]^{-1} = \mathrm{A}(s)\mathbf{B}_{+}^{-1}(s)\mathbf{B}_{\mathrm{n}}(s)\left[\mathrm{A}_{\mathrm{n}}(s)\mathbf{I} - \mathbf{B}_{\mathrm{n}}(s)\right]^{-1} \tag{25}$$

2.2. Sampled data systems

In many practical cases the *MIMO* process model is given in a special, inverse stable form. This is especially valid for sampled (or discrete-time: DT) processes

$$\boldsymbol{G} = \boldsymbol{G}_{-}\boldsymbol{G}_{+} = z^{-d}\boldsymbol{G}_{+} = \bar{\boldsymbol{G}}_{+}\bar{\boldsymbol{G}}_{-} = \bar{\boldsymbol{G}}_{+}z^{-d} \qquad \boldsymbol{G}_{+} = \bar{\boldsymbol{G}}_{+} \tag{26}$$

Here for all inputs in the main diagonal the time-delay is z^{-d}. All other variants can be taken into account in $\boldsymbol{G}_{+}$. In this case the YOULA-parameter is

$$\boldsymbol{Q} = \boldsymbol{G}_{+}^{-1}\boldsymbol{R}_{\mathrm{n}} \qquad \bar{\boldsymbol{Q}} = \boldsymbol{R}_{\mathrm{n}}\bar{\boldsymbol{G}}_{+}^{-1} \tag{27}$$

Using these parameters the regulator (16) and (18) becomes

$$\begin{aligned} \boldsymbol{C} &= \boldsymbol{Q}\left(\mathbf{I} - \boldsymbol{P}\boldsymbol{Q}\right)^{-1} = \boldsymbol{G}_{+}^{-1}\boldsymbol{R}_{\mathrm{n}}\left(\mathbf{I} - \boldsymbol{R}_{\mathrm{n}}z^{-d}\right)^{-1} = \boldsymbol{G}_{+}^{-1}\left(\mathbf{I} - \boldsymbol{R}_{\mathrm{n}}z^{-d}\right)^{-1}\boldsymbol{R}_{\mathrm{n}} \\ \bar{\boldsymbol{C}} &= \left(\mathbf{I} - \bar{\boldsymbol{Q}}\bar{\boldsymbol{P}}\right)^{-1}\bar{\boldsymbol{Q}} = \left(\mathbf{I} - \boldsymbol{R}_{\mathrm{n}}z^{-d}\right)^{-1}\boldsymbol{R}_{\mathrm{n}}\boldsymbol{G}_{+}^{-1} = \boldsymbol{R}_{\mathrm{n}}\left(\mathbf{I} - \boldsymbol{R}_{\mathrm{n}}z^{-d}\right)^{-1}\boldsymbol{G}_{+}^{-1} \end{aligned} \tag{28}$$

Here $\boldsymbol{G}_{+} = \bar{\boldsymbol{G}}_{+}$ is considered and the identity

$$\boldsymbol{R}_{\mathrm{n}}\left(\mathbf{I} - \boldsymbol{R}_{\mathrm{n}}z^{-d}\right)^{-1} = \left(\mathbf{I} - \boldsymbol{R}_{\mathrm{n}}z^{-d}\right)^{-1}\boldsymbol{R}_{\mathrm{n}} \tag{29}$$

can be simply checked. The closed system for the two-type of regulators is exactly the same

$$\begin{aligned} \boldsymbol{y} &= \boldsymbol{R}_{\mathrm{r}}z^{-d}\boldsymbol{y}_{\mathrm{r}} + \left(\mathbf{I} - \boldsymbol{R}_{\mathrm{n}}z^{-d}\right)\boldsymbol{y}_{\mathrm{n}} = \boldsymbol{y}_{\mathrm{t}} + \boldsymbol{y}_{\mathrm{d}} \\ \boldsymbol{y} &= \boldsymbol{R}_{\mathrm{r}}z^{-d}\boldsymbol{y}_{\mathrm{r}} + \left(\mathbf{I} - \boldsymbol{R}_{\mathrm{n}}z^{-d}\right)\boldsymbol{y}_{\mathrm{n}} = \boldsymbol{y}_{\mathrm{t}} + \bar{\boldsymbol{y}}_{\mathrm{d}} \end{aligned} \tag{30}$$

thus $\boldsymbol{y}_{\mathrm{d}} = \bar{\boldsymbol{y}}_{\mathrm{d}}$. Note that for this case $\boldsymbol{G}_{\mathrm{r}} = \boldsymbol{G}_{\mathrm{n}} = \mathbf{I}$ is chosen, since the effect of the invariant factor $\boldsymbol{G}_{-} = z^{-d}\mathbf{I}$ cannot be attenuated.

The DT "naive" model of the *MIMO* process is

$$\boldsymbol{G}(z) = \frac{1}{\mathrm{A}(z)}\mathbf{B}(z) \;\; ; \;\; \mathbf{B}_{+} = \mathbf{B} \;\; ; \;\; \mathbf{B}_{-} = z^{-d}\mathbf{I} \tag{31}$$

and the sampled YOULA-parametrized *MIMO* regulator is obtained by performing the analogous computations providing (25)

$$\begin{aligned} \boldsymbol{C}(z) &= \mathrm{A}(z)\mathbf{B}^{-1}(z)\mathbf{B}_{\mathrm{n}}(z)\left[\mathrm{A}_{\mathrm{n}}(z)\mathbf{I} - z^{-d}\mathbf{B}_{\mathrm{n}}(z)\right]^{-1} = \\ &= \mathrm{A}(z)\mathbf{B}_{+}^{-1}(z)\mathbf{B}_{\mathrm{n}}(z)\left[\mathrm{A}_{\mathrm{n}}(z)\mathbf{I} - z^{-d}\mathbf{B}_{\mathrm{n}}(z)\right]^{-1} \end{aligned} \tag{32}$$

It is worth to check that the similarly computed sampled YOULA-parametrized *SISO* regulator has the form

$$C = \mathrm{A}(z)B^{-1}(z)B_{\mathrm{n}}(z)\left[\mathrm{A}_{\mathrm{n}}(z) - z^{-d}B_{\mathrm{n}}(z)\right]^{-1} = \mathrm{A}(z)B_{+}^{-1}(z)B_{\mathrm{n}}(z)\left[\mathrm{A}_{\mathrm{n}}(z) - z^{-d}B_{\mathrm{n}}(z)\right]^{-1} \quad (33)$$

In these expressions the reference model has also the "naive" form. Let us assume now that $\boldsymbol{R}_{\mathrm{n}}$ is given in left side *MFD* form, i.e.,

$$\boldsymbol{R}_n = \boldsymbol{A}_n^{-1}(z)\boldsymbol{B}_{\boldsymbol{n}}(z) = [\boldsymbol{I} + \widetilde{\boldsymbol{A}}_n(z^{-1})]^{-1}\boldsymbol{B}_{\boldsymbol{n}}(z^{-1}) \quad (34)$$

In this case the output of the regulator can be computed by a two-step algorithm. Let us denote the output by the vector $\boldsymbol{c}[k]$. It is reasonable to use (18) according to which the necessary computation has the form

$$\boldsymbol{c} = \bar{\boldsymbol{C}}\boldsymbol{e} = \left(\mathbf{I} - \boldsymbol{R}_{\mathrm{n}}\bar{\boldsymbol{G}}_{-}\right)^{-1}\boldsymbol{R}_{\mathrm{n}}\bar{\boldsymbol{G}}_{+}^{-1}\boldsymbol{x} \qquad \boldsymbol{x} = \bar{\boldsymbol{G}}_{+}^{-1}\boldsymbol{e} \quad (35)$$

Here the auxiliary variable $\boldsymbol{x}[k]$ is introduced. Using these equations the regulator can be written in the form of vector difference equation form linear in parameters

$$\boldsymbol{c} = \left(\mathbf{B}_{\mathbf{n}}\mathbf{N}_{\mathrm{L}}^{-} - \widetilde{\mathbf{A}}_{\boldsymbol{n}}\right)\boldsymbol{c} + \boldsymbol{B}_{\boldsymbol{n}}\boldsymbol{x} \quad (36)$$

where $\boldsymbol{x}[k]$ can also be given in similar form

$$\boldsymbol{x} = \boldsymbol{D}_L\boldsymbol{e} - \mathbf{N}_{\mathrm{L}}^{+}\boldsymbol{x} \quad (37)$$

In the equations of the regulator the following simple notations are used

$$\bar{\boldsymbol{G}}_{+}^{-1} = \left[\mathbf{N}_{\mathrm{L}}^{+}(z)\right]^{-1}\mathbf{D}_{\mathrm{L}}(z) \qquad \bar{\boldsymbol{G}}_{-} = \mathbf{N}_{\mathrm{L}}^{-} \qquad \mathbf{N}_{\mathrm{L}}^{+} = \mathbf{I} + \widetilde{\mathbf{N}}_{\mathrm{L}}^{+} \quad (38)$$

3. Decoupling control of the *MIMO* process models

The decoupling control of *M*ulti-*I*nput-*M*ulti-*O*utput (*MIMO*) processes is not a simple problem. In general case, considering *MIMO* process models, each input signal has effect on each output signal. The same is valid for the all elements of the output disturbance. It is an important practical task to construct control system where each reference signal has effect only on the corresponding output signal. Similarly it is a favorable case when a certain output disturbance has effect on a given output signal and has no effect at all on the other outputs. The joint solutions of the above tasks are called decoupling or decoupling control. The practical solutions available in the literature usually apply two approaches [12], [14], [15].

The first approach applies state feedback where the decoupling vector can be chosen by algebraic method in order to reach partial or complete decoupling. These methods are very complicated, do not illustrate well how the decoupling operates, therefore they are not widely used in the engineering practice [14].

The other approach introduces process model structures (*P* and *V* structures) what handle the feed-forward and feedback elements of the *TFM* separately. The analysis of

these elements makes easier the design of the necessary control though they do not provide systematic solution and do not give the theoretical limits of the decoupling [14].

Let us investigate the decoupling for sampled systems where the *TFM* of the process is assumed as

$$\boldsymbol{G} = \boldsymbol{G}_{\mathrm{D}} + \boldsymbol{G}_{\mathrm{A}} = \boldsymbol{G}_{\mathrm{D}}\left(\boldsymbol{I} + \boldsymbol{G}_{\mathrm{D}}^{-1}\boldsymbol{G}_{\mathrm{A}}\right) = \left(\boldsymbol{I} + \boldsymbol{G}_{\mathrm{A}}\boldsymbol{G}_{\mathrm{D}}^{-1}\right)\boldsymbol{G}_{\mathrm{D}} \tag{39}$$

Here $\boldsymbol{G}_{\mathrm{D}}$ contains the diagonal elements, i.e., it is a diagonal matrix, $\boldsymbol{G}_{\mathrm{A}}$ does the elements outside the diagonal (antidiagonal elements) in the original structure. The block scheme of the *MIMO* processes is usually feed-forward like as it is shown on Fig. 4 for two-variable case. The operation of the decoupling regulators is usually demonstrated on two-input two-output simple *MIMO* systems where the essence of the method can be understood in the simplest way. In the industrial practice the input and output variables are usually considered in pairs if the technology allows. These kinds of schema are used next to illustrate the methods.

The decoupler, serially connected with the *MIMO* process and providing the decoupling effect, is noted by $\boldsymbol{D}$. One of the most natural decoupling could be reached by the compensator $\boldsymbol{D} = \boldsymbol{D}_{\mathrm{o}} = \boldsymbol{G}^{-1}$, i.e., by the inverse of the process, what would mean complete decoupling $\boldsymbol{D}_{\mathrm{o}}\,\boldsymbol{G} = \boldsymbol{I}$. But the inverse is usually not realisable and there is almost never need to eliminate the complete dynamics of the process. In general case the structure of the decoupler $\boldsymbol{D}$ corresponds to the process model shown on Fig. 4 if the elements G_{ij} are simply substituted by D_{ij}.

Considering the engineering aspects the ideal decoupling would contain the process dynamics $\boldsymbol{G}_{\mathrm{D}}$ in the main diagonal what could be reached by the following compensator

$$\boldsymbol{D} = \boldsymbol{D}_{\mathrm{i}} = \boldsymbol{G}^{-1}\boldsymbol{G}_{\mathrm{D}} \tag{40}$$

Observe that this case also requires the inverse of the process though in certain cases there are more chances to realize the elements of the product $\boldsymbol{G}^{-1}\boldsymbol{G}_{\mathrm{D}}$ than those of $\boldsymbol{G}^{-1}$.

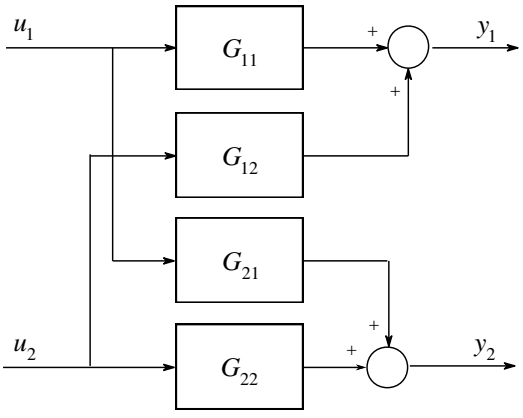

Figure 4. Block scheme of two-variable MIMO process

There are models for decoupling where the feed-forward and feedback effects appear mixed. Such topology is shown in Fig. 5. This structure is called V-topology or inverse (inverted) structure [12], [15].

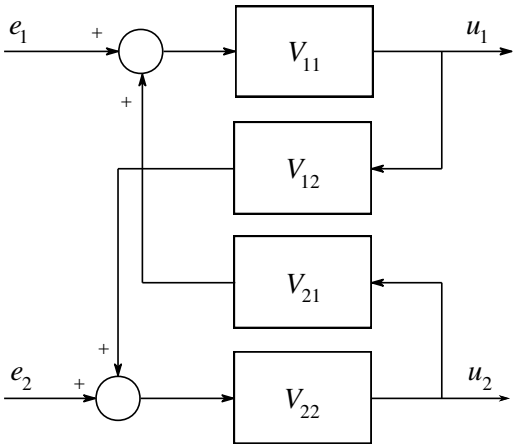

Figure 5. Block scheme of the decoupler of V-topology

The relationships of the resulting model can be written as

$$\begin{bmatrix} u_1 \\ u_2 \end{bmatrix} = \begin{bmatrix} V_{11} & 0 \\ 0 & V_{22} \end{bmatrix} \begin{bmatrix} e_1 \\ e_2 \end{bmatrix} + \begin{bmatrix} V_{11} & 0 \\ 0 & V_{22} \end{bmatrix} \begin{bmatrix} 0 & V_{12} \\ V_{21} & 0 \end{bmatrix} \begin{bmatrix} u_1 \\ u_2 \end{bmatrix} \tag{41}$$

Analogously with the notations introduced in (39) we can write now that

$$\boldsymbol{u} = \boldsymbol{V}_{\mathrm{D}}\, \boldsymbol{e} + \boldsymbol{V}_{\mathrm{D}}\, \boldsymbol{V}_{\mathrm{A}}\, \boldsymbol{u} \tag{42}$$

where the decomposition

$$\boldsymbol{V} = \boldsymbol{V}_{\mathrm{D}} + \boldsymbol{V}_{\mathrm{A}} \tag{43}$$

for diagonal and antidiagonal components is similar what was used for the process model. Based on (39) we can write that

$$\boldsymbol{u} = \left(\boldsymbol{I} - \boldsymbol{V}_{\mathrm{D}}\, \boldsymbol{V}_{\mathrm{A}}\right)^{-1} \boldsymbol{V}_{\mathrm{D}}\, \boldsymbol{e} = \boldsymbol{D}_{\mathrm{V}}\, \boldsymbol{e} \tag{44}$$

The V-topology can be simply used for the design of a decoupling compensator. Let us use the following equation for the design of the decoupling

$$\boldsymbol{G}\, \boldsymbol{D}_{\mathrm{V}} = \boldsymbol{G}_{\mathrm{D}} \left(\boldsymbol{I} + \boldsymbol{G}_{\mathrm{D}}^{-1}\, \boldsymbol{G}_{\mathrm{A}}\right) \left(\boldsymbol{I} - \boldsymbol{V}_{\mathrm{D}}\, \boldsymbol{V}_{\mathrm{A}}\right)^{-1} \boldsymbol{V}_{\mathrm{D}} \tag{45}$$

Observe that if in the decoupler $\boldsymbol{V}_{\mathrm{D}}\, \boldsymbol{V}_{\mathrm{A}} = -\boldsymbol{G}_{\mathrm{D}}^{-1}\, \boldsymbol{G}_{\mathrm{A}}$ is chosen then the ideal decoupling $\boldsymbol{G}\, \boldsymbol{D}_{\mathrm{V}} = \boldsymbol{G}_{\mathrm{D}}\, \boldsymbol{V}_{\mathrm{D}}$ is ensured. It can be stated that the elements of $\boldsymbol{V}_{\mathrm{D}}$ can

provide the decoupled, already single variable regulator in the control loop. The realization of the above compensation is ensured by the following choices

$$\boldsymbol{V}_{\mathrm{A}} = -\boldsymbol{G}_{\mathrm{A}} \qquad \boldsymbol{V}_{\mathrm{D}} = \boldsymbol{G}_{\mathrm{D}}^{-1} \tag{46}$$

These relationships explain the introduction of the V-topology since the prescribed operations are so simple that they can be performed manually.

Using the design relationships (46) it can be seen that the V-topology shown here corresponds to the following decoupling compensator

$$\boldsymbol{D}_{\mathrm{V}} = \boldsymbol{G}^{-1}\, \boldsymbol{G}_{\mathrm{D}}\, \boldsymbol{V}_{\mathrm{D}} \tag{47}$$

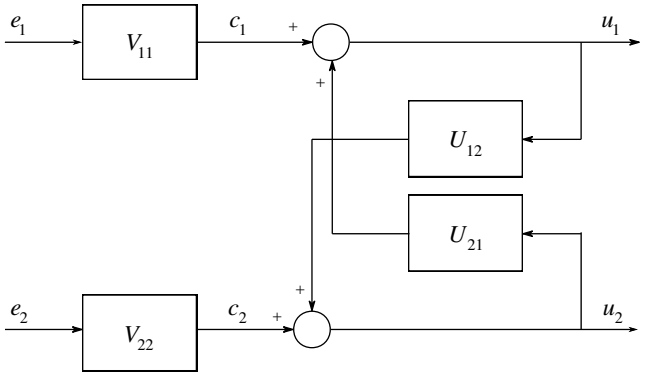

Figure 6. Block scheme of the decoupler of the U-topology

The practice of the decoupling tasks inspired the introduction of a very useful structure what can be seen in the right side of the Fig. 6 between the variables $\boldsymbol{c}$ and $\boldsymbol{u}$. Let us call this U-topology where U (unity) refers to the channels having unity transfer. It is well seen from the comparison with the V-topology that the U-topology can be obtained by the choices $U_{11} = 1$ and $U_{22} = 1$, thus corresponds to $\boldsymbol{V}_{\mathrm{D}} = \boldsymbol{I}$. Let us write $\boldsymbol{D}_{\mathrm{U}}$ for this case and substituting $\boldsymbol{V}_{\mathrm{D}} = \boldsymbol{I}$ into $\boldsymbol{D}_{\mathrm{V}}$ we get

$$\boldsymbol{D}_{\mathrm{U}} = \boldsymbol{D}_{\mathrm{V}}\big|_{\boldsymbol{V}_{\mathrm{D}}=\boldsymbol{I}} = \left(\boldsymbol{I} - \boldsymbol{U}_{\mathrm{A}}\right)^{-1} \tag{48}$$

Here it is assumed that, in comply with the notations of (39) and (43), $\boldsymbol{U} = \boldsymbol{I} + \boldsymbol{U}_{\mathrm{A}}$. After identical rearrangements we get

$$\boldsymbol{D}_{\mathrm{U}} = \left(\boldsymbol{I} - \boldsymbol{U}_{\mathrm{A}}\right)^{-1} = \left[\boldsymbol{G}_{\mathrm{D}}\left(\boldsymbol{I} - \boldsymbol{U}_{\mathrm{A}}\right)\right]^{-1} \boldsymbol{G}_{\mathrm{D}} = \left(\boldsymbol{G}_{\mathrm{D}} - \boldsymbol{G}_{\mathrm{D}}\boldsymbol{U}_{\mathrm{A}}\right)^{-1} \boldsymbol{G}_{\mathrm{D}} \tag{49}$$

Choosing $\boldsymbol{U}_{\mathrm{A}} = -\boldsymbol{G}_{\mathrm{D}}^{-1}\, \boldsymbol{G}_{\mathrm{A}}$ the final form of the decoupler becomes

$$\boldsymbol{D}_{\mathrm{U}} = \left(\boldsymbol{G}_{\mathrm{D}} + \boldsymbol{G}_{\mathrm{A}}\right)^{-1} \boldsymbol{G}_{\mathrm{D}} = \boldsymbol{G}^{-1}\, \boldsymbol{G}_{\mathrm{D}} \tag{50}$$

Using the compensator the decoupling is obtained as

$$\boldsymbol{G}\,\boldsymbol{D}_{\mathrm{U}} = \left(\boldsymbol{G}_{\mathrm{D}} + \boldsymbol{G}_{\mathrm{A}}\right)\left(\boldsymbol{G}_{\mathrm{D}} + \boldsymbol{G}_{\mathrm{A}}\right)^{-1}\boldsymbol{G}_{\mathrm{D}} = \boldsymbol{G}_{\mathrm{D}} \tag{51}$$

Compared to the V-topology the effect of the main diagonal elements are still missing. It can be easily substituted if a diagonal element $\boldsymbol{V}_{\mathrm{D}}$ is serially connected to the compensator $\boldsymbol{D}_{\mathrm{U}}$. This effect is illustrated on the left side of Fig. 6 between the variables $\boldsymbol{e}$ and $\boldsymbol{c}$. This means at the same time that the relation between the two compensators can be simply written as

$$\boldsymbol{G}_{\mathrm{V}} = \boldsymbol{G}_{\mathrm{U}}\,\boldsymbol{V}_{\mathrm{D}} = \boldsymbol{G}^{-1}\,\boldsymbol{G}_{\mathrm{D}}\boldsymbol{V}_{\mathrm{D}} \tag{52}$$

There is the following simple relationship between the V- and U-topology

$$\boldsymbol{V} = \boldsymbol{V}_{\mathrm{D}} + \boldsymbol{V}_{\mathrm{A}} = \boldsymbol{V}_{\mathrm{D}}\left(\boldsymbol{I} + \boldsymbol{V}_{\mathrm{D}}^{-1}\boldsymbol{V}_{\mathrm{A}}\right) = \boldsymbol{V}_{\mathrm{D}}\left(\boldsymbol{I} + \boldsymbol{U}_{\mathrm{A}}\right) = \boldsymbol{V}_{\mathrm{D}}\,\boldsymbol{U} \tag{53}$$

what explaines all the above results.

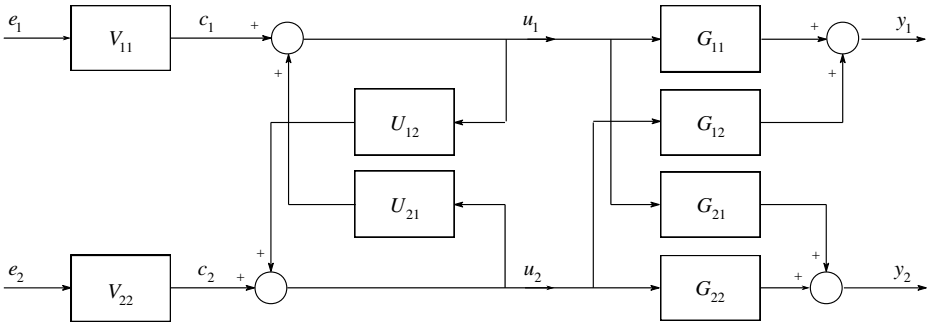

Figure 7. Joint block scheme of the decoupler and the process

The joint block scheme of the process and the decoupler of the U-topology is summarized in the Fig. 7. The cross-effects can be eliminated by the equations $G_{12} = -U_{21}G_{11}$ and $G_{21} = -U_{12}G_{22}$, whence the equations $U_{12} = -G_{21}/G_{22}$ and $U_{21} = -G_{12}/G_{11}$ are obtained for the decoupler. Due to the simplicity this method is widely used in the industrial practice of the decoupling by pairs.

This structure is beloved in the practical applications because the two inputs (V_{11} and U_{21} or V_{22} and U_{12}) of the summing elements allow to use standard PLC elements where the regulators (now V_{11} and V_{22}) appear together with the feed-forward elements (now U_{21} and U_{12}) what is usually the conventional tool of the classical solution of the noise compensation.

Besides the aboves, however, the decoupling can be performed by further simple topologies. The unity values of the diagonal elements can be used also for feed-forward

structures. This method is used to be called simple or simplified decoupling method [9]. The corresponding S-topology of the decoupling block scheme is shown in Fig. 8.

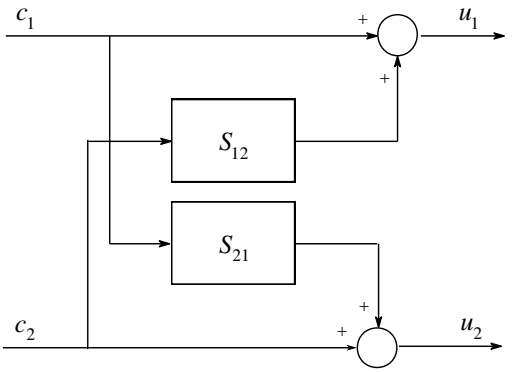

Figure 8. Block scheme of the decoupler of the S-topology

The basic relationship of the model can be written as

$$\boldsymbol{u} = \begin{bmatrix} u_1 \\ u_2 \end{bmatrix} = \begin{bmatrix} 1 & S_{12} \\ S_{21} & 1 \end{bmatrix} \begin{bmatrix} c_1 \\ c_2 \end{bmatrix} = \left(\boldsymbol{I} + \boldsymbol{S}_A\right)\boldsymbol{c} \tag{54}$$

Introduce the following notation for the inverse of the process

$$\boldsymbol{G}^{-1} = \left(\boldsymbol{G}_{\mathrm{D}} + \boldsymbol{G}_{\mathrm{A}}\right)^{-1} = \bar{\boldsymbol{G}}_{\mathrm{D}} + \bar{\boldsymbol{G}}_{\mathrm{A}} \tag{55}$$

Let $\boldsymbol{S}_{\mathrm{A}} = \bar{\boldsymbol{G}}_{\mathrm{A}}\,\bar{\boldsymbol{G}}_D^{-1}$ be, then

$$\left(\boldsymbol{I} + \boldsymbol{S}_A\right) = \boldsymbol{I} + \bar{\boldsymbol{G}}_{\mathrm{A}}\,\bar{\boldsymbol{G}}_D^{-1} = \left(\boldsymbol{I} + \bar{\boldsymbol{G}}_{\mathrm{A}}\,\bar{\boldsymbol{G}}_D^{-1}\right)\bar{\boldsymbol{G}}_{\mathrm{D}}\,\bar{\boldsymbol{G}}_D^{-1} = \left(\bar{\boldsymbol{G}}_{\mathrm{D}} + \bar{\boldsymbol{G}}_{\mathrm{A}}\right)\bar{\boldsymbol{G}}_D^{-1} = \boldsymbol{G}^{-1}\,\bar{\boldsymbol{G}}_D^{-1} \tag{56}$$

Using the S-compensator the decoupling becomes

$$\boldsymbol{G}\,\boldsymbol{G}^{-1}\,\bar{\boldsymbol{G}}_D^{-1} = \bar{\boldsymbol{G}}_D^{-1} \tag{57}$$

Thus the decoupling is fulfilled but there are very complicated transfer functions in the diagonals, namely the reciprocals of the main diagonal of $\boldsymbol{G}^{-1}$.

It is worth noting that the decouplers of feedback topology are welcome in sampled time applications because the actuator signal can be easily computed and programmed using (44) from the following expression

$$\boldsymbol{u} = \boldsymbol{V}_{\mathrm{D}}\,\boldsymbol{e} - \boldsymbol{V}_{\mathrm{D}}\,\boldsymbol{V}_{\mathrm{A}}\,\boldsymbol{u} = \boldsymbol{V}_{\mathrm{D}}\left(\boldsymbol{e} - \boldsymbol{V}_{\mathrm{A}}\,\boldsymbol{u}\right) = \boldsymbol{G}_{\mathrm{D}}^{-1}\left(\boldsymbol{e} + \boldsymbol{G}_{\mathrm{A}}\,\boldsymbol{u}\right) \tag{58}$$

4. Decoupling control using YOULA-parametrized *MIMO* regulators

The *YP*-parametrized *MIMO* regulator, introduced in Section 2, makes also possible to solve the decoupling problem. The real advantage of this approach is that it is clearly observable whether the decoupling is possible or not.

According to (17) and choosing $\boldsymbol{G}_{\mathrm{r}} = \mathbf{I}$ and $\boldsymbol{G}_{\mathrm{n}} = \mathbf{I}$, the overall transfer characteristic of the closed system obtained by YOULA-parametrization for *MIMO* systems has the form

$$\boldsymbol{y} = \boldsymbol{P}_{-}\boldsymbol{R}_{\mathrm{r}}\,\boldsymbol{y}_{\mathrm{r}} + \left(\mathbf{I} - \boldsymbol{P}_{-}\boldsymbol{R}_{\mathrm{n}}\right)\boldsymbol{y}_{\mathrm{n}} = \boldsymbol{y}_{\mathrm{t}} + \boldsymbol{y}_{\mathrm{d}} \tag{59}$$

It is well seen that if the invariant *MIMO* process factor $\boldsymbol{P}_{-}$ is non-diagonal, then it is impossible to apply decoupling regulator. If $\boldsymbol{P}_{-}$ is diagonal or $\boldsymbol{P}_{-} = \mathbf{I}$, then choosing diagonal $\boldsymbol{R}_{\mathrm{r}}$ or $\boldsymbol{R}_{\mathrm{n}}$ [8], [9], the tracking and noise rejection decoupling can be performed. If $\boldsymbol{P}_{-}$ is diagonal, then the diagonal inner matrix filters $\boldsymbol{G}_{\mathrm{r}}$ or $\boldsymbol{G}_{\mathrm{n}}$ can also be applied for the optimal compensation of the invariant factors. In the case of diagonal reference models providing decoupling, the design of the main diagonal elements of the inner filters is completely the same as in the optimization methods shown for scalar (*SISO*) systems [6].

5. Decoupling examples

Example 1.

Consider a very simple *MIMO* process, whose *TFM* is $\boldsymbol{P}(s) = \mathbf{B}(s)/\mathrm{A}(s)$, i.e.,

$$\boldsymbol{P}(s) = \begin{bmatrix} \dfrac{1}{1+s} & \dfrac{1}{1+2s} \\ 0 & \dfrac{1}{1+4s} \end{bmatrix} = \frac{1}{(1+s)(1+2s)(1+4s)} \begin{bmatrix} (1+2s)(1+4s) & (1+s)(1+4s) \\ 0 & (1+s)(1+2s) \end{bmatrix} \tag{60}$$

Choose such reference models what can perform both the speeding up and decoupling design goals

$$\boldsymbol{R}_{\mathrm{n}}(s) = \frac{1}{\mathrm{A}_{\mathrm{n}}(s)}\mathbf{B}_{\mathrm{n}}(s) = \frac{1}{(1+0.5s)}\begin{bmatrix} 1 & 0 \\ 0 & 1 \end{bmatrix} = \frac{1}{(1+0.5s)}\mathbf{I} \tag{61}$$

After the calculations of (25) the following regulator is obtained

$$\boldsymbol{C}(s) = \begin{bmatrix} \dfrac{1+s}{0.5s} & -\dfrac{(1+s)(1+4s)}{0.5s(1+2s)} \\ 0 & \dfrac{1+4s}{0.5s} \end{bmatrix} \tag{62}$$

whose elements contain signal forming of *PI* and *PID* character.

Example 2.

Investigate now a DT process where the impulse *TFM* of the process is

$$\boldsymbol{G}(z)=\begin{bmatrix} \dfrac{0.5z^{-1}}{1-0.5z^{-1}} & \dfrac{0.2z^{-1}}{1-0.8z^{-1}} \\ 0 & \dfrac{z^{-1}-0.5z^{-2}}{1-1.7z^{-1}+0.2z^{-1}} \end{bmatrix} \tag{63}$$

Apply again the speeding up and decoupling design goals using the following reference model

$$\boldsymbol{R}_{\mathrm{n}}(z)=\begin{bmatrix} \dfrac{0.8z^{-1}}{1-0.2z^{-1}} & 0 \\ 0 & \left(\dfrac{0.9z^{-1}}{1-0.1z^{-1}}\right)^2 \end{bmatrix}=\frac{\begin{bmatrix} 0.8z^{-1}\left(1-0.1z^{-1}\right)^2 & 0 \\ 0 & \left(0.9z^{-1}\right)^2\left(1-0.2z^{-1}\right) \end{bmatrix}}{\left(1-0.2z^{-1}\right)\left(1-0.1z^{-1}\right)^2} \tag{64}$$

After the calculations given by (25), the impulse *TFM* of the obtained matrix regulator is

$$\boldsymbol{C}(z)=\begin{bmatrix} C_{11}(z) & C_{12}(z) \\ C_{21}(z) & C_{22}(z) \end{bmatrix} \tag{65}$$

where

$$C_{11}(z)=\frac{1.6\left(1-0.5z^{-1}\right)}{1-z^{-1}} \qquad C_{12}(z)=\frac{-0.32\left(1-1.7z^{-1}+0.2z^{-2}\right)}{\left(1-z^{-1}\right)\left(1-0.8z^{-1}\right)} \tag{66}$$

$$C_{21}(z)=0 \qquad C_{22}(z)=\frac{0.81z^{-1}\left(1-1.7z^{-1}+0.2z^{-2}\right)}{\left(1-z^{-1}\right)\left(1+0.8z^{-1}\right)\left(1-0.5z^{-1}\right)} \tag{67}$$

All elements of the regulator can be realized what is the consequence of the specially chosen reference model *TFM*. Since all non-trivial elements of $\boldsymbol{R}_{\mathrm{n}}$ have unity gain, therefore the scalar regulators have integrating character (i.e., all elements have the pole $z=1$).

Example 3.

An aircraft obviously has a very complex dynamics [1], [10], [13], which can be described by many state, input and/or output variables. Experts states that the vital lateral dynamics, however, can be described by relatively simple models which have four state variables and two major input signals. The input variables are the aileron δ_{a}

and the rudder δ_r. For the small changes $\Delta\delta_a$ and $\Delta\delta_r$ in the vicinity of a working point we can introduce the following input vector

$$\boldsymbol{u} = \left[\Delta\delta_a \quad \Delta\delta_r\right]^T \tag{68}$$

so the next state equation well approaches the dynamics [10], [13]

$$\dot{\boldsymbol{x}} = \begin{bmatrix} Y_\beta & (\approx 0) & (\approx -1) & \frac{g}{V} \\ L_\beta & L_p & L_r & 0 \\ N_\beta & N_p & N_r & 0 \\ 0 & 1 & 0 & 0 \end{bmatrix} \boldsymbol{x} + \begin{bmatrix} 0 & Y_{\delta_r} \\ L_{\delta_a} & L_{\delta_r} \\ N_{\delta_a} & N_{\delta_r} \\ 0 & 0 \end{bmatrix} \boldsymbol{u} = \mathbf{A}\boldsymbol{x} + \mathbf{B}\boldsymbol{u}$$
$$\boldsymbol{y} = \mathbf{C}\boldsymbol{x} \tag{69}$$

Here $\mathbf{A}$ and $\mathbf{B}$ contain the so-called dimensional derivatives typical for a given aircraft. The subscripts δ_a and δ_r refer to the aileron and rudder input, respectively. Introduce the following variables: the sideslip angle β, the roll rate p, the yaw rate r and the roll angle ϕ. The small changes of the above variables produce the elements of the state vector, i.e.,

$$\boldsymbol{x} = \left[\Delta\beta \quad \Delta p \quad \Delta r \quad \Delta\phi\right]^T \tag{70}$$

The output variables depend on the selection of the structure of matrix $\mathbf{C}$. The following special selection, for example,

$$\boldsymbol{C} = \begin{bmatrix} 0 & 1 & 0 & 0 \\ 0 & 0 & 0 & 1 \end{bmatrix} \tag{71}$$

means that the output variables are the roll rate p and the roll angle ϕ, i.e., for their small changes

$$\boldsymbol{y} = \left[\Delta p \quad \Delta\phi\right]^T \tag{72}$$

It is an interesting task to design a simple decoupling regulator in order to reach the independent regulation of the roll rate and roll angle, or other selected output variables. The parameter matrices of the above state equation are available for different types of aircrafts in the literature. First choose an aircraft where this model is stable. A possible model according to [12] is

$$\dot{\boldsymbol{x}} = \begin{bmatrix} -0.099593 & 0 & -1 & 0.1056796 \\ -1.700982 & -1.184647 & 0.223908 & 0 \\ 0.407420 & -0.056276 & -0.188010 & 0 \\ 0 & 1 & 0 & 0 \end{bmatrix} \boldsymbol{x} + \begin{bmatrix} 0 & 0.740361 \\ 0.531304 & 0.049766 \\ 0.005685 & -0.106592 \\ 0 & 0 \end{bmatrix} \boldsymbol{u} =$$
$$= \mathbf{A}\boldsymbol{x} + \mathbf{B}\boldsymbol{u} \tag{73}$$

From the eigenvalues $\{-0.0603+0.7555i;-0.0603-0.7555i;-1.3198;-0.0319\}$ of the matrix **A**, two is complex conjugate and one is very slow. Let now the output variables be the sideslip angle β and the yaw rate r, i.e.,

$$\boldsymbol{y}=\left[\Delta\beta \quad \Delta r\right]^{\mathrm{T}} \tag{74}$$

This task can be solved by the choice

$$\mathbf{C}=\begin{bmatrix}1 & 0 & 0 & 0\\ 0 & 0 & 1 & 0\end{bmatrix} \tag{75}$$

To the decoupling choose the diagonal reference models

$$\boldsymbol{R}_{\mathrm{n}}(s)=\frac{1}{\mathrm{A}_{\mathrm{n}}(s)}\mathbf{B}_{\mathrm{n}}(s)=\frac{1}{(1+0.5s)}\begin{bmatrix}1 & 0\\ 0 & 1\end{bmatrix}=\frac{2}{s+2}\mathbf{I}=\boldsymbol{R}_{\mathrm{r}} \tag{76}$$

Using (25) we can compute the decoupling regulator as

$$\mathbf{C}(s)=\begin{bmatrix}\mathrm{C}_{11}(s) & \mathrm{C}_{12}(s)\\ \mathrm{C}_{21}(s) & \mathrm{C}_{22}(s)\end{bmatrix} \tag{77}$$

where

$$\mathrm{C}_{11}(s)=\frac{50.6501(s-2.862)(s+1.383)(s-0.04035)}{s(s+3.687)(s+3.687)} \tag{78}$$

$$\mathrm{C}_{12}(s)=\frac{351.803(s+1.154)(s+0.3676)(s-0.004883)}{s(s+3.687)(s+3.687)} \tag{79}$$

$$\mathrm{C}_{21}(s)=\frac{2.7014(s-3.79)(s-1.15)(s+0.9645)}{s(s+3.687)(s+3.687)} \tag{80}$$

$$\mathrm{C}_{22}(s)=\frac{2.7014(s-14.08)(s+0.1335)}{s(s+3.687)(s+3.687)} \tag{81}$$

It can be checked by simple calculations that the overall characteristic of the closed system is

$$\boldsymbol{y}=\begin{bmatrix}\Delta\beta\\ \Delta r\end{bmatrix}=\frac{2}{s+2}\mathbf{I}\begin{bmatrix}\Delta\delta_{\mathrm{a}}\\ \Delta\delta_{\mathrm{r}}\end{bmatrix}+\frac{2}{s+2}\mathbf{I}\,\boldsymbol{y}_{\mathrm{n}} \tag{82}$$

i.e., the decoupling is realized both for tracking and noise rejection. Each element of the *MIMO* regulator is realizable integrating regulator with third order transfer functions. Of course, depending on the feature of the task, different reference models can be chosen for $\boldsymbol{R}_{\mathrm{r}}$ and $\boldsymbol{R}_{\mathrm{n}}$.

On the basis of [13], the state equation of an unstable aircraft can be obtained by linearization around the working point

$$\dot{\boldsymbol{x}} = \begin{bmatrix} -0.05 & -0.003 & -0.98 & 0.2 \\ -1.0 & -0.75 & 1.0 & 0 \\ 0.3 & -0.3 & -0.15 & 0 \\ 0 & 1 & 0 & 0 \end{bmatrix} \boldsymbol{x} + \begin{bmatrix} 0 & 0 \\ 1.7 & -0.2 \\ 0.3 & -0.6 \\ 0 & 0 \end{bmatrix} \boldsymbol{u} = \mathbf{A}\boldsymbol{x} + \mathbf{B}\boldsymbol{u} \tag{83}$$

where the relative gain for the aileron and rudder are $g_1 = 1.0$ and $g_2 = \delta_r / \delta_a$.

The dynamic model of most of the aircrafts for the above state variables, however, is unstable. The YOULA-parametrization based regulators can be applied only for stable processes. The solution may the usual two-step method, where first an inner control loop is applied to stabilize the system.

The eigenvalues of the matrix $\mathbf{A}$ are $\{-0.0035 \pm 0.8834i; -0.9821; -0.0391\}$. The two complex conjugate poles and one of the real poles are stable, the other pole is unstable. This latter one corresponds to the instability of the so-called spiral dynamics. Different types of stabilizing regulators can be applied. The simplest case when the stabilization is solved by state feedback. Choose the following design poles: $\{-0.0035 \pm 0.8834i; -0.9821; -0.0391\}$, i.e., mirror the unstable pole on the complex axis. This pole assigning task can be solved by the following state feedback matrix

$$\boldsymbol{K} = \begin{bmatrix} -0.5606 & -0.3848 & 0.5529 & 0.5071 \\ -0.7622 & 0.2099 & -1.0143 & 0.6824 \end{bmatrix} \tag{84}$$

Let the output variables be the sideslip β and roll angle ϕ , i.e.,

$$\boldsymbol{y} = \begin{bmatrix} \Delta\beta & \Delta\phi \end{bmatrix}^{\mathrm{T}} \tag{85}$$

and the corresponding control matrix is

$$\boldsymbol{C} = \begin{bmatrix} 1 & 0 & 0 & 0 \\ 0 & 0 & 0 & 1 \end{bmatrix} \tag{86}$$

Similarly to the previous case the elements of the *MIMO* regulator are

$$\mathrm{C}_{11}(s) = \frac{0.42517\left(s^2 + 0.5416s + 0.6217\right)}{s} \tag{87}$$

$$\mathrm{C}_{12}(s) = \frac{1.2513\left(s^2 - 0.0332s + 0.7768\right)}{s} \tag{88}$$

$$\mathrm{C}_{21}(s) = \frac{3.6139\left(s + 0.8423\right)\left(s + 0.107\right)}{s} \tag{89}$$

$$C_{22}(s)=\frac{0.63584\left(s^2-1.395s+1.124\right)}{s} \tag{90}$$

Here we got *PID* regulators in each element of the matrix regulator. The overall characteristic of the closed system is

$$\boldsymbol{y}=\begin{bmatrix}\Delta\beta\\ \Delta\phi\end{bmatrix}=\frac{2}{s+2}\mathbf{I}\begin{bmatrix}\Delta\delta_a\\ \Delta\delta_r\end{bmatrix}+\frac{2}{s+2}\mathbf{I}\,\boldsymbol{y}_n \tag{91}$$

Acknowledgement

This work was supported in part by the Control Engineering Research Group of the HAS, at the Budapest University of Technology and Economics and by the project TAMOP 4.2.2.A-11/1/KONV-2012-2012, at the Széchenyi University of Győr.

References

[1] Allerton, D.: *Principles of Flight Simulation*, John Wiley & Sons, 2009
[2] Bányász, Cs., Keviczky, L.: *Youla-parametrized MIMO controller design for stable multivariable processes*, Int. Conf. on Control CONTROL'2010, Coventry, UK, pp. 126-131, 2010
[3] Etkin, B., Reid, L.D.: *Dynamics of Flight Stability and Control*, John Wiley & Sons, 1996
[4] Ghosh, A., Das S.K.: *Open-loop decoupling of MIMO plants*, IEEE Trans. on Aut. Contr., vol. AC-54, pp. 1977-1981, 2009
[5] Harold, L.W.: *Inverted decoupling – a neglected technique*, IEEE Trans. Aut. Control, vol. AC-36, 1, pp. 3-10, 1997
[6] Keviczky, L., Bányász, Cs.: *Iterative identification and control design using KB-parametrization*, In: Control of Complex Systems, Eds: Åström, K.J., Albertos, P., Blanke, M., Isidori, A., Schaufelberger, W., Sanz, R., Springer, pp. 101-121, 2001
[7] Keviczky, L., Bányász, Cs.: *Youla-parametrized controllers for stable multivariable processes*, Acta Technica Jaurinensis, vol. 3, no. 2, pp. 187-196, 2010
[8] Keviczky, L., Bányász, Cs.: *Decoupling autopilot MIMO controller design*, 31st IASTED Conf. on Modelling, Identification and Control MIC'11, Innsbruck, Austria, 2011
[9] Keviczky, L., Bányász, Cs.: *MIMO controller design for decoupling aircraft lateral dynamics*, 9th IEEE Conf. on Control and Automation, ICCA'11, Santiago, Chile, pp. 1079-1084, 2011
[10] McLean, D.: *Automatic Flight Control Systems*, Prentice Hall, 1990
[11] Maciejowski, J.M.: *Multivariable Feedback Design*, Addison Wesley, 1989
[12] Morari, M., Zafiriou, E.: *Robust Process Control*, Prentice-Hall, London, 1989
[13] Nelson, R.C.: WCB/McGraw-Hill, 1998
[14] Qing-Guo, W.: *Decoupling Control*, Springer, 2003
[15] Skogestad, S., Poslethwaite, I.: *Multivariable Feedback Control: Analysis and Design*, Wiley, second edition, 2005

Arbitary Pole-Placement in the LQ Control Paradigm

L. Keviczky, J. Bokor

Széchenyi István University, Győr
Computer and Automation Research Institute and Control Engineering Research Group
Hungarian Academy of Sciences
H-1111 Budapest, Kende u 13-17, Hungary
Phone: +361-466-5435
e-mail: keviczky@sztaki.hu; bokor@sztaki.hu

Abstract: The specific relationships between the classical pole-placement state feedback, the Riccati equation based LQ paradigm and the Kalman frequency domain approach are discussed. It is shown that arbitrary pole placement is not possible by standard LQ optimality. A possible solution of this anomaly is to use more general LQ criterion with specific weights on the state, input and crossterm.

Keywords: LQ problem, Kalman equation, optimality

1. Introduction

In the early time of control theory the optimization of transient processes in dynamic systems used a quadratic criterion, i.e., the integral square of error

$$I_2 = \int_0^\infty e^2(t)\mathrm{d}t = \int_{-\infty}^{\infty} E(-s)E(s)\mathrm{d}s = \frac{1}{\pi}\int_0^\infty |E(j\omega)|^2 \,\mathrm{d}\omega \,. \tag{1}$$

Here $e(t)$ is the error signal of a closed-loop control system. The second half of (1) is the so-called Parseval theorem [3], [6], using the strictly proper $E(s)$, the Laplace transform of $e(t)$.

This integral criterion was very popular, because the evaluation of (1) could be performed analytically and easily computed even by the early slow computers (by preprogrammed formulas). The general theory was called Wiener approach [3] and thousands of papers were published for the different optimal designs. The first critics came from the industry: the optimal regulators minimizing (1) were not acceptable in the practice, because they resulted a very large (20~25 %) overshoot in the step response transients.

One way to overcome this problem was first to introduce a more general quadratic integral criterion, penalizing the different state variables as

$$I_{2(n)} = \int_0^\infty \left[x^2 + \tau_1^2\dot{x}^2 + \cdots + \tau_n^2\left(x^{(n)}\right)^2\right]\mathrm{d}t \tag{2}$$

which is called generalized quadratic criterion. It is not difficult to show that (2) has an equivalent form

$$I_{2(n)} = \int_0^\infty \left[x^2 + \alpha\dot{x} + \cdots + \alpha_n x^{(n)}\right]^2 \mathrm{d}t \tag{3}$$

where $x(\infty) = \dot{x}(\infty) = \cdots = x^{(n-1)}(\infty) = 0$ and $c_0 = \alpha_1 x_0^2$, $x_0 = x(0)$. The coefficients of the two forms depend on each other by the Rekasius-Feldbaum equations [1], [2]

$$\begin{gathered} \tau_1^2 = \alpha_1^2 - 2\alpha_0\alpha_2 \\ \tau_2^2 = \alpha_2^2 - 2\alpha_1\alpha_3 + 2\alpha_0\alpha_4 \\ \tau_3^2 = \alpha_3^2 - 2\alpha_2\alpha_4 + 2\alpha_1\alpha_3 - 2\alpha_0\alpha_4 \\ \vdots \\ \tau_n^2 = \alpha_n^2 \end{gathered} \tag{4}$$

From (3) the minimum can be easily seen, if $x(t)$ fulfils the differential equation

$$\alpha_n x^{(n)} + \alpha_{n-1} x^{(n-1)} + \cdots + \alpha_1 x + \alpha_0 = 0;\ \alpha_0 = 1. \tag{5}$$

Here the signal $x(t)$ is more general than $e(t)$, because it can be one of the state variables of a linear system.

2. State feedback (*SFB*)

Consider a *SISO* continuous time linear time invariant (*LTI*) dynamic plant described by the state variable representation (*SVR*)

$$\begin{gathered} \frac{\mathrm{d}\boldsymbol{x}}{\mathrm{d}t} = \dot{x} = \boldsymbol{A}\boldsymbol{x} + \boldsymbol{b}u \\ y = \boldsymbol{c}^{\mathrm{T}}\boldsymbol{x} \end{gathered} \tag{6}$$

Here u, y and $\boldsymbol{x}$ are the input, output and state variables of the controlled process and T stands for transposition. The transfer function representation (*TFR*) of the open-loop system can be calculated by

$$P(s) = \frac{\mathrm{B}(s)}{\mathrm{A}(s)} = \boldsymbol{c}^{\mathrm{T}}\left(s\boldsymbol{I} - \boldsymbol{A}\right)^{-1}\boldsymbol{b} = \boldsymbol{c}^{\mathrm{T}}\boldsymbol{\Phi}(s)\boldsymbol{b} \tag{7}$$

where $\boldsymbol{I}$ is the unit matrix,

$$\begin{gathered} \boldsymbol{\Phi}(s) = \left(s\boldsymbol{I} - \boldsymbol{A}\right)^{-1} = \mathrm{L}\left\{e^{\boldsymbol{A}t}\right\} = \frac{\boldsymbol{\Psi}(s)}{\mathrm{A}(s)} \\ \boldsymbol{\Psi}(s) = \mathbf{adj}\left(s\boldsymbol{I} - \boldsymbol{A}\right) \end{gathered} \tag{8}$$

and

$$B(s) = s^n + b_1 s^{n-1} + \cdots + b_{n-1}s + b_n = \boldsymbol{c}^{\mathrm{T}}\boldsymbol{\Psi}(s)\boldsymbol{b} \tag{9}$$

$$A(s) = s^n + a_1 s^{n-1} + \cdots + a_{n-1}s + a_n = \det(s\boldsymbol{I} - \boldsymbol{A}) \tag{10}$$

are the numerator and denominator polynomials, respectively. If the feedback is restricted to a linear *SFB*, then the classical solution can be written as

$$u = k_{\mathrm{r}}\, r - \boldsymbol{k}^{\mathrm{T}} \boldsymbol{x} \tag{11}$$

where r is the reference signal, k_{r} is a calibrating constant and $\boldsymbol{k}^{\mathrm{T}}$ is the linear *SFB* vector. It is easy to check that the transfer function from the reference signal r to the output y is [4]

$$T_{\mathrm{ry}}(s) = \boldsymbol{c}^{\mathrm{T}} \left(s\boldsymbol{I} - \boldsymbol{A} + \boldsymbol{b}\boldsymbol{k}^{\mathrm{T}} \right)^{-1} \boldsymbol{b}\, k_{\mathrm{r}} = \frac{k_{\mathrm{r}}\, \mathrm{B}(s)}{\mathrm{A}(s) + \boldsymbol{k}^{T} \boldsymbol{\Psi}(s) \boldsymbol{b}} \tag{12}$$

where k_{r} is obtained by requiring that the static gain of T_{ry} should be equal to one

$$k_{\mathrm{r}} = \frac{\boldsymbol{k}^{\mathrm{T}} \boldsymbol{A}^{-1} \boldsymbol{b} - 1}{\boldsymbol{c}^{\mathrm{T}} \boldsymbol{A}^{-1} \boldsymbol{b}} \tag{13}$$

The usual classical design goal is to determine the feedback gain $\boldsymbol{k}^{\mathrm{T}}$ so that the closed-loop system has the characteristic polynomial

$$R(s) = s^n + r_1 s^{n-1} + \cdots + r_{n-1} s + r_n \tag{14}$$

The solution formally means equating the characteristic polynomial of the closed-loop with the desired polynomial ("pole placement method")

$$\mathrm{R}(s) = \det\left(s\boldsymbol{I} - \boldsymbol{A} + \boldsymbol{b}\boldsymbol{k}^{T} \right) = \mathrm{A}(s) + \boldsymbol{k}^{T} \boldsymbol{\Psi}(s) \boldsymbol{b} = \mathrm{A}(s) + \mathrm{K}(s) \tag{15}$$

to compute $\boldsymbol{k}^{\mathrm{T}}$. The solution always exists if $P(s)$ is controllable.

If the *TFR* of the process is known then one can easily form a controllable canonical form $\left\{ \boldsymbol{A}_{\mathrm{c}}, \boldsymbol{b}_{\mathrm{c}}, \boldsymbol{c}_{\mathrm{c}}^{\mathrm{T}} \right\}$ with

$$A_c = \begin{bmatrix} -\boldsymbol{a}_c^{\mathrm{T}} \\ \boldsymbol{I}, \boldsymbol{0} \end{bmatrix} \quad \boldsymbol{a}_c = [a_1, a_2, \cdots, a_n]^{\mathrm{T}} \quad \boldsymbol{b}_c = [1, 0, \cdots, 0]^{\mathrm{T}} \quad \boldsymbol{c}_c = [c_1, c_2, \cdots, c_n]^{\mathrm{T}} \tag{16}$$

and now the feedback gain is obtained from (15) as

$$\boldsymbol{k}_c^{\mathrm{T}} = [r_1 - a_1, r_2 - a_2, \cdots, r_n - a_n] = [k_1, k_2, \cdots, k_n] \tag{17}$$

because

$$\boldsymbol{\Psi}_c(s) \boldsymbol{b}_c = [s^{n-1}, \cdots, s, 1]^{\mathrm{T}} \tag{18}$$

and

$$\boldsymbol{k}_c^{\mathrm{T}} \boldsymbol{\Psi}_c(s) \boldsymbol{b}_c = k_1 s^{n-1} + \cdots k_{n-1} s + k_n = K(s). \tag{19}$$

The calibration factor is calculated by

$$k_{\mathrm{r}} = \frac{a_n + (r_n - a_n)}{b_n} = \frac{a_n}{b_n} \tag{20}$$

The *SVR* of the closed-loop system is described by

$$\frac{\mathrm{d}\boldsymbol{x}}{\mathrm{d}t} = \left(\boldsymbol{A} - \boldsymbol{b}\boldsymbol{k}^{\mathrm{T}}\right)\boldsymbol{x} + k_{\mathrm{r}}\,\boldsymbol{b}\,r = \bar{\boldsymbol{A}} + k_{\mathrm{r}}\,\boldsymbol{b}\,r$$
$$y = \boldsymbol{c}^{\mathrm{T}}\boldsymbol{x} \tag{21}$$

It is easy to see from equation (12) that $T_{\mathrm{ry}}(s)$ is now

$$T_{\mathrm{ry}}(s) = \frac{k_{\mathrm{r}}\,\mathrm{B}(s)}{\mathrm{R}(s)} \tag{22}$$

i.e., besides reaching the desired pole-placement the *SFB* leaves the open-loop zeros untouched.

3. The *LQR* (*L*inear system - *Q*uadratic criterion - *R*egulator) problem

Not only the bad transient of the error signal obtained from the optimal quadratic criterion was the problem, but also the big amplitude jumps necessary to the control action. An other way suggested to overcome the combined problem was the introduction of a penalty for the energy of the control signal. This optimization was formulated by the more general [3], [4] quadratic criterion

$$I = \frac{1}{2}\int_0^{\infty}\left[\boldsymbol{x}^{\mathrm{T}}(t)\boldsymbol{W}_{\mathrm{x}}\boldsymbol{x}(t) + w_{\mathrm{u}}u^2(t)\right]\mathrm{d}t \tag{23}$$

where $\boldsymbol{x}(t)$ is the state vector, $u(t)$ is the input of the process, respectively. The positive definite $\boldsymbol{W}_{\mathrm{x}}$ stands for penalizing the variations in the state space, w_{u} is for penalizing the energy of the control action, which is more general than (2). The solution, minimizing (23) is again a negative *SFB* [7]

$$u(t) = -\boldsymbol{k}_{\mathrm{LQ}}^{\mathrm{T}}\,\boldsymbol{x}(t) \tag{24}$$

where $\boldsymbol{k}_{\mathrm{LQ}}^{\mathrm{T}}$ is given by

$$\boldsymbol{k}_{\mathrm{LQ}}^{\mathrm{T}} = \frac{1}{w_{\mathrm{u}}}\boldsymbol{b}^{\mathrm{T}}\boldsymbol{P} \tag{25}$$

where the symmetric positive semi definite matrix $\boldsymbol{P}$ can be obtained from the solution of the algebraic Riccati equation [4]

$$\boldsymbol{P}\boldsymbol{A} + \boldsymbol{A}^{\mathrm{T}}\boldsymbol{P} - \frac{1}{w_{\mathrm{u}}}\boldsymbol{P}\boldsymbol{b}\boldsymbol{b}^{\mathrm{T}}\boldsymbol{P} = -\boldsymbol{W}_{\mathrm{x}} \tag{26}$$

Analytic solution is not possible, because this equation is nonlinear in $\boldsymbol{P}$, therefore only numeric solution can be obtained by MATLAB© and other *CACSD* programs.

Introducing the orthogonal factorization

$$\boldsymbol{W}_{\mathrm{x}} = \boldsymbol{G}^{\mathrm{T}}\boldsymbol{G} \tag{27}$$

the closed-loop system is stable if the auxiliary process

$$\boldsymbol{v} = \boldsymbol{G}\boldsymbol{x} \tag{28}$$

is observable.

The characteristic polynomial coefficients are computed now from

$$[r_1, r_2, \cdots, r_n]^{\mathrm{T}} = \boldsymbol{k}_{\mathrm{LQ}}^{\mathrm{T}} + [a_1, a_2, \cdots, a_n]^{\mathrm{T}} \tag{29}$$

Note that this *SFB* also provides the same $T_{\mathrm{ry}}(s)$ as (22) before.

A joint use of time domain optimality criteria, prescribed constraints and pole locations are often required in practice. Optimal and partially optimal pole placement based on optimality criteria (58) was studied in [19], [20], [21] and [22]. It can be shown, however, that [20] does not provide solution for the general problem (illustrated by the examples later), mainly due to the fact that it uses only the weights $\boldsymbol{W}_{\mathrm{x}}$, $\boldsymbol{W}_{\mathrm{u}}$ but not the cross term $\boldsymbol{W}_{\mathrm{ux}}$.

4. The frequency domain solution of the *LQR* problem

The *LQR* approach is widely used for control problems in all over the world, however, in a practical problem it is not an easy task to find the best $\boldsymbol{W}_{\mathrm{x}}$ and w_{u} weights, which are usually obtained by trial and error iterative methods. The *LQR* problem has an almost forgotten frequency domain solution, too, which will give us a deterministic design process to find useful relationships between the classical pole placement *SFB* solution and the *LQR* paradigm. It can be shown that the simpler dyadic factorization [3]

$$\boldsymbol{W}_{\boldsymbol{x}} = \boldsymbol{g}\boldsymbol{g}^{\mathrm{T}} \quad \boldsymbol{g} = [g_1, \cdots, g_{n-1}, g_n]^{\mathrm{T}} \tag{30}$$

can also be used. The frequency domain condition of the minimum of (23) is called the Kalman equation [3] or sometimes it is named frequency domain identity (FDI)

$$w_{\mathrm{u}}\left|1 + \boldsymbol{k}^{\mathrm{T}}\boldsymbol{\Phi}(s)\boldsymbol{b}\right|^2 = w_{\mathrm{u}} + \left|\boldsymbol{g}^{\mathrm{T}}\boldsymbol{\Phi}(s)\boldsymbol{b}\right|^2 \tag{31}$$

Assuming unity weight $w_{\mathrm{u}} \equiv 1$ the equation becomes even simpler

$$\left|1 + \boldsymbol{k}^{\mathrm{T}}\boldsymbol{\Phi}(s)\boldsymbol{b}\right|^2 = 1 + \left\|\boldsymbol{g}^{\mathrm{T}}\boldsymbol{\Phi}(s)\boldsymbol{b}\right\|_2^2 = 1 + \left|\boldsymbol{g}^{\mathrm{T}}\boldsymbol{\Phi}(s)\boldsymbol{b}\right|^2 \tag{32}$$

Using the well known relationship of complex functions

$$\left\{Z(s)\right\}^2 = \left|Z(s)\right|^2 = Z(s)Z(-s) \tag{33}$$

and introducing the (n-1)-th order polynomial G(s) as the numerator of

$$H(s) = \boldsymbol{g}^{\mathrm{T}}\boldsymbol{\Phi}(s)\boldsymbol{b} = \frac{\boldsymbol{G}(s)}{\boldsymbol{A}(s)} = \frac{g_1 s^{n-1} + \cdots + g_{n-1}s + g_n}{\boldsymbol{A}(s)} \tag{34}$$

the equation (32) can be rearranged into a new form

$$\underbrace{[A(s)+\boldsymbol{k}^{\mathrm{T}}\boldsymbol{\Psi}(s)\boldsymbol{b}]}_{R(s)}\underbrace{[A(-s)+\boldsymbol{k}^{\mathrm{T}}\boldsymbol{\Psi}(-s)\boldsymbol{b}]}_{R(-s)}=A(s)A(-s)+\underbrace{[\boldsymbol{g}^{\mathrm{T}}\boldsymbol{\Psi}(s)\boldsymbol{b}]}_{G(s)}\underbrace{[\boldsymbol{g}^{\mathrm{T}}\boldsymbol{\Psi}(-s)\boldsymbol{b}]}_{G(-s)} \tag{35}$$

which provides the quadratic polynomial solution of the Kalman equation. Thus the final quadratic equation, ensuring relationship between the process $\mathrm{A}(s)$, design $\mathrm{R}(s)$ and weighting $\mathrm{G}(s)$ polynomials, is

$$\mathrm{R}(s)\mathrm{R}(-s)=\mathrm{A}(s)\mathrm{A}(-s)+\mathrm{G}(s)\mathrm{G}(-s) \qquad |\mathrm{R}(s)|^2=|\mathrm{A}(s)|^2+|\mathrm{G}(s)|^2 \tag{36}$$

or in the general form

$$w_{\mathrm{u}}|\mathrm{R}(s)|^2=w_{\mathrm{u}}|\mathrm{A}(s)|^2+|\mathrm{G}(s)|^2 \tag{37}$$

Observe that the solution tends to $\mathrm{R}(s)=\mathrm{A}(s)$ if $W_{\mathrm{u}}\to\infty$ and $\boldsymbol{g}^{\mathrm{T}}\boldsymbol{x}=0$ if $w_{\mathrm{u}}\to 0$. Do not forget that $\mathrm{K}(s)$ and $\mathrm{G}(s)$ are of $(n-1)$-th order [8].

5. Some anomalies in the *LQR* problem

The solution of the polynomial equation can be a direct coefficient comparison or a spectral factorization approach [5]. Consider some examples in the sequel.

Example 1

Consider a first order example with

$$\mathrm{A}(s)=s+a_1 \qquad \mathrm{R}(s)=s+r_1 \qquad \mathrm{G}(s)=g_1 \tag{38}$$

The two sides of (35) are

$$-s^2-r_1s+r_1s+r_1^2=-s^2-a_1s+a_1s+a_1^2+g_1^2 \tag{39}$$

and the solution is

$$r_1^2=a_1^2+g_1^2>0 \tag{40}$$

and

$$k_1=r_1-a_1=\sqrt{a_1^2+g_1^2}-a_1>0 \tag{41}$$

If we want to ensure (place) a required pole then the necessary weight in the *LQR* problem is

$$g_1=\sqrt{r_1^2-a_1^2} \tag{42}$$

It is easy to see that only such r_1 can be placed, which fulfills the condition

$$r_1^2>a_1^2\Rightarrow|r_1|>|a_1|\Rightarrow r_1>|a_1| \tag{43}$$

for stable design polynomial $R(s)$. So this example shows that only a faster pole can be placed by the *LQR* optimization comparing to the original process pole.

Example 2

Consider a second order example with

$$A(s)=s^2+a_1s+a_2 \qquad R(s)=s^2+r_1s+r_2 \qquad G(s)=g_1s+g_2 \tag{44}$$

The two sides of (35) are now

$$\left(s^2+r_1s+r_2\right)\left(s^2-r_1s+r_2\right)=\left(s^2+a_1s+a_2\right)\left(s^2-a_1s+a_2\right)+\left(g_1s+g_2\right)\left(-g_1s+g_2\right) \tag{45}$$

and the solutions are

$$r_2=\sqrt{a_2^2+g_2^2}>a_2 \tag{46}$$

$$r_1=\sqrt{2\left(\sqrt{a_2^2+g_2^2}-a_2\right)+\left(a_1^2+g_1^2\right)}=\sqrt{2\left(r_2-a_2\right)+\left(a_1^2+g_1^2\right)}>a_1>0 \tag{47}$$

The *SFB* to be applied is given by

$$k_1=r_1-a_1>0 \qquad k_2=r_2-a_2>0 \tag{48}$$

For pole placement the necessary *LQR* weights are

$$g_2=\sqrt{r_2^2-a_2^2} \tag{49}$$

and

$$g_1=\sqrt{r_2^2-a_1^2-2\left(r_2-a_2\right)}=\sqrt{2\left(\mu_r^2-\mu_a^2\right)} \tag{50}$$

where

$$\mu_r^2=\frac{r_1^2-2r_2}{2}=\frac{\left(s_1^r\right)^2+\left(s_2^r\right)^2}{2} \tag{51}$$

and

$$\mu_a^2=\frac{a_1^2-2a_2}{2}=\frac{\left(s_1^a\right)^2+\left(s_2^a\right)^2}{2} \tag{52}$$

It is easy to see that there are such $\{r_1,r_2\}$ domains, which can not be reached by any $\{g_1,g_2\}$ selection. These conditions are

$$r_2^2>a_2^2\Rightarrow|r_2|>|a_2|\Rightarrow r_2>|a_2| \tag{53}$$

and

$$r_2 \geq \frac{r_1^2}{2} - 2\mu_a^2 = \frac{r_1^2}{2} - \left(a_1^2 - 2a_2\right) \tag{54}$$

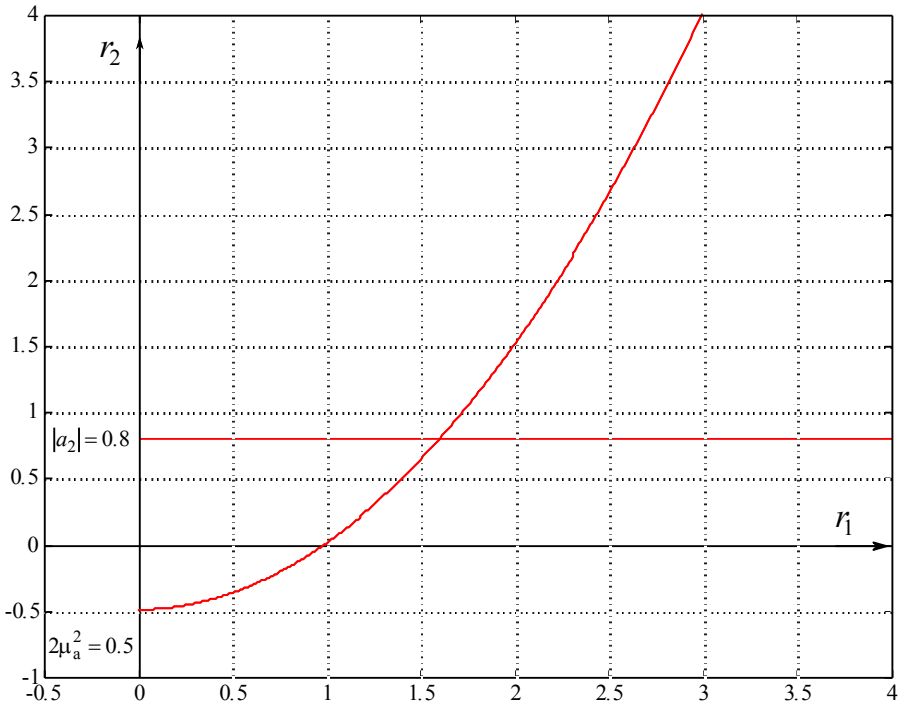

Figure 1. Unreachable design parameter domains

These conditions are graphically demonstrated on Fig.1, where the shaded area shows the unreachable design parameters for the case of open-loop process parameters $|a_2| = 0.8$ and $2\mu_a^2 = 0.5$.

One can check these results either via the solution of the Riccati equation (very time consuming method) or by the spectral factorization approach

$$R(s)R(-s) = \left[A(s)A(-s) + G(-s)G(s)\right]^{+}\left[A(s)A(-s) + G(-s)G(s)\right]^{-} \tag{55}$$

as the solution of (36), i.e., by

$$R(s) = \left[A(s)A(-s) + G(s)G(-s)\right]^{+} \tag{56}$$

6. Solutions for *LQ*-pole placement

We can not explain the above anomalies physically and provide unique solutions, however, offer some applicable solutions. Therefore it is necessary to discuss first the original *MIMO LQR* problem.

Infinite-horizon, continuous-time *LQ* Regulator (*LQR*)

For a continuous-time *MIMO* linear system described by

$$\begin{gathered}\frac{\mathrm{d}\boldsymbol{x}}{\mathrm{d}t}=\dot{\boldsymbol{x}}=\boldsymbol{A}\boldsymbol{x}+\boldsymbol{B}\boldsymbol{u}\\ \boldsymbol{x}(0)=\boldsymbol{x}_0\end{gathered} \tag{57}$$

with a *LQ* cost functional (performance index) defined as

$$J(\boldsymbol{x}_0,\boldsymbol{u})=\frac{1}{2}\int_0^\infty\left(\boldsymbol{x}^{\mathrm{T}}\boldsymbol{W}_{\mathrm{x}}\boldsymbol{x}+\boldsymbol{u}^{\mathrm{T}}\boldsymbol{W}_{\mathrm{u}}\boldsymbol{u}\right)\mathrm{d}t \tag{58}$$

with $\boldsymbol{W}_{\mathrm{x}}\geq 0$ and $\boldsymbol{W}_{\mathrm{u}}>0$, the stabilizing feedback control law that minimizes the value of the cost is

$$\boldsymbol{u}=\boldsymbol{K}\boldsymbol{x} \tag{59}$$

where $\boldsymbol{K}$ is given by

$$\boldsymbol{K}=-\boldsymbol{W}_{\mathrm{u}}^{-1}\boldsymbol{B}^{\mathrm{T}}\boldsymbol{P} \tag{60}$$

and $\boldsymbol{P}=\boldsymbol{P}^{\mathrm{T}}>0$ is the solution of the continuous time algebraic Riccati equation

$$\boldsymbol{A}^{\mathrm{T}}\boldsymbol{P}+\boldsymbol{P}\boldsymbol{A}-\boldsymbol{P}\boldsymbol{B}\boldsymbol{W}_{\mathrm{u}}^{-1}\boldsymbol{B}^{\mathrm{T}}\boldsymbol{P}+\boldsymbol{W}_{\mathrm{x}}=\boldsymbol{0} \tag{61}$$

It is possible to construct an even more general *LQR* performance index, which penalizes the interaction of the state and control variables, too:

$$J(\boldsymbol{x}_0,\boldsymbol{u})=\frac{1}{2}\int_0^\infty\left(\boldsymbol{x}^{\mathrm{T}}\boldsymbol{W}_{\mathrm{x}}\boldsymbol{x}+2\boldsymbol{u}^{\mathrm{T}}\boldsymbol{W}_{\mathrm{ux}}\boldsymbol{x}+\boldsymbol{u}^{\mathrm{T}}\boldsymbol{W}_{\mathrm{u}}\boldsymbol{u}\right)\mathrm{d}t \qquad \boldsymbol{W}_{\mathrm{x}}\geq 0 \qquad \boldsymbol{W}_{\mathrm{u}}>0 \tag{62}$$

where the stabilizing feedback control law that minimizes the value of the cost is again

$$\boldsymbol{u}=\boldsymbol{K}\boldsymbol{x}$$

but here $\boldsymbol{K}$ is given by

$$\boldsymbol{K}=-\boldsymbol{W}_{\mathrm{u}}^{-1}\left(\boldsymbol{W}_{\mathrm{ux}}+\boldsymbol{B}^{\mathrm{T}}\boldsymbol{P}\right) \tag{63}$$

and $\boldsymbol{P}=\boldsymbol{P}^{\mathrm{T}}>0$ is now the solution of a more complex algebraic Riccati equation

$$\boldsymbol{P}\boldsymbol{A}+\boldsymbol{A}^{\mathrm{T}}\boldsymbol{P}-\left(\boldsymbol{P}\boldsymbol{B}+\boldsymbol{W}_{\mathrm{ux}}^{\mathrm{T}}\right)\boldsymbol{W}_{\mathrm{u}}^{-1}\left(\boldsymbol{W}_{\mathrm{ux}}+\boldsymbol{B}^{\mathrm{T}}\boldsymbol{P}\right)+\boldsymbol{W}_{\mathrm{x}}=\boldsymbol{0} \tag{64}$$

These results are standard facts of the *LQR* theory. For the sake of completeness a sketch of the proof for the sufficiency is given as follows: assume that $\boldsymbol{W}_{\mathrm{ux}}>0$, $\boldsymbol{W}_{\mathrm{x}}\geq 0$, $\boldsymbol{W}_{\mathrm{ux}}$ are given. Then it will be shown that (62) is minimized by $\boldsymbol{K}$ in (60). The Riccati equation can be rewritten as

$$\boldsymbol{P}\boldsymbol{A}+\boldsymbol{A}^{\mathrm{T}}\boldsymbol{P}-\boldsymbol{K}\boldsymbol{W}_{\mathrm{u}}^{-1}\boldsymbol{K}+\boldsymbol{W}_{\mathrm{x}}=\boldsymbol{0} \tag{65}$$

Pre- and post-multiplying by $\boldsymbol{x}^{\mathrm{T}}$ and $\boldsymbol{x}$, respectively and substituting $\boldsymbol{Ax} = \dot{\boldsymbol{x}} - \boldsymbol{Bu}$, it follows:

$$\boldsymbol{x}^{\mathrm{T}}\boldsymbol{P}(\dot{\boldsymbol{x}} - \boldsymbol{Bu}) + (\dot{\boldsymbol{x}} - \boldsymbol{Bu})^{\mathrm{T}}\boldsymbol{Px} - \boldsymbol{x}^{\mathrm{T}}\boldsymbol{K}^{\mathrm{T}}\boldsymbol{W}_{\boldsymbol{u}}\boldsymbol{Kx} + \boldsymbol{x}^{\mathrm{T}}\boldsymbol{Wx} = \boldsymbol{0}$$

Using $-\boldsymbol{W}_{\mathrm{u}}\boldsymbol{K} = \boldsymbol{B}^{\mathrm{T}}\boldsymbol{P} + \boldsymbol{W}_{\mathrm{ux}}$ and $\frac{\mathrm{d}}{\mathrm{d}t}(\boldsymbol{x}^{\mathrm{T}}\boldsymbol{Px}) = \dot{\boldsymbol{x}}^{\mathrm{T}}\boldsymbol{Px} + \boldsymbol{x}^{\mathrm{T}}\boldsymbol{P}\dot{\boldsymbol{x}}$, one arrives at

$$\boldsymbol{x}^{\mathrm{T}}\boldsymbol{W}_{\mathrm{x}}\boldsymbol{x} + 2\boldsymbol{u}^{\mathrm{T}}\boldsymbol{W}_{\mathrm{ux}}\boldsymbol{x} + \boldsymbol{u}^{\mathrm{T}}\boldsymbol{W}_{\mathrm{u}}\boldsymbol{u} = -\frac{\mathrm{d}}{\mathrm{d}t}\left(\boldsymbol{x}^{\mathrm{T}}\boldsymbol{Px}\right) + \left(\boldsymbol{u} - \boldsymbol{Kx}\right)^{\mathrm{T}}\boldsymbol{W}_{\mathrm{u}}\left(\boldsymbol{u} - \boldsymbol{Kx}\right)$$

and by integration

$$J\left(\boldsymbol{x}_0, \boldsymbol{u}\right) = \frac{1}{2}\boldsymbol{x}^{\mathrm{T}}\left(t_0\right)\boldsymbol{P}_{t_0}\boldsymbol{x}\left(t_0\right) + \frac{1}{2}\int_{t_0}^{\infty}\left(\boldsymbol{u} - \boldsymbol{Kx}\right)^{\mathrm{T}}\boldsymbol{W}_{\mathrm{u}}\left(\boldsymbol{u} - \boldsymbol{Kx}\right)\mathrm{d}t$$

is obtained. Obviously $J_{\min}\left(\boldsymbol{x}_0\right) = \frac{1}{2}\boldsymbol{x}^{\mathrm{T}}\left(t_0\right)\boldsymbol{P}_{t_0}\boldsymbol{x}\left(t_0\right)$ if $\boldsymbol{u} = \boldsymbol{Kx}$.

Inverse optimality for *LQR* performance

Given a stabilizing feedback $\boldsymbol{u} = \boldsymbol{Kx}$ for (57) one can formulate the problem whether there exists an *LQR* problem of the form (58) or (62) that has the given feedback as a solution, i.e., the feedback is optimal. If the pair $\left(\boldsymbol{A}, \boldsymbol{B}\right)$ is controllable, then for any given spectrum Λ there is a feedback gain $\boldsymbol{K}_{\Lambda}$ such that $\lambda\left(\boldsymbol{A} + \boldsymbol{BK}_{\Lambda}\right) = \Lambda$. Concerning the pole-placement problem one can state that a spectrum Λ is *LQ* optimal if there is an associated $\boldsymbol{K}_{\Lambda}$ such that it is a solution of the RICCATI equation with a $\boldsymbol{W}_{\mathrm{x}} \geq 0$.

It turns out that the problem associated to the performance index (58) is nontrivial while the general case, corresponding to (62) can be always solved.

The MIMO KALMAN-FDI

In frequency domain the solution of the problem leads to the so called return difference condition. Its single input formulation is due to Kalman and was later extended by Anderson and Moore [9].

Specifically, $\boldsymbol{K}$ is optimal for $\boldsymbol{W}_{\mathrm{x}} = \boldsymbol{W}_{\mathrm{x}}^{\mathrm{T}} \geq 0$ and $\boldsymbol{W}_{\mathrm{u}} = \boldsymbol{W}_{\mathrm{u}}^{\mathrm{T}} > 0$ if and only if $\boldsymbol{A} + \boldsymbol{BK}$ is stable and there exists an $\boldsymbol{W}_{\mathrm{u}} = \boldsymbol{W}_{\mathrm{u}}^{\mathrm{T}} > 0$ that satisfies the return difference inequality:

$$\left[\boldsymbol{I} + \boldsymbol{H}_{\mathrm{LQ}}\left(-s\right)\right]^{\mathrm{T}}\boldsymbol{W}_{\mathrm{u}}\left[\boldsymbol{I} + \boldsymbol{H}_{\mathrm{LQ}}\left(s\right)\right] \geq \boldsymbol{W}_{\mathrm{u}} \tag{66}$$

for all $s = j\omega$, $\omega \in \mathbb{R}$ or equivalently the Kalman-FDI is also satisfied:

$$\left[\boldsymbol{I} + \boldsymbol{H}_{\mathrm{LQ}}\left(-s\right)\right]^{\mathrm{T}}\boldsymbol{W}_{\mathrm{u}}\left[\boldsymbol{I} + \boldsymbol{H}_{\mathrm{LQ}}\left(s\right)\right] = \boldsymbol{W}_{\mathrm{u}} + \boldsymbol{H}\left(-s\right)\boldsymbol{H}\left(s\right) \tag{67}$$

where

$$\boldsymbol{H}_{\mathrm{LQ}}\left(s\right) = \boldsymbol{K}\left(s\boldsymbol{I} - \boldsymbol{A}\right)^{-1}\boldsymbol{B} \qquad \boldsymbol{H}\left(s\right) = \boldsymbol{G}\left(s\boldsymbol{I} - \boldsymbol{A}\right)^{-1}\boldsymbol{B} \qquad \boldsymbol{W}_{\mathrm{x}} = \boldsymbol{G}^{\mathrm{T}}\boldsymbol{G} \tag{68}$$

Choosing $\boldsymbol{W}_{\mathrm{u}} = w_{\mathrm{u}}\boldsymbol{I}$, $w_{\mathrm{u}} > 0$ one has:

Proposition 1 *Consider* (58)*, then the static state feedback gain* $\boldsymbol{K}$ *is optimal for some* $\boldsymbol{W}_{\mathrm{x}} > 0$, $\boldsymbol{W}_{\mathrm{u}} > 0$ *if and only if*

$$\mathrm{Re}\lambda_i\left\{\boldsymbol{A}+\boldsymbol{B}\boldsymbol{K}\right\} < 0 \quad \forall\ i$$
$$\sigma_i\left\{\boldsymbol{1}+\boldsymbol{K}(i\omega-\boldsymbol{A})^{-1}\boldsymbol{B}\right\} > 1 \quad \forall\ i \quad \forall\ \omega$$

where σ_i denotes the singular values. For *SISO* systems the Kalman-FDI becomes:

$$w_{\mathrm{u}}\left[1+H_{\mathrm{LQ}}(-s)\right]\left[1+H_{\mathrm{LQ}}(s)\right] = w_{\mathrm{u}} + H(-s)H(s) \tag{69}$$

where $H(s) = \frac{G(s)}{A(s)}$ and

$$H_{\mathrm{LQ}}(s) = \boldsymbol{k}^{\mathrm{T}}(s\boldsymbol{I}-\boldsymbol{A})^{-1}\boldsymbol{b} = \boldsymbol{k}^{\mathrm{T}}\boldsymbol{\Phi}(s)\boldsymbol{b} = \frac{\boldsymbol{k}^{\mathrm{T}}\boldsymbol{\Psi}(s)\boldsymbol{b}}{A(s)}.$$

Denoting the closed loop characteristic align by $R(s)$,

$$R(s) = \det\left(s\boldsymbol{I}-\boldsymbol{A}-\boldsymbol{b}\boldsymbol{k}^{\mathrm{T}}\right) = \det(s\boldsymbol{I}-\boldsymbol{A})\det\left[1+\boldsymbol{k}^{\mathrm{T}}(s\boldsymbol{I}-\boldsymbol{A})^{-1}\boldsymbol{b}\right]$$

leading to

$$R(s) = A(s)\left[1+H_{\mathrm{LQ}}(s)\right]$$

if $w_{\mathrm{u}} \equiv 1$ is chosen. From the Kalman-FDI one obtains:

$$w_{\mathrm{u}}\frac{\mathrm{R}(s)\mathrm{R}(-s)}{\mathrm{A}(s)\mathrm{A}(-s)} = w_{\mathrm{u}} + \frac{\mathrm{G}(s)\mathrm{G}(-s)}{\mathrm{A}(s)\mathrm{A}(-s)} \qquad \frac{\mathrm{R}(s)\mathrm{R}(-s)}{\mathrm{A}(s)\mathrm{A}(-s)} = 1 + w_{\mathrm{u}}^{-1}\frac{\mathrm{G}(s)\mathrm{G}(-s)}{\mathrm{A}(s)\mathrm{A}(-s)} \tag{70}$$

which corrresponds to (36). We now give a simple test for a given state feedback gain $\boldsymbol{k}$ to decide if it can be an *LQ* optimal gain.

Proposition 2 *Assume that with* $u = \boldsymbol{k}^{\mathrm{T}}\boldsymbol{x}$ *the closed loop is stable. Then* $\boldsymbol{k}$ *is optimal for some* $\boldsymbol{W}_{\mathrm{x}} \geq 0$, *and* $w_{\mathrm{u}} > 0$ *if and only if*

$$\left|\frac{R(i\omega)}{A(i\omega)}\right| \geq 1 \quad \forall\ \omega \tag{71}$$

Proof. If $\boldsymbol{k}$ is *LQ* optimal, then the closed loop is stable and from the Kalman-FDI follows that $\left[1+H_{\mathrm{LQ}}\right] \geq 1$ and (71) is satisfied. On the contrary, if $\boldsymbol{k}$ is stabilizing and (71) is satisfied, one can find a $\boldsymbol{W}_{\mathrm{x}} \geq 0$ and $w_{\mathrm{u}} > 0$ such that the Kalman-FDI is

satisfied, too, i.e., $\boldsymbol{k}$ is *LQ* optimal with this $\boldsymbol{W}_{\mathrm{x}}$ and w_{u}.

Example 3
Let the system be given as

$$\dot{x} = -2x + u$$

i.e., $\boldsymbol{A} = A = a = -2$, $\boldsymbol{B} = B = b = 1$. The open loop (plant) transfer function is

$$P(s) = \frac{1}{s+2} = \frac{b_1}{s+a_1} \qquad A(s) = s + a_1$$

Applying state feedback $u = k\,x$, allocate the pole to $p_1 = -r_1 = -1$, i.e. $\mathrm{R}(s) = s + r_1$. This will be performed by $k = 1$ and the closed loop system will be

$$\dot{\bar{x}} = -1\bar{x} + u$$

i.e.,

$$R(s) = s + r_1 = s + 1$$

Plotting the Bode diagram for

$$\left|\frac{R(i\omega)}{A(i\omega)}\right| = \frac{1}{2}\frac{|1+i\omega|}{|1+i\omega/2|}$$

one can deduce that this is below the 0 dB for small frequencies and asymptotically approaches 0 dB if $\omega \to \infty$. This shows that this *k* cannot be optimal for the *LQR* performance index (58).

It is seen that using static state feedback, it is not possible to "slow down" the system since $r_1 > a_1$ has to be satisfied for *LQ* optimality.

Time domain conditions

In time domain inverse optimality of the feedback gain can be described through the concept of passivity.

For a *LTI* system passivity, equivalent in this case to the positive realness, is assured in accordance with the following lemma, often termed as the KALMAN-YACUBOVICH-POPOV lemma:

Lemma 1 *A stable system* (57) *is passive, if and only if, there exists a matrix* $\boldsymbol{P} = \boldsymbol{P}^{\mathrm{T}} > 0$ *such that*

$$\begin{aligned} \boldsymbol{P}\boldsymbol{A} + \boldsymbol{A}^{\mathrm{T}}\boldsymbol{P} &= -\boldsymbol{W}_{\mathrm{x}} \le 0 \\ \boldsymbol{P}\boldsymbol{B} &= \boldsymbol{C}^{\mathrm{T}} \end{aligned} \tag{72}$$

with $\boldsymbol{C} \in \mathbb{R}^{m \times n}$ a suitable output matrix for system (61). Then, inverse optimality is given by the following result:

Proposition 3 *A stable feedback gain-matrix* $\boldsymbol{K}$ *is optimal for a given input weighting matrix* $\boldsymbol{W}_{\mathrm{u}} > 0$ *and some state weighting matrix* $\boldsymbol{W}_{\mathrm{x}} \ge 0$, *i.e., it minimizes a performance index of the form of* (58)*, if and only if, the closed-loop system with gain-*

matrix

$$\bar{\boldsymbol{K}} = \frac{1}{2}\boldsymbol{K} \tag{73}$$

is passive for an output matrix $\boldsymbol{C} = -\boldsymbol{W}_{\mathrm{u}}\boldsymbol{K}$.

Inverse optimality for *LQR* performance (67)

Including the cross term $\boldsymbol{W}_{\mathrm{ux}}$ in the *LQR* performance index makes the problem trivial. For a stabilizing state feedback $\boldsymbol{K}$ one can find the extended matrix $\boldsymbol{W}$ (see (75)) such, that $\boldsymbol{K}$ is *LQ* optimal according to the performance (62). The procedure of deriving such weighting matrices, however, is neither trivial, nor unique. We show one possible solution that follows the procedure in [12].

It is obvious, that for any $\boldsymbol{W}_{\mathrm{u}} > 0$ the stabilizing feedback $\boldsymbol{u} = \boldsymbol{K}\boldsymbol{x}$ is optimal for the performance index:

$$J(x_0, \boldsymbol{u}) = \frac{1}{2}\int_0^{\infty} (\boldsymbol{u} - \boldsymbol{K}\boldsymbol{x})^{\mathrm{T}} \boldsymbol{W}_{\mathrm{u}} (\boldsymbol{u} - \boldsymbol{K}\boldsymbol{x})\,\mathrm{d}t \tag{74}$$

i.e., $\boldsymbol{W}_{\mathrm{x}} = \boldsymbol{K}^{\mathrm{T}}\boldsymbol{W}_{\mathrm{u}}\boldsymbol{K} \geq 0$ and $\boldsymbol{W}_{\mathrm{ux}} = -\boldsymbol{W}_{\mathrm{u}}\boldsymbol{K}$ in (58). Observe that this corresponds to the solution $\boldsymbol{P} = \boldsymbol{0}$ of the Riccati equation.

A more standard solution is given by the following result:

Proposition 4 *For a given stabilizing feedback* $\boldsymbol{K}$ *there exists a feedback law* $\boldsymbol{u} = \boldsymbol{K}\boldsymbol{x}$ *and an extended matrix*

$$\boldsymbol{W} = \begin{bmatrix} \boldsymbol{W}_{\mathrm{x}} & \boldsymbol{W}_{\mathrm{ux}} \\ \boldsymbol{W}_{\mathrm{ux}}^{\mathrm{T}} & \boldsymbol{W}_{\mathrm{u}} \end{bmatrix} > 0 \tag{75}$$

such that

$$\int_0^{\infty} [\boldsymbol{x}^{\mathrm{T}} \boldsymbol{u}^{\mathrm{T}}] \begin{bmatrix} \boldsymbol{W}_{\mathrm{x}} & \boldsymbol{W}_{\mathrm{ux}} \\ \boldsymbol{W}_{\mathrm{ux}}^{\mathrm{T}} & \boldsymbol{W}_{\mathrm{u}} \end{bmatrix} \begin{bmatrix} \boldsymbol{x} \\ \boldsymbol{u} \end{bmatrix} \mathrm{d}t \rightarrow \min_{\boldsymbol{K} \in \boldsymbol{K}_s \mathrm{tab}} \tag{76}$$

if

$$\|\boldsymbol{W}_{\mathrm{u}}\| > \frac{\|\boldsymbol{B}^{\mathrm{T}}\boldsymbol{P}\|}{2\|\boldsymbol{P}(\boldsymbol{A} + \boldsymbol{B}\boldsymbol{K})\|} \tag{77}$$

where $\boldsymbol{P} = \boldsymbol{P}^{\mathrm{T}} > 0$ *satisfies the Lyapunov equation*

$$\boldsymbol{P}(\boldsymbol{A} + \boldsymbol{B}\boldsymbol{K}) + (\boldsymbol{A} + \boldsymbol{B}\boldsymbol{K})^{\mathrm{T}} \boldsymbol{P} < 0 \tag{78}$$

Then

$$\boldsymbol{W}_{\mathrm{x}} = -\boldsymbol{P}(\boldsymbol{A}+\boldsymbol{B}\boldsymbol{K}) - (\boldsymbol{A}+\boldsymbol{B}\boldsymbol{K})^{\mathrm{T}}\boldsymbol{P} + \boldsymbol{K}^{\mathrm{T}}\boldsymbol{W}_{\mathrm{u}}\boldsymbol{K} + \boldsymbol{K}^{\mathrm{T}}\boldsymbol{B}^{\mathrm{T}}\boldsymbol{P} + \boldsymbol{P}\boldsymbol{B}\boldsymbol{K} \tag{79}$$

$$\boldsymbol{W}_{\mathrm{ux}} = -(\boldsymbol{B}^{\mathrm{T}}\boldsymbol{P} + \boldsymbol{W}_{\mathrm{u}}\boldsymbol{K}) \tag{80}$$

Example 4

Consider the *Example 3* again. Let

$$\dot{x} = -2x + u$$

and apply the state feedback $k = 1$. The closed loop system $\dot{\bar{x}} = -1\bar{x} + u$ becomes stable and "slower". It can be shown that this $k = 1$ is optimal for the *LQR* performance index

$$\int_0^{\infty} \left(5x^2 - 4xu + u^2\right)\mathrm{d}t \tag{81}$$

Indeed, using the Riccati-equation with

$$\boldsymbol{A} = A = a = -2 \qquad \boldsymbol{B} = B = b = 1 \qquad \boldsymbol{W}_{\mathrm{x}} = W_{\mathrm{x}} = w_{\mathrm{x}} = 5$$
$$\boldsymbol{W}_{\mathrm{ux}} = W_{\mathrm{ux}} = w_{\mathrm{ux}} = -2 \qquad \boldsymbol{W}_{\mathrm{u}} = W_{\mathrm{u}} = w_{\mathrm{u}} = 1$$

and

$$-4p^2 - (p-2)^2 + 5 = 0$$

and choosing the positive solution $p = 1$, the state feedback is given by

$$k = -w_{\mathrm{u}}^{-1}(bp + w_{\mathrm{ux}}) = -(1-2) = 1$$

and the closed loop matrix $\bar{\boldsymbol{A}} = \bar{A} = \bar{a} = a + bk = -2 + 1 = -1$ as required, i.e., $p_1 = -r_1 = -1$. So the closed-loop is slower-

This result was obtained by using the method in Proposition 4. Pick any $p > 0$ such that it is a solution of the Lyapunov equation $2p(a+bk) < 0$. Since $\bar{a} = a + bk = -1$ and $2p(-1) < 0$ for all $p > 0$, one can choose $p = 1$ and compute

$$w_{\mathrm{u,min}} = \frac{(bp)^2}{2p|\bar{a}|} = \frac{1}{2}$$

Choose any $w_{\mathrm{u}} > w_{\mathrm{u,min}}$, e.g., let $w_{\mathrm{u}} = 1$, then $w_{\mathrm{x}} = 2 + 1 + 2 = 5$ and $w_{\mathrm{ux}} = -(1+1) = -2$. Notice that this solution is not unique, any $W_{\mathrm{u}} = w_{\mathrm{u}} \geq 1$ would do, e.g., $w_{\mathrm{u}} = 2$ results in $w_{\mathrm{x}} = 10$, $w_{\mathrm{ux}} = -4$.

7. Conclusions

The paper presents the specific historical comparison of the relationships between the classical quadratic integral criterion, the pole-placement state feedback, the algebraic Riccati equation based *LQR* paradigm and Kalman's frequency domain approach.

Then two low order examples are shown how the obtained quadratic polynomial equation can be used. It is shown that arbitrary pole placement is not possible by standard classical *LQ* optimality by choosing only $\boldsymbol{W}_{\mathrm{x}}$, $\boldsymbol{W}_{\mathrm{u}}$ weights. For a second order case the unreachable domains are graphically demonstrated.

The *MIMO LTI* case is discussed next with more general *LQR* criterion which penalizes the interaction between the state and input variables. In this framework it is possible to obtain *LQR* solutions for the whole parameter space, but the design of the crossterm weight $\boldsymbol{W}_{\mathrm{ux}}$ is necessary, too. The uniqueness of the proposed solution is not guaranteed.

Acknowledgement

This work was supported in part by the Control Engineering Research Group of the HAS, at the Budapest University of Technology and Economics and by the project TAMOP 4.2.2.A-11/1/KONV-2012-2012, at the Széchenyi University of Győr.

References

[1] Rekasius, Z.V.: *A general performance index for analytica of control systems*, *IRE Transactions on Automatic Control*, p. 217, 1960

[2] Feldbaum, A.A.: *Theoretical foundations of automatic systems* (in Russian), State Publishing House in Physics and Mathematics, Moscow, 1960

[3] Csáki, F.: *State-space methods for control systems,* Akadémiai Kiadó, Budapest, 1978

[4] Kailath, T.: *Linear systems,* Prentice Hall, 1980

[5] Grimble, M.J., Kucera, V.: *Polynomial methods for control systems design*, Springer, Berlin, 1996

[6] Åström, K.J.: *Control system design,* Lecture Notes, University of California, Santa Barbara, 2002

[7] Bányász, Cs., Keviczky, L.: *State-feedback solutions via transfer function representations*, Journal of Systems Science, vol. 30, no. 2, pp. 21-34, 2004

[8] Keviczky, L., Bányász, Cs.*: Model error properties of observer-based state-feedback controller*, 6. Int. Conf. System identification and control problems SICPRO'07, Moscow, Russia, pp. 879-888, 2007

[9] Anderson, B.D.O., Moore, J.B.: *Optimal control, Linear Quadratic Methods,* Prentice-Hall, 1989

[10] Casti, J.: *The linear-quadratic control problem: some recent results and outstanding problems*, SIAM Review, vol. 22, no. 4, pp. 459-485, 1980

[11] Cigler, J., Kucera, V.: *Pole-by-Pole shifting via a linear-quadratic regulation*, 17th Int. Conf. on Process Control, Strbske Pleso, Slovakia, pp. 1-9, 2009

[12] Gattami, A., Rantzer, A.: *Linear quadratic performance criteria for cascade control,* Conf. on Decision and Control and European Control Conference CDC-ECC'05, pp. 3632-3637, 2005

[13] Jameson, A.: *Inverse problem of linear optimal control*, SIAM Journal on Control. vol. 11, no. 1, pp. 1-19, 1973

[14] Medanic, J., Tharp, H.S., Perkins, W.R.: *Pole placement by performance criterion modification*, IEEE Trans. on Aut. Control, vol. 33, no. 5, pp. 469-472, 1988

[15] Mehdi, D., Hamid, Al M., Perrin, F.: *Robustness and optimality of linear quadratic controller for uncertain systems*, Automatica, vol. 32, no. 7, pp. 1081-1083, 1996

[16] Molinari, B.: *The stable regulator problem and its inverse,* IEEE Trans. on Aut. Control, vol. 18, no. 5, pp. 454-459, 1973

[17] Willems, J.*: Least squares stationary optimal control and the algebraic Riccati equation*, IEEE Trans. on Aut. Control, vol. 16, no. 6, pp. 621-634, 2003

[18] Yao, D., Zhang, S., Zhou, X.: *LQ control via semi-definite programming*, 38th IEEE Conference on Decision and Control CDC99, pp. 1027-1032, 1999

[19] Sugimoto, K.: *Partial pole placement by LQ regulators: an inverse problem approach*, IEEE Trans. on Aut. Control, vol. 43, no. 5, pp. 706-708, 1998

[20] Alexandridis, A.T., Galanos, G.D.: *Optimal pole-placement for linear multi-input controllable systems*, IEEE Trans. Circuits Syst., vol. CAS-34, pp. 1602-1604, 1987

[21] Alexandridis, A.T.: *Algorithm for the design of state feedback controllers by optimal eigenstructure assignment*, Proc. ECC European Control Conference, vol. 4b, pp. 3365-3369, 1995

[22] Iracleous, D.P., Alexandridis, A.T.: *A simple solution to the optimal eigenvalue assignment problem*, IEEE Trans. on Aut. Control, vol. 44, no. 10, pp. 1746–1749, 1999

Plug and Play Design in the Electric Vehicle Systems

P. Gáspár, L. Keviczky, Z. Szabó

Széchenyi István University, Győr
MTA SZTAKI, Systems and Control Laboratory
Kende u, 13-17, Budapest, Hungary
Phone: +36 1 279 6171
e-mail: szaboz@sztaki.hu

Abstract: The plug and play concept focuses on the design of complex control systems with multiple functional building blocks. Each of the blocks fulfills certain specifications, is designed separately and might be delivered by different vendors. Concerning vehicle systems complexity is handled in the integrated design framework built around a supervisory architecture. This paper investigates the possibilities of the plug and play design built in the supervisory integrated control. The supervisory control makes decisions about the necessary interventions, guarantees coordination between components and meets performance specifications. The well-defined interfaces provide that the decisions are propagated between the supervisor and the local components. Therefore the interfaces between components have crucial roles. The concept of the plug and play design is presented and several design methods based on the weighting strategy in the closed-loop interconnection structure are proposed.

Keywords: electric vehicle, plug and play, robust control, qLPV design

1. Introduction

The demand for the integrated vehicle control methodologies including the driver, the vehicle and the road arises at several research centers and automotive suppliers, see, e.g., [6], [16]. The purpose of the integrated control is to combine and supervise all controllable subsystems affecting vehicle dynamic responses. In more details it means that multiple-objective performances from available actuators must be improved, sensors must be used in several control tasks, the number of independent control systems must be reduced and at the same time the flexibility of control systems must be enhanced, see e.g. [2], [4], [9].

A possible approach to the integrated control may be to set the design problem for the entire vehicle and include all the performance demands in a single specification. In the framework of available design techniques the formulation and successful solution of complex multi-objective control tasks are highly nontrivial. In the integration of various

control components, which operate only in some limited part of the overall operating regime of the plant, the multiple model approach is proposed.

Another approach to the integrated control is the supervisory decentralized control structure where the components are designed independently, see, e.g., [5], [15]. The role of the supervisor in the integrated control is to guarantee the coordination of the local controllers in order to meet global performance specifications, guarantee priority between controllers and reduce conflicts between them. The concepts of an agent and a multi-agent system is proposed by [12]. Conflicts between agents, which naturally arise in such systems due to the dependencies between the partial problems the agents solve, are handled by supervisory activities by adequately coordinating the agents.

The integrated control creates the possibility of the plug and play design, which is important in the industrial applications. In [11] the plug and play control concept is presented and a number of problems and solutions are proposed for the industrial requirements. In [13] a hierarchical control architecture applied to several complex dynamic systems is presented.

In this paper the concept of the plug and play design in connection with the integrated supervisory control is presented for vehicle systems. In the design of the integrated control the LPV (Linear Parameter Varying) methods play an important role. LPV methods are well elaborated and successfully applied to various industrial problems. Moreover, in LPV methods both performance specifications and model uncertainties are taken into consideration.

2. Concept of the supervisory integrated control

2.1. Architecture of the integrated control

The integrated control proposed in the paper is based on a supervisory decentralized control structure, which is illustrated in Figure 1. The supervisor is a high-level controller which is able to handle the effects of individual control components on vehicle dynamics. The advantage of this solution is that the components with their sensors and actuators can be designed by the suppliers independently.

The supervisor has information about the current operational mode of the vehicle, i.e., the various vehicle maneuvers or the different fault operations gathered from monitoring components. In addition it is able to make decisions about the necessary interventions into the vehicle components. The communication between the supervisor and the local control components is performed by using a CAN bus and a well-defined interface.

A local controller must meet the predefined performance specifications based on the measured signals. The main point of the proposed approach is that in the control design of the local components scheduling variables received from the supervisor are used as a key of the integration. The controller is able to modify or reconfigure its normal operations in order to focus on other performances instead of the actual performances. It is often able to detect different faults and can adapt to the dynamic properties of the faulty plant or changes in the environment. In this way the operation of a local controller can be extended to reconfigurable and fault-tolerant functions.

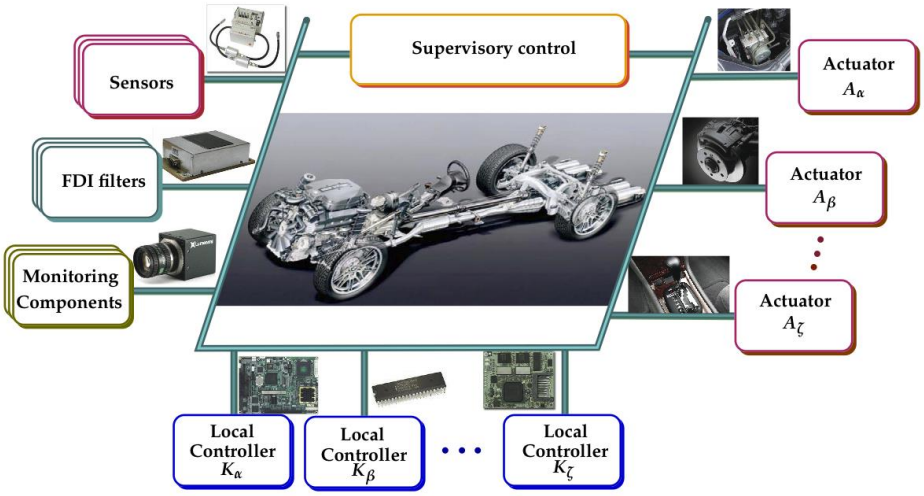

Figure 1. The supervisory decentralized architecture of integrated control

The solution of the problem is that the performance specifications are formalized in a parameter-dependent way in which this parameter depends on the monitoring and fault information. Moreover, the local controller sends messages about the changes to the supervisor and it receives messages from the supervisor about the special requirements. The local controllers often have a hierarchical structure, in which the high-level controller is distinguished from the low-level actuator.

2.2. LPV control of vehicle systems

In the decentralized architecture the signals are propagated between the supervisor and the local components through a well-defined encoded interface. This interface uses the monitoring signals as scheduling variables of the individual LPV controllers introduced to distinguish the performances that correspond to different operational modes. The advantage of this architecture is that local LPV controllers are designed independently provided that the monitoring signals are taken into consideration in the formalization of their performance specifications.

The design of a local controller is based on the standard closed-loop interconnection structure of the model $G(\rho)$, the compensator, and elements associated with the uncertainty models and performance objectives. A typical interconnection structure is shown in Figure 1.

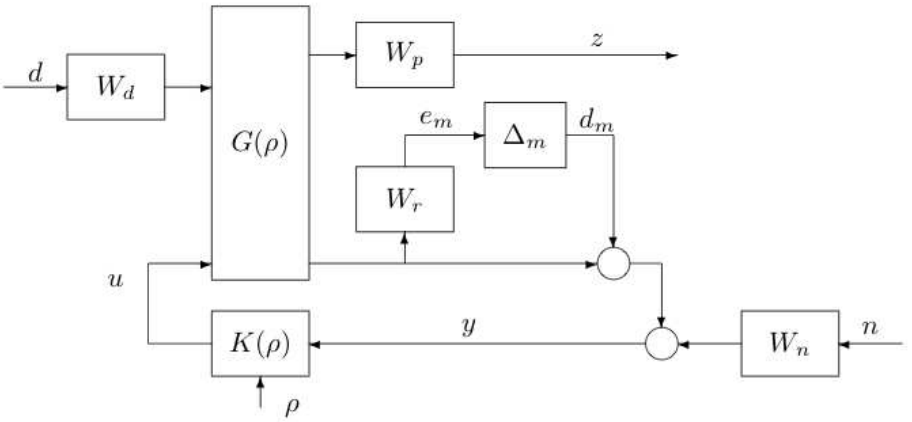

Figure 2. The closed-loop interconnection structure

In this framework performance requirements z are imposed by a suitable choice of the weighting functions W_p. Usually the purpose of weighting functions W_p is to define penalty functions, i.e., weights should be large where small signals are desired and small where large performance outputs can be tolerated. The proposed approach realizes the reconfiguration of the performance objectives by an appropriate scheduling of these weighting functions. The values of the monitoring signals are usually built into the weighting functions applied for performance requirements.

In the augmented plant the uncertainties, such as unmodelled dynamics and parameter uncertainty, are represented by a weighting function W_r and a block Δ_m. The transfer function Δ_m is assumed to be stable and unknown with the norm condition, $\|\Delta_m\|_\infty < 1$. It is assumed that the transfer function W_r is known, and it reflects the size of the uncertainty in the model. The purpose of the weighting functions W_d and W_n is to reflect the disturbance and sensor noises.

Finally, the control problem can be formulated in the general $P - K - \Delta$ structure, where P is the generalized plant and Δ contains both the uncertainties and the scheduling variables, see Figure 2.

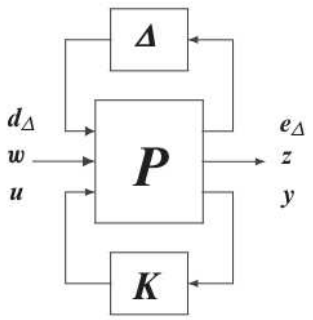

Figure 3: The $P - K - \Delta$ structure

In the design of local controllers the quadratic LPV performance problem is to choose the parameter-varying controller in such a way that the resulting closed-loop system is quadratically stable and the induced $\mathcal{L}_2$ norm from the disturbance and the performances is less than the value γ. The minimization task is the following:

$$\inf_{K} \sup_{\Delta} \sup_{\|w\|_2 \neq 0, w \in \mathcal{L}_2} \frac{\|z\|_2}{\|w\|_2}. \tag{1}$$

The existence of a controller that solves the quadratic LPV γ-performance problem can be expressed as the feasibility of a set of Linear Matrix Inequalities (LMIs), which can be solved numerically. Stability and performance are guaranteed by the design procedure, for details see [1], [10].

3. Plug and play design

3.1. Motivation of the plug and play design

In the decentralized supervisory control the concept of the plug and play method plays and important role. If a new control component is added, an old control is replaced by a new one, or an old component is removed, the structure of the system (or the control) changes. In these cases the conventional control should be redesigned, which is expensive and takes a long time. This is often not acceptable due to the cost associated with the control design procedure. In the supervisory control concept the supervisory logic must be modified on the highest level. The ultimate goal is to provide a design method for a plug and play control architecture, i.e., the possibility to use sensors and actuators provided by different vendors interchangeably on a core system by guaranteeing a performance level and leaving the global controller intact.

If a new component is added or an old one is replaced by a new one, the dynamics of the entire system may change. A possible way to model the effects of the different components is by using a monitoring signal with its operation range. Then controllers are designed at selected operation points within the range, and finally a family of controllers are implemented as a single controller. As a consequence, during the operation of the system the monitoring signal is used in order to select the appropriate control and adapt to the current operating conditions.

A possible solution of the plug and play design is to apply a set of controllers and the selection of the appropriate control is based on a switching method and monitoring signals. The operation range is divided into several grid points. Then controllers are designed for all the grid points and a finite set of controllers is constructed. The advantage of the solution is that the local controllers are always able to adapt to the new situations by using the monitoring signals.

The vehicle, however, has a large number of monitoring signals, which must be taken into consideration during the operation. There are a few examples. The changes of the adhesion coefficient influence road stability, it may also cause a μ split problem. The saturation of an actuator may cause the unstable operation of a control system. The performance degradation of an actuator leads to insufficient control actions. The fault operation of a sensor may result in the fault intervention of an actuator. As the number of the monitoring signals increases the number of controllers significantly increases.

The solution for the plug and play method proposed in the paper is based on a high-level supervisory control. It is a complex control, which includes monitoring components as additional scheduling variables. It leads to a special LPV structure, since some of the scheduling variables are constant during the operation. For example the fact of an actuator fault, the mass of the vehicle, the height of center of gravity or the actuator dynamics are fixed, thus scheduling variables must be selected constant during the operation.

In what follows this principle is illustrated for the vehicle dynamics example considered in the paper. Each of the actuators and sensors is listed and the weighting policy is presented.

3.2. Actuators

Bound limiter

The intervention of an actuator is related to its construction and operation limits. The construction limit must be taken into consideration all the time, e.g. the value of front-wheel steering must not exceed its upper bound $\delta_{\max}$. Brake control also has an operation limit M_{brmax}, which is related to the adhesion factor. The skidding is monitored by the estimation of the longitudinal slips κ.

In order to avoid reaching the steering limit, differential braking and the wheel camber angle must be increased. In order to avoid the skidding of tires, the value of differential braking must be reduced and other control inputs must be increased. Due to the redundancy of the action of different actuators for the same vehicle dynamics the integrated control framework makes it possible to handle this problem by reconfiguration.

Rate limiter

Usually, in the control design the control input of the actuators is assumed to be arbitrarily fast. However, if the bandwidth of the actuators or the signals is disregarded, the control signal does not meet the industrial requirements. Thus, the rate bound on the control input must be estimated and taken into consideration in the control design. In the design a gain is used as a scheduling variable in the weighting function which is applied for the control input. Then a rate bound on the scheduling variable is applied. In the LPV framework the solution leads to the application of the parameter dependent Lyapunov function (PDLF), see [14].

Balance between actuators

The actuator selection depends on several factors such as construction limits, energy requirement and the actuator dynamics. The maximal control input of the steering is determined by their physical construction limits, while in the case of the braking system the constraints are the tire-road adhesion conditions. It is necessary to avoid the skidding of tires, thus in such a case the generation of differential braking must be reduced. The skidding of tires can be monitored by the estimation of the longitudinal slips of the tires κ. These constraints must also be taken into consideration in the control design and must be guaranteed by the supervisor.

Moreover, the activation of the different components have an energy requirement. By using differential braking the velocity of the vehicle is reduced, which must be compensated for by the driveline with additional energy. Therefore the use of differential braking must be avoided during acceleration and front-wheel steering is preferred. During deceleration the brake is already being used, thus the lateral dynamics is handled by the braking for practical reasons. Thus differential braking is preferred, but close to the limit of skidding, front-wheel steering must also be generated.

According to the inertia of steering, the bandwidths of steering is lower than the bandwidth of differential braking. The fast operation of actuators is an important feature mainly at high velocities. At higher velocities it is recommended to use differential braking, while at lower velocities steering actuation is preferred for practical reasons. The weighting functions for the front wheel steering, brake yaw-moment and suspension moment are selected in the following form:

$$W_{act,\delta} = \rho_\delta / \delta_{max} \tag{2}$$

$$W_{act,Mbr} = \rho_{br} / M_{brmax} \tag{3}$$

respectively, where δ_{max} and γ_{max} are determined by the constructional maximum of the steering and the camber angle, while M_{brmax} is the maximum of the brake yaw-moment. Weighting factors ρ_{br}, ρ_δ are chosen to influence the priority of the actuators. Figure 4 shows the characteristics of the weighting factors.

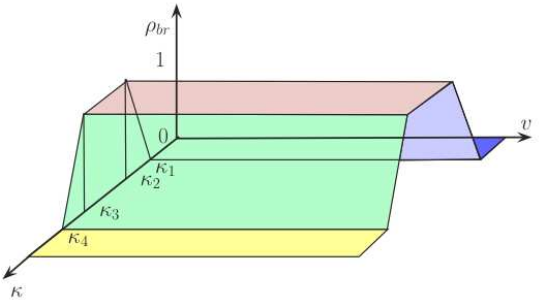

a. Parameter ρ_{st}

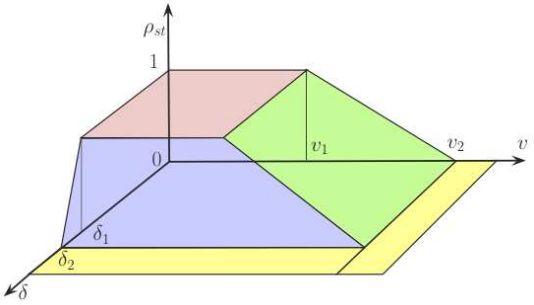

b. Parameter ρ_{br}

Figure 4: Selection of parameters ρ_{st} and ρ_{br}

When the vehicle is being driven the front wheel steering is actuated, which is determined by factor ρ_{st}, see Figure 4(a). The value is reduced between δ_1 and δ_2, which represents the constructional criterion of the steering system. When the brakes are being applied the tire longitudinal slip angle affects factor ρ_{br}, see Figure 4(b). In this interval differential braking is preferred for practical reasons. It requires an interval to reduce tire skidding and it also requires an interval to prevent chattering between steering and differential braking. Therefore four parameters are designed: κ_1 and κ_2 are used to prevent chattering between steering and braking and κ_3 and κ_4 are applied to prevent the skidding of tires. The weights also depend on the velocity of the vehicle. The effect of the velocity on the weighting factors is the consequence of the interaction between the bandwidth values of the actuators.

3.3. Sensors

The monitoring parameters are critical in the operation of the supervisor, thus in the cooperation of the local control systems. The more signals are used in the control of the entire vehicle the more accurately and safety the control systems can operate. In the following a few important monitoring signals are listed.

Tracking error

In the control design the purpose is to handle the tracking problem. In trajectory tracking the reference signal is the yaw rate defined by the steering angle of the driver $\dot{\psi}_{\mathrm{ref}}$, while the actual yaw rate is a measured signal $\dot{\psi}$. The performance signal is the tracking error, which is the difference between the actual yaw rate and the yaw rate command. The weighting function of the tracking error is selected as:

$$W_{z,e_{\dot{\psi}}} = \gamma_e \frac{T_{d1}s+1}{T_{d2}s+1}, \tag{4}$$

where T_{di} are time constants. Here, it is required that the steady state value of the tracking error should be below $1/\gamma_e$ in steady-state.

Roll dynamics

In order to reduce the chassis roll angle, the dynamic displacement of the height of the roll center $|\Delta h|$ is reduced. In this solution a signal h_{ref} is introduced and applied as a reference signal for the tracking task: $\Delta h_M = |h_{ref} - h_M|$, in which h_M is calculated from the measured γ according to the suspension geometry.

When the roll angle ϕ increases significantly, the variable-geometry suspension control must minimize the roll angle. This configuration is achieved by the selection $h_{ref} = h_{ref,max}$. Note that it is possible to achieve vehicle maneuvers in which there is a balance between two performances, i.e., the reduction of the half-track change and that of the roll angle. In these configurations h_{ref} is selected in an interval $h_M < h_{ref} < h_{ref,max}$. When the suspension system must focus on the trajectory tracking, i.e., in emergency maneuvers, the scheduling variable $\rho_{susp} = 1$ is selected, and the safety factor overrides the other performances. The selection of the variables h_{ref} is the following: $h_{ref} = h_M$ if $\phi \leq \phi_1$, $h_{ref} = (h_{ref,max} - h_M)(\phi - \phi_1)/(\phi_2 - \phi_1) + h_M$ if $\phi_1 \leq \phi \leq \phi_2$, otherwise $h_{ref} = h_{ref,max}$. where ϕ_1, ϕ_2 are design parameters. Note

that h_{ref} is also a supervisory variable, since in an emergency it is modified by the set of the scheduling variable $\rho_{susp} = 1$.

FDI sensors

The fault-tolerant control requires fault information in order to guarantee performances and modify its operation. At the level of local control design the reconfiguration is achieved by scheduling the performance weights by a signal ρ_κ related to the fault information and provided by a fault decision block. As a simple example, one might consider $\rho_\kappa = f_{act}/f_{max}$, where f_{act} is an estimation of the failure (output of the FDI filter) and f_{max} is an estimation of the maximum value of the potential failure (fatal error). The value of a possible fault is normalized into the interval $\rho_\kappa = [0, 1]$. The estimated value f_{act} represents the rate of the performance degradation of an active components.

The operation of the fault-tolerant control is based on two factors: the failure or performance degradation has already been detected and the fault information ρ_κ and the necessary intervention possibilities are built into its control design. Instead of a switching type controller reconfiguration the control structure changes due to a reconfiguration of the performance goal achieved by a scheduling of the performance weights. In order to achieve that, the signals of various fault scenarios provided by FDI filters are built in the performance specifications of the controller.

For example when performance degradation occurs in the operation of a brake circuit the brake yaw moment must be substituted for by using the steering and suspension to provide trajectory tracking. In addition, the effect of the degradation of the brake yaw moment is asymmetric. For example, in the case of a left-hand-side brake circuit fault in the rear the brake is not able to turn the vehicle anti-clockwise, therefore positive M_{br} is not allowed, i.e., $\rho_{br} = 0$. However, if $M_{br} < 0$ then $\rho_{br} > 0$. Consequently, if there is one fault in the brake system the weight of braking ρ_{br} depends on the sign of the desired brake yaw moment M_{br} and a gain $\rho_{\kappa,i}$. In the realization of the gain $\rho_{\kappa,i}$, either $\rho_{\kappa,left}$ or $\rho_{\kappa,right}$ must be set. The modification of ρ_{br} is based on the sign of the desired brake yaw moment and the parameters $\rho_{\kappa,i}$, i.e., $\rho_{br,new} = \rho_{\kappa,i}\rho_{br}$, where $\rho_{\kappa,i}$ is the scheduling parameter.

3.4. Uncertainties

In order to cope with the complexity problem integrated control design has already reduced the design task to subsystems and individual components. These elements are joined together by a correctly defined interface. This interface connects high level (virtual) signals to actuators and sensors. If a plug and play setting is considered on the connecting points the presence of an uncertainty, usually unmodelled dynamics, should be considered.

The properties of the assumed uncertainty set depend on the diversity of the possible devices that are allowed to be used for a given component. Thus, the specific task for the plug and play design is to specify these uncertainties by setting suitable weights at the given points. These uncertainty models are usually more complex those used in a baseline integrated control design.

The uncertainties of the model are caused by neglected components, unknown or little known parameters. The uncertainties are modelled by both unmodelled dynamics and parametric uncertainties. The estimation of the uncertain interval around its nominal value is important in the control design. If the uncertain interval is selected too large, the designed controller will be conservative. The unmodelled dynamics can be reduced by using a more accurate estimation of a component in the model. For example, if parametric uncertainties of mechanical components are known, the uncertainties for unmodelled dynamics can also be reduced.

As an example, in the suspension design uncertainties are usually modelled as a complex full block with multiplicative uncertainty at the plant input. The weighting function of the unmodelled dynamics is selected $W_{r,comp} = \rho_{g1}(T_{r1}s + 1)/(T_{r2}s + 1)$, with time constant T_{ri} in such a way that in the low frequency domain, uncertainties are about $\rho_{g1}(\%)$ and, in the upper frequency domain they are up to 100%. Parameters in the vertical vehicle model always contain uncertainties, which can be described by their nominal values and ranges of possible variations, e.g., the mass, the damping coefficient, the spring coefficient. If parametric uncertainties are built into the control design, the magnitude of the unmodelled dynamics may be reduced. In the latter case the uncertainty structure contains an uncertainty block, which represents the ignored actuator dynamics and real uncertainty blocks. Thus, it is possible to select the weighting function significantly smaller than in the previous case. It means that in the low frequency domain the modelling error is $\rho_{g2}(= \rho_{g1})$: $W_{r,mix} = \rho_{g2}(T_{r3}s + 1)(T_{r4}s + 1)$.

In addition to these uncertainties in the plug and play framework it is necessary to consider uncertainties related to the interfaces. As an example the high level suspension module produces forces as requested control inputs while the plug and play actuator module receives these forces as reference signals. During the specification on this interface proper weights are necessary in order to guarantee the interoperability. For the high level design the weight specifies a required performance that tells the high level controller to produce force requests compatible with the available actuators. Moreover, the dynamics of the actuator will not necessary be able to follow the requested force, thus an unmodelled dynamics should be modelled on the inputs side. On the actuator side the weight specifies the performance of the tracking problem in order to provide the requested actual forces.

4. Analysis of the entire system

The verification of the specification for the supervisor is a highly nontrivial task and can be performed in the same setting as for the baseline supervisory integrated design.

In order to provide a formal verification of the achieved control performance on a global level, the problem must be formulated globally. Only on this extended level are the performance variables which are relevant for the whole vehicle available. Once the local controllers have been designed, however, it is possible to perform an analysis step in the same robust control framework on a global level, for details see [3], [7]. Concerning the performance assessment the plug and play setting makes it necessary to use a robust LPV setting.

This is a highly computation-intensive procedure, that may be set, as an example, in the robust LPV framework [14], or in the integral quadratic framework [8]. Moreover the presence of competing multi-objective criteria deny the applicability of this global approach. E.g., in emergency events certain performance components gain absolute priority over others, thus requiring a given performance level for the ignored performance components is not justified. On the other hand the local design guarantees the prescribed performance level for the critical components. Therefore in practice the formal global verification is often omitted and the quality of the overall control scheme is assessed through simulation experiments.

The relationship between the supervisor and the local controllers guarantees that the system meets the specified performances. Applying parameter-dependent weighting a balance between different controllers is achieved. In different critical cases related to extreme maneuvers or performance degradations/faults in sensors or actuators the controllers reconfigure their operations. However, situations in which different critical performances must be achieved simultaneously may occur. These difficult situations are necessary to examine in different time domain scenarios using a simulation software.

For example in a high-speed cornering maneuver the risk of a rollover increases significantly. The performances are in contradiction: deviating from the lane might cause the vehicle to run off the road while increasing roll dynamics might lead to rollover. This maneuver requires an intensive cooperation between the steering and the brake control systems. The supervisor sends critical signals to the controllers and consequently these control systems are activated. However, in order to reduce the rollover risk the yaw signals are modified and consequently, the deviation from the predefined path may increase. In contrast reducing the deviation from the path might increase the rollover risk. Since both interventions are critical the supervisor is not able to resolve the problem entirely, thus the performances are handled by the actuators with performance degradation.

5. Conclusion

In the paper the principles of the plug and play design in connection with the supervisory integrated control system have been presented. The relationship between the supervisor and the local plug and play controllers is ensured by a proper parameter dependent weighting strategy that guarantees that the system meets the specified performances. The weighting strategy leads to a complex control task, which includes different types of monitoring components as additional scheduling variables in the LPV design. Concerning actuators, sensors, functions and uncertainties the proposed method is illustrated through several examples based on the weighting strategy in the closed-loop interconnection structure.

Acknowledgment

The research has been conducted as part of the project TÁMOP-4.2.2.A-11/1/KONV-2012-0012: Basic research for the development of hybrid and electric vehicles. The Project is supported by the Hungarian Government and co-financed by the European Social Fund.

References

[1] Bokor, J., Balas, G.: *Linear parameter varying systems: A geometric theory and applications*, 16th IFAC World Congress, vol. 6. part 1. Prague, 2005

[2] Burgio, G., Zegelaar, P: *Integrated vehicle control using steering and brakes*, International Journal of Control, vol. 79, pp. 534-541, 2006

[3] D'Andrea, R., Dullerud, G.E.: *Distributed control design for spatially interconnected systems*, IEEE Transactions on Automatic Control, vol. 48, no. 9, pp. 1478-1495, 2003

[4] Gordon,T., Howell, M., Brandao, F.: *Integrated control methodologies for road vehicles*, Vehicle System Dynamics, vol. 40, pp. 157-190, 2003

[5] Gáspár, P., Szabó, Z., Bokor, J.: *LPV design of reconfigurable and integrated control for road vehicles,* 50th IEEE Conference on Decision and control, Orlando, pp. 2505-2510, 2011

[6] He, J., Crolla, D.A., Levesley, M.C., Manning, W.J.: *Coordination of active steering, driveline, and braking for integrated vehicle dynamics control*. Proceedings of the Institution of Mechanical Engineers Part D Journal of Automobile Engineering, pp. 1401-1421, 2006

[7] Langbort, C., Chandra, R.S., D'Andrea, R.: *Distributed control design for systems interconnected over an arbitrary graph*, IEEE Transactions on Automatic Control, vol. 49, no. 9, pp. 1502-1519, 2004

[8] Megretski, A., Rantzer, A.: *System analysis via integral quadratic constraints*, IEEE Transactions on Automatic Control, vol. 42, no. 6, pp. 819-829, 1997

[9] Poussot-Vassal, C., Sename, O., Dugard, L., Savaresi, S.M.: *Vehicle dynamic stability improvements through gain-scheduled steering and braking control*, Vehicle Systems Dynamics, vol. 49, no. 10, pp. 1597-1621, 2011

[10] Scherer, C.W.: *LPV control and full block multipliers*, Automatica, vol. 27, no. 3, pp. 325-485, 2001

[11] Stoustrup, J.: *Plug and play control: Control technology towards new challenges,* European Journal of Control, vol. 15, no. 3, pp. 311-330, 2009

[12] Wang, J., Xin, M.: *Multi-agent consensus algorithm with obstacle avoidance via optimal control approach*, International Journal of Control, vol. 83, no. 12, pp. 2606-2621, 2010

[13] Wills, L., Kannan, S., Sander, S., Guler, M.: *An open platform for reconfigurable control*, IEEE Control Systems Magazine, pp. 49-64, 2001

[14] Wu, F., Yang, X.H., Packard, A., Becker, G.: *Induced L_2 norm controller for LPV systems with bounded parameter variation rates,* Journal of Robust and Nonlinear Control, vol. 6, pp. 983-988, 1996

[15] Xiao, H.S., Chen, W.W., Zhou, H.H., Zu, J.W.: *Integrated control of active suspension system and electronic stability programme using hierarchical control strategy: theory and experiment*, Vehicle System Dynamics, vol. 49, pp. 381-397, 2011

[16] Yu, F., Li, D.F., Crolla, D.A.: *Integrated vehicle dynamics control: State-of-the art review*, IEEE Vehicle Power and Propulsion Conference, Harbin, China, pp. 1-6, 2008

A control-oriented qLPV modeling framework

Z. Szabó, P. Gáspár, L. Keviczky

Széchenyi István University, Győr
MTA SZTAKI, Systems and Control Laboratory
Kende u, 13-17, Budapest, Hungary
Phone: +36 1 279 6171
e-mail:szaboz@sztaki.hu

Abstract: This paper proposes a framework for selecting affinely parametrized quasi Linear Parameter Varying (qLPV) model structures that facilitates solutions to specific control design tasks encountered in vehicle dynamics applications. Moreover it facilitates the selection of the scheduling variables and provides a framework to decide whether the controller performance can be improved by introducing some estimated parameters as scheduling variables, i.e., if some adaptive strategy is needed or not. The proposed scheme is an iterative process: in every step a suitable model transformation is applied to generate a finite element convex polytopic representation in order to obtain a qLPV model. Then the LMI feasibility of a robust control objective is verified, which is closely related to the original control task. This step provides a selection criterion that sorts out the suitable models from a finite set of model candidates generated by the iterative method.

Keywords: electric vehicle, nonlinear modelling, robust control, qLPV design

1. Introduction and motivation

In a control design problem a control law must be designed for a not entirely known system in order to reach given performance specifications. For a successful analysis and design, it is crucial to obtain a model that captures the essential behaviors of the system under consideration.

In modern control design the approximation of nonlinear models with linear models is often based on a qLPV description. This approach is based on the possibility of rewriting the plant in a form in which nonlinear terms can be hidden by using suitably defined scheduling variables by maintaining the linear structure of the model. An advantage of qLPV models is that in the entire operational interval nonlinear systems can be defined and a well-developed linear system theory to analyze and design nonlinear control system can be used.

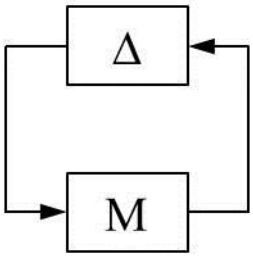

Figure 1. General feedback configuration

The models are augmented with performance specifications and uncertainties. Weighting functions are applied to the performance signals to meet performance specifications and guarantee a tradeoff between performances. The uncertainties are modelled by both unmodelled dynamics and parametric uncertainties. As a result of this construction a Linear Fractional Transformation (LFT) interconnection structure, which is the basis of control design, is achieved, see Figure 1.

These representations provide a particular structure to the LPV system, also known as a $M - \Delta$ configuration, whereby the parameter-varying, uncertain or nonlinear terms are located in the diagonal Δ operator and the time invariant part is described by the operator M. An LFT based model set is widely considered to be the most general representation adopted in robust controller design.

It is apparent that there is a great amount of analogy between classical adaptive schemes and the qLPV design philosophy, see [1], [2]. The parameters that are estimated during operational time and which are used to tune the actual controller in an adaptive scheme play the same role as the scheduling variables in the qLPV context. From this latter perspective the difference consists in the acquisition of the scheduling variable, namely, in the adaptive case the values of the scheduling variable are not directly available by the measurement and need to be obtained by a specific estimation process based on the directly available data. This observation leads us to propose a unified view of both control design strategies cast in the qLPV design framework by extending the set of scheduling variables with parameters that might not be directly measured but estimated using a suitable designed procedure. The idea was tested through certain applications, see [3].

The solution to the LPV control synthesis problem is formulated as a parameter dependent LMI optimization problem, i.e. a convex problem for which efficient optimization techniques are available. This control structure is applicable whenever the value of parameter is available in real-time. The resulting controller is time-varying and smoothly scheduled by the values of the scheduling variables. Therefore qLPV models with Linear Matrix Inequalities (LMI), as the main design tool, seem to be the most efficient approach to achieve robust and non-conservative results.

Besides the weighting functions (performance and uncertainty weights) the model structure itself -- which is not unique -- influences decisively the success of the design and control quality. Concerning the latter the role of the uncertainty structure

(modeling) is well known. It is less understood that in the LFT framework the choice of the scheduling variables affects the model in the same way as the uncertainties, moreover for a given model their choice is also non-unique, in general. The aim of this paper is to provide a systematic framework in which the search for a suitable model- concerning both uncertainty and scheduling variable structure- for a given control task can be performed.

1.1. The proposed modeling framework

The starting point is a (nominal) model

$$\begin{pmatrix} \dot{x} \\ z \\ y \end{pmatrix} = S(\theta, \pi) \begin{pmatrix} x \\ d \\ u \end{pmatrix} \tag{1}$$

where z is the performance vector, θ contains the measured variables, i.e., components/functions of y and some measured/estimated parameters, u is the control input, while d is the disturbance vector. The set of uncertain parameters is denoted by π.

The goal is to give a description of the type

$$\mathrm{S}(\theta, \pi) = \mathrm{S}_0 + \sum_{\mathrm{i} \in \mathrm{I}} \rho_{\mathrm{i}}(\theta)\delta_{\mathrm{j}}(\pi)\mathrm{S}_{\mathrm{i,j}} \tag{2}$$

of the system which facilitates the control design task as much as possible where ρ_i will be the scheduling variables of the design while δ_j will catch the effect of the parametric uncertainties.

Robust control is handled based on the feedback connection depicted on Figure 0 and the associated well-posedness theorem, for details see [5]:

Theorem 1 *Let a subset* $\nabla \in \mathbb{C}^{k \times l}$ *and a matrix* $M \in \mathbb{R}^{l \times k}$ *be given. The following statements are equivalent:*

1. the feedback system on Figure 0 is well-posed, i.e., $det(I - \Delta M) \neq 0$ for all $\Delta \in \nabla$
2. there exist a symmetric matrix $P \in \mathbb{R}^{(k+l)\times(k+l)}$ such that

$$\begin{pmatrix} \mathrm{I} & \mathrm{M} \end{pmatrix} \mathrm{P} \begin{pmatrix} \mathrm{I} \\ \mathrm{M}^{\mathrm{T}} \end{pmatrix} < 0, \tag{3}$$

$$\begin{pmatrix} \Delta & \mathrm{I} \end{pmatrix} \mathrm{P} \begin{pmatrix} \Delta^* \\ \mathrm{I} \end{pmatrix} \geq 0 \quad \forall \Delta \in \nabla. \tag{4}$$

The constraint set in (4) is convex, however, it is usually not easily dealt with, since represents an infinity number of conditions. One way to overcome this difficulty is to approximate the exact set by a tractable one. By choosing appropriate inner/outer approximations one may develop computable lower/upper bounds for certain performances, e.g., stability margins.

As a possible solution, a uniformly and automatically executable Tensor Product (TP) model transformation method based on the recently developed Higher Order Singular Value Decomposition (HOSVD) concept has been proposed, see [7], [6]. The

TP model transformation offers uniform, tractable and readily executable numerical ways and creative manipulations to generate convex (polytopic) representations of LPV models upon which LMI-based design techniques are immediately executable. The result of the TP model transformation is a TP model that belongs to the class of polytopic models, where the parameter-dependent weightings of the vertex systems are one-dimensional functions of the elements of the parameter vector.

This form offers a relatively simple way to describe various convex hull generations in terms of matrix operations. The obtained structures are not unique, however the framework provides an efficient background to introduce a set of rules, heuristics and algorithms that provide us with a set of candidate model structures on which further analysis and final model selection can be carried out.

The selection criteria in the proposed framework can be tailored according to the given control task. The idea is to set an LMI feasibility problem related to a control-relevant task, e.g., robust stability with state feedback, robust performance with state feedback, etc., while solvability and the level of the achieved performances (if applicable) will provide the desired selection method.

The proposed framework facilitates the execution of the following program:

- build an qLPV model of the type (2),
- put the given model in the LFT form, e.g.,

$$\mathrm{S}(\theta,\pi) = \mathrm{S}_{1,1} + \mathrm{S}_{12}\Delta(\mathbb{I} - \mathrm{S}_{2,2}\Delta)^{-1}\mathrm{S}_{21} \tag{5}$$

where $\Delta = \begin{bmatrix} diag(\delta_i) & 0 \\ 0 & diag(\rho_j) \end{bmatrix}$ and $S_{i,j}$ are constant matrices,

- solve an LMI feasibility problem related to the control task,
- evaluate the results.

In order to make the method reliable the framework must provide efficient numerical techniques to perform each step. The aim of the paper is to propose such a framework.

The layout of the paper is the following: in Section 2 a brief description of the TP method is given. Section 3 gives details how the LMI problems suitable for the desired selection can be set. In Section 4 an example is provided to illustrate the proposed method. Finally, Section 5 contains some concluding remarks and future directions.

2. Tensor Product (TP) transformation for qLPV modeling

Tensor Product (TP) modeling, in broad sense, is an approximation technique where the approximating functions are in a tensor product form. The motivation is straightforward: one dimensional functions are much easier to calculate with, handle and visualize. A family of methods use tensor products of continuous univariate basis functions, e.g., non-uniform rational B-splines.

Consider a parameter-varying state-space model with input $\mathrm{u(t)}$, output $\mathrm{y(t)}$ and state vector $\mathrm{x(t)}$

$$\begin{bmatrix}\dot{\mathrm{x}}(\mathrm{t})\\ \mathrm{y}(\mathrm{t})\end{bmatrix} = \mathrm{S}(\mathrm{q}(\mathrm{t}))\begin{bmatrix}\mathrm{x}(\mathrm{t})\\ \mathrm{u}(\mathrm{t})\end{bmatrix} \tag{6}$$

with the parameter-varying system matrix

$$\mathrm{S}(\mathrm{q}(\mathrm{t})) = \begin{pmatrix}\mathrm{A}(\mathrm{q}(\mathrm{t})) & \mathrm{B}(\mathrm{q}(\mathrm{t}))\\ \mathrm{C}(\mathrm{q}(\mathrm{t})) & \mathrm{D}(\mathrm{q}(\mathrm{t}))\end{pmatrix}. \tag{7}$$

The time varying N-dimensional parameter vector $\mathbf{q}(t) \in \Omega$ is an element of the closed hypercube $\Omega = [a_1, b_1] \times [a_2, b_2] \times \cdots \times [a_N, b_N] \subset \mathbb{R}^N$.

For practical reasons a finite element TP modeling is applied which uses a tensor defined by the values of $\mathbf{S}(\mathbf{q}(t))$ on a suitable discretization of Ω (usually a grid), i.e., a piecewise linear approximation of the multivariate map $\mathbf{S}(\mathbf{q}(t))$. Based on this data TP model transformation generates the HOSVD-based canonical form of LPV models [8], i.e.,

$$\begin{pmatrix}\dot{\mathrm{x}}(\mathrm{t})\\ \mathrm{y}(\mathrm{t})\end{pmatrix} = (\mathcal{S} \bigotimes_{\mathrm{n}=1}^{\mathrm{N}} \mathrm{w}_{\mathrm{n}}(\mathrm{q}_{\mathrm{n}}(\mathrm{t})))\begin{pmatrix}\mathrm{x}(\mathrm{t})\\ \mathrm{u}(\mathrm{t})\end{pmatrix}. \tag{8}$$

$\bigotimes_i$ denotes the i-mode tensor product as defined in [7]. For further details we refer to [6], [9].

This procedure extracts the unique structure of a given LPV model in the same sense as the HOSVD does for tensors and matrices, in a way such that:

- the number of LTI components are minimized;
- the weighting functions are univariate functions of the parameter vector in an orthonormed system for each parameter;
- the LTI systems are also in orthogonal position;
- the LTI systems and the weighting functions are ordered according to the higher-order singular values of the parameter vector.

Based on the higher-order singular values (that express the rank properties of the given model for each element of the parameter vector in L_2 norm), the TP model transformation offers a trade-off between the complexity of further design and the accuracy of the resulting TP model.

One of the advantages of the TP model transformation is that it can be executed uniformly (irrespective of whether the model is given in the form of analytical equations resulting from physical considerations, or as an outcome of soft computing based identification techniques such as neural networks or fuzzy logic based methods, or as a result of a black-box identification), without analytical interaction, within a reasonable amount of time. The obtained structure can be directly used for an LFT type modeling without any further preprocessing step.

Consider the map defined by the ordering $(i_1, \dots i_N) \rightarrow \mathbf{r}$ in the multi base number system defined by $(I_1, I_2, \dots, I_N)$. According to this indexing the weighting functions are denoted by

$$\mathrm{w_r(q(t)) = \prod_k w_{k,i_k}(q_k(t)) \in [0,1]},$$

where $w_{k,j}(q_k(t)) \in [0,1]$ is the j-th one variable weighting function defined on the k-th dimension of Ω, while the corresponding *vertex systems* are $\mathbf{S_r} = \mathbf{S}_{i_1,i_2,\dots,i_N}$. Using this index transformation one can write the TP model in the typical polytopic form:

$$\mathrm{S(q(t)) = \sum_{r=1}^{R} w_r(q(t))S_r}. \tag{9}$$

Remark: Having $q(t) = [\theta(t), \pi]$ and the functions w_{n,i_n} are univariate the further splitting of the sum, i.e., $w_{\mathbf{r}}(q(t)) = \rho(\theta)_{\mathbf{r}}\delta(\pi)_{\mathbf{r}}$ is straightforward.

2.1. Multi-affine models

In many cases the convexity of the resulting TP model is required. The convex hull of $S(q)$ might not be polytopic, however for design purposes a finite, polytopic (outer) approximation is needed. Convexity is ensured by the following conditions:

$$\mathrm{\forall n \in [1,N], i, q_n(t): w_{n,i}(q_n(t)) \in [0,1]}; \tag{10}$$

$$\mathrm{\forall n \in [1,N], q_n(t): \sum_{i=1}^{I_n} w_{n,i}(q_n(t)) = 1}. \tag{11}$$

These conditions ensure that $\mathbf{S}(\mathbf{q}(t))$ is within the convex hull of the LTI vertex systems $\mathbf{S}_r$ for any $\mathbf{q}(t) \in \Omega$.

One of the main advantages of the TP model transformation is that we can find the convex representation via numerical matrix operations instead of analytical interactions. This approximation is highly nonunique and the TP approach provides a systematic approach in which different convex descriptions can be built. The TP model transformation was extended to generate different types of convex polytopic models, [10]. The generated convex hull of the polytopic models considerably influences the feasibility of the LMI-based design and the resulting performance level.

There are many ways to define the vertex systems and the type of the convex hull determined by the vertex system can be defined by the weighting functions. The applications of TP models specifies special requirements for the weighting functions.

For illustration purposes consider $\mathrm{S(q) = [q - q^2 \quad 2q]}$ where $\mathrm{q \in [-3,3]}$. In Figure 1 one can see the systems $\mathcal{S} = \mathrm{S(q)}$ (in blue). The dotted red lines depicts the directions given by the HOSVD while in green is depicted the smallest box that contains the convex hull $\tilde{\mathcal{S}}$ of $\mathcal{S}$. Another convex hull is depicted in magenta, that corresponds to a TP model. The corresponding weights are depicted in Figure 2.

It is worth noting that both the TP model transformation and the LMI-based control design methods are numerically executable one after the other, and this makes the resolution of a wide class of problems possible in a straightforward and tractable, numerical way.

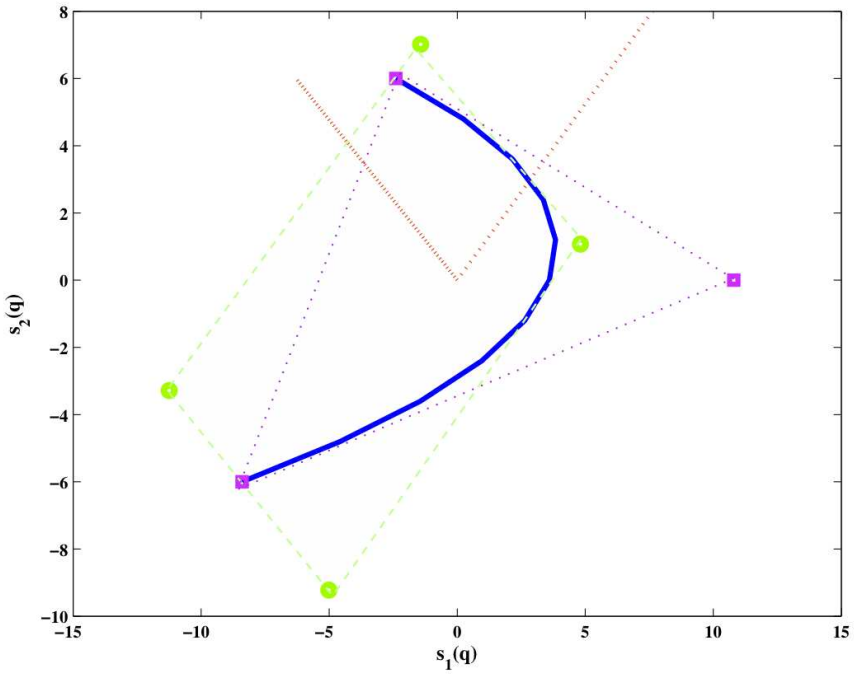

Figure 2. Different convex approximations

3. Setting LMI feasibility problems

Modern control design strategies strongly use LMI techniques. The variety of the control tasks affect the complexity of the resulting algorithms. For the purposes of this paper robust control objectives that lead to efficiently solvable LMI feasibility problems are to be selected.

Since output feedback control objectives often lead to non--convex bilinear matrix inequalities (BMI), which have computationally hard solution algorithms, this class of problems are not suitable candidates for a selection criteria. State feedback problems, however, usually lead to LMI feasibility problems, which can be solved more efficiently.

The easiest control objective is to stabilize the system. Let us recall that an LPV system is quadratically stable if $A(\rho)P + PA^T(\rho) < 0$ is fulfilled with a $P = P^T > 0$ matrix for all the parameters $\rho \in \mathcal{P}$. A necessary and sufficient condition for a system to be quadratically stable is that this condition holds for all the corner points of the parameter space, i.e., one can obtain a finite system of LMIs that must be fulfilled for $A(\rho)$ with a suitable positive definite matrix P, see [11], [12].

It follows that for the closed--loop system, i.e, for the matrices $A_c(\delta, \rho) = A(\delta, \rho) + B(\delta, \rho)K(\rho)$ the matrix inequality $A_c^T(\rho)P + PA_c(\rho) < 0$ must hold for suitable $K(\rho)$ and $P = P^T > 0$. By introducing the auxiliary variable $L(\rho) = PK(\rho)$, one can reduce the problem to a set of LMIs that must be solved at the corner points of the parameter

space. This method makes possible to handle in a fairly straightforward way the parameter dependent feedback situation. However the method may lead to big LMI feasibility problems. This drawback can be eliminated by using relaxation techniques, e.g., for details see [13].

The drawback of using merely stabilizability as a selection criterion is that there is no direct information provided about the performance of the controller since there is no explicit performance criteria formulated in the problem. By doing simulations on relevant test scenarios, however, the different controllers, hence the different models, can be evaluated.

Fortunately, problems that contain meaningful performance specifications can be formulated in terms of LMI feasibility conditions. These problems can be set for systems of generalized LFT type:

$$\begin{pmatrix} \dot{x}(t) \\ z_u(t) \\ z_p(t) \\ y(t) \end{pmatrix} = \begin{pmatrix} A & B_u & B_p & B \\ C_u & D_{uu} & D_{up} & E_u \\ C_p & D_{pu} & D_{pp} & E_p \\ C & F_u & F_p & 0 \end{pmatrix} \begin{pmatrix} x(t) \\ w_u(t) \\ w_p(t) \\ u(t) \end{pmatrix}$$

$$\begin{pmatrix} w_u(t) \\ z_u(t) \end{pmatrix} \in \mathcal{S}(\Delta(t)) \subset \mathbb{R}^{m_u+k_u} \tag{12}$$

with the time-varying parameters satisfying $\Delta(t) \in \nabla$. It is assumed that $\mathcal{S}(\Delta)$ admits the explicit description $\mathcal{S}(\Delta) = Im(\mathbf{S}(\Delta))$ with a continuous matrix function $\mathbf{S}(\Delta)$ of full column rank. Furthermore, we suppose that (12) is well-posed, and that there exists a nominal value $\Delta_0 \in \nabla$ for which $Im\begin{pmatrix} 0 \\ I_{k_u} \end{pmatrix} \in \mathcal{S}(\Delta_0)$.

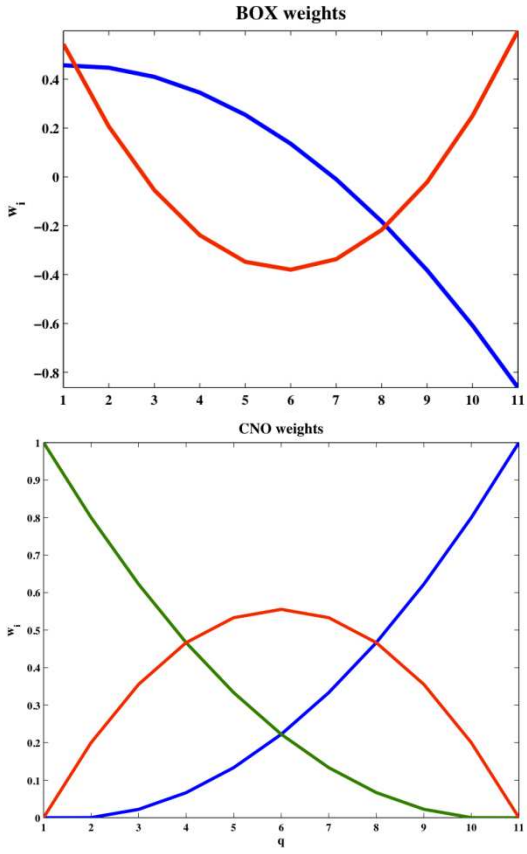

Figure 3. Weights for the different TP models

A -state-feedback or output feedback- controller is searched to fulfill a quadratic performance index:

$$\int_0^\infty \begin{bmatrix} w \\ z \end{bmatrix}^T \begin{bmatrix} Q_p & S_p \\ S_p^T & R_p \end{bmatrix} \begin{bmatrix} w \\ z \end{bmatrix} \leq -\varepsilon ||w||^2,$$

e.g., for an $\mathbb{L}^2$--gain specification one has $Q_p = -\gamma^2 \mathbb{I}, S_p = 0$ and $R_p = \mathbb{I}$. For these problems the performance index γ is an indicator on the quality of the controller.

An output-feedback LPV controller for (12) is described as

$$\begin{pmatrix} \dot{x}_c(t) \\ u(t) \\ z_c(t) \end{pmatrix} = \begin{pmatrix} A_c & B_{c1} & B_{c2} \\ C_{c1} & D_{c11} & D_{c12} \\ C_{c2} & D_{c21} & D_{c22} \end{pmatrix} \begin{pmatrix} x_c(t) \\ y(t) \\ w_c(t) \end{pmatrix}$$

$$\begin{pmatrix} w_c(t) \\ z_c(t) \end{pmatrix} \in \mathcal{S}_c(\Delta(t)) \subset \mathbb{R}^{m_c+k_c} \tag{13}$$

and consists of an LTI system in which the on-line measured parameter $\Delta(t)$ enters via an implicit constraint imposed by $\mathcal{S}_c(\Delta)$. Here $\mathcal{S}_c(\Delta)$ is a subspace that depends continuously on $\Delta \in \nabla$ and that satisfies $Im\begin{pmatrix} 0 \\ I_{k_c} \end{pmatrix} \in \mathcal{S}_c(\Delta_0)$.

An LPV controller can be obtained by using the following result, for details see e.g. [14], [15], [16]:

Theorem 2 (LPV synthesis) *There exist a controller (13) such that closed-loop system is well-posed and stable if and only if there exist X, Y, multipliers $P = \begin{pmatrix} Q & S \\ S^T & R \end{pmatrix}$ and $\tilde{P} = \begin{pmatrix} \tilde{Q} & \tilde{S} \\ \tilde{S}^T & \tilde{R} \end{pmatrix}$ with $P > 0$ on $\mathcal{S}(\Delta)$ and $\tilde{P} < 0$ on $\mathcal{S}(\Delta)^{\perp}$ for all $\Delta \in \nabla$ that satisfy the matrix inequalities*

$$\begin{pmatrix} X & I \\ I & Y \end{pmatrix} \geq 0, \tag{14}$$

$$\Psi^T \begin{pmatrix} * & & \\ & * & \\ & & * \end{pmatrix}^T \begin{pmatrix} 0 & X & 0 & 0 & 0 & 0 \\ X & 0 & 0 & 0 & 0 & 0 \\ 0 & 0 & Q & S & 0 & 0 \\ 0 & 0 & S^T & R & 0 & 0 \\ 0 & 0 & 0 & 0 & Q_p & S_p \\ 0 & 0 & 0 & 0 & S_p^T & R_p \end{pmatrix} \begin{pmatrix} I & 0 & 0 \\ A & B_u & B_p \\ 0 & I & 0 \\ C_u & D_{uu} & D_{up} \\ 0 & 0 & I \\ C_p & D_{pu} & D_{pp} \end{pmatrix} \Psi < 0, \tag{15}$$

$$\Phi^T \begin{pmatrix} * & & \\ & * & \\ & & * \end{pmatrix}^T \begin{pmatrix} 0 & Y & 0 & 0 & 0 & 0 \\ Y & 0 & 0 & 0 & 0 & 0 \\ 0 & 0 & \tilde{Q} & \tilde{S} & 0 & 0 \\ 0 & 0 & \tilde{S}^T & \tilde{R} & 0 & 0 \\ 0 & 0 & 0 & 0 & \tilde{Q}_p & \tilde{S}_p \\ 0 & 0 & 0 & 0 & \tilde{S}_p{}^T & \tilde{R}_p \end{pmatrix} \begin{pmatrix} -A^T & -C_u^T & -C_p^T \\ I & 0 & 0 \\ -B_u^T & -D_{uu}^T & -D_{pu}^T \\ 0 & I & 0 \\ -B_p^T & -D_{up}^T & -D_{pp}^T \\ 0 & 0 & I \end{pmatrix} \Phi > 0, \tag{16}$$

where $\Phi = \begin{pmatrix} \Phi_1 \\ \Phi_2 \\ \Phi_3 \end{pmatrix} = \mathrm{Ker}\begin{pmatrix} B^T & E_u^T & E_p^T \end{pmatrix}$ and $\Psi = \begin{pmatrix} \Psi_1 \\ \Psi_2 \\ \Psi_3 \end{pmatrix} = \mathrm{Ker}\begin{pmatrix} C & F_u & F_p \end{pmatrix}$.

This basic setting for the controller synthesis can be varied depending on the problem at hand and on the actual demands. The information on the change rate of the measured scheduling variables can be introduced through the slightly extended design

equations derived in [17] and [18]. The details of the controller construction are fairly standard, hence, are omitted. Some details on the construction of controller scheduling variables, however, are relevant for our topic:

Relaxation: the LMI conditions on the scaling matrices P and $\widetilde{\mathrm{P}}$ must hold on an infinite set. In order to make the problem tractable a so called relaxation technique, i.e., sufficient conditions that must hold on a finite set, are needed. However, this might lead to a conservative design, hence we want to reduce the relaxation "gap" .

Having convex weighting functions a sufficient condition for the double summation: $\sum_{i,j} w_i w_j P_{ij} > 0$ is

$$\mathrm{X_{ij}} = \mathrm{X_{ji}^T}, \mathrm{X_{ii}} \leq \mathrm{P_{ii}}, \mathrm{X_{ij}} + \mathrm{X_{ji}} \leq \mathrm{P_{ij}} + \mathrm{P_{ji}}, \mathrm{j} \neq \mathrm{i},$$

$$\mathrm{Y} = [\,\mathrm{X_{ij}}\,] > 0.$$

A recursive version can be formulated for multi-convex TP summations: $\sum_{\mathbf{i,j}} w_\mathbf{i} w_\mathbf{j} P_\mathbf{ij} > 0$:

$$\mathrm{X_{ikjs}} = \mathrm{X_{jsik}^T}, \mathrm{X_{ikik}} \leq \mathrm{P_{ikik}}, \mathrm{X_{ikjs}} + \mathrm{X_{jsik}} \leq \mathrm{P_{ikjs}} + \mathrm{P_{jsik}},$$

$$\sum_{\mathrm{i,j}} \mathrm{w_i w_j Y_{ij}} > 0, \quad \mathrm{Y_{ij}} = [\,\mathrm{X_{isjk}}\,], \quad (\mathrm{i,k}) \rightarrow \mathrm{i}.$$

Using the later technique stability can be proved even the stability domain is not convex, see [19]

Scheduling variables: the scheduling variables of the controller can be obtained applying the following procedure; perturb $\tilde{P}$, if required, to render it non-singular. Choose U such that its columns form an orthogonal basis of the image of $P - \tilde{P}^{-1}$. Define

$$\mathrm{M}(\Delta) = \mathrm{T^T}([\mathrm{U^T}(\mathrm{P} - \widetilde{\mathrm{P}}^{-1})\mathrm{U}]^{-1} - \mathrm{U^T S}(\Delta)(\mathrm{S}(\Delta)^\mathrm{T}\mathrm{PS}(\Delta))^{-1}\mathrm{S}(\Delta)^\mathrm{T}\mathrm{U})\mathrm{T}, \qquad (17)$$

where T is non-singular with

$$\mathrm{M}(\Delta_0) = \mathrm{diag}(\mathrm{M_-}, \mathrm{M_+}), \quad \mathrm{M_-} < 0, \quad \mathrm{M_+} > 0.$$

Set $k_c = dim(M_+)$ and $m_c = dim(M_-)$. If $\mathbf{S}_c(\Delta)$ denotes the orthogonal projector onto the eigenspace of $M(\Delta)$ with respect to its positive eigenvalues, the continuous controller scheduling subspace of dimension k_c is given by $\mathcal{S}_c(\Delta) = Im(\mathbf{S}_c(\Delta))$.

Since expression (17) is quite complicated in general, by using a TP transform technique, one can obtain an affine parametrisation of the controllers scheduling block in terms of the original scheduling variables. Thus a more suitable expression that can be easily implemented is obtained.

4. Simulation example

In Figure 4. a two-degree-of-freedom quarter-car model is shown with body mass $\mathrm{m_s}$, unsprung mass $\mathrm{m_u}$, suspension stiffness $\mathrm{k_s}$, suspension damping $\mathrm{b_s}$ and tire

stiffness k_t. The displacements of the sprung mass, the unsprung mass and their derivatives are q_1, q_2, $\dot{q}_1$ and $\dot{q}_2$, respectively. The system is excited by the road disturbance w and controlled by a force F.

Control performances of the suspension system are to keep sprung mass acceleration and suspension deflection small, and simultaneously limit the control force.

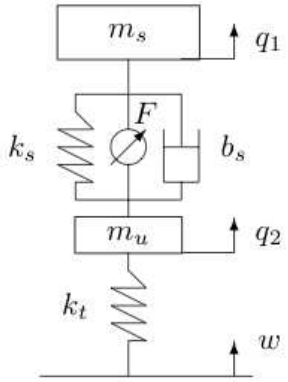

Figure 4. Quarter-car model

The vertical dynamics of the suspension system is formalized in the following way:

$$m_s\ddot{q}_1 = F_{ks} + F_{bs} - F, \tag{18}$$

$$m_u\ddot{q}_2 = -F_{ks} - F_{bs} - k_t(q_2 - w) + F, \tag{19}$$

where $F_{bs} = b_s^l\dot{d} - b_s^{sym}\dot{d}sgn(\dot{d}) + b_s^{nl}\sqrt{|\dot{d}|}sgn(\dot{d})$ is the suspension damping force and $F_{ks} = k_s^l d + k_s^{nl}d^3$ is the suspension spring force, with $d = q_2 - q_1$. The parts of the nonlinear suspension stiffness (k_s) are a linear coefficient k_s^l and a nonlinear coefficient k_s^{nl} while the nonlinear suspension damping b_s consists of a linear coefficient b_s^l and two nonlinear coefficients b_s^{nl} and b_s^{sym}, [20]. The measured outputs are d and $\dot{d}$.

The performance outputs are the passenger comfort (heave acceleration) ($z_a = \ddot{x}_1$), the suspension deflection ($z_s = x_s - x_u$) and the control input (z_u). The purpose of weighting functions W_{p_a}, W_{p_d}, and W_{p_u} in the closed-loop interconnection structure is to keep the heave acceleration, suspension deflection, wheel travel, and control input small over the desired frequency range. These weighting functions can be considered as penalty functions, i.e., weights should be large in a frequency range where small signals are desired and small where larger performance outputs can be tolerated.

The weighting functions for heave acceleration and suspension deflection are selected as $W_{p_a} = \phi_a W_{p_a,0}(s)$ and $W_{p_d} = \phi_d W_{p_d,0}(s)$, where parameter-dependent gains are applied to obtain trade-off between passenger comfort and road holding. A large gain ϕ_a and a small gain ϕ_d correspond to a design that emphasize passenger comfort. On the other hand, choosing ϕ_a small and ϕ_d large corresponds to a design that focuses on suspension deflection.

The LPV controller schedules on suspension deflection, and focuses on minimizing either the heave acceleration or suspension deflection response, depending on the magnitude of the vertical suspension deflection. In order to achieve the shift in focus from vertical acceleration to suspension deflection the weights associated with these signals are chosen to be parameter-dependent. In the mechanism two parameters are defined: c_1 and c_2. When the suspension deflection d is below c_1, the gain ϕ_a is selected to be constant and the gain ϕ_d is zero. When the deflection is between c_1 and c_2 the gains change linearly. When the value of the suspension deflection is greater than c_2, the gain ϕ_d is constant and the gain ϕ_a is zero, see Figure 5 for ϕ_d.

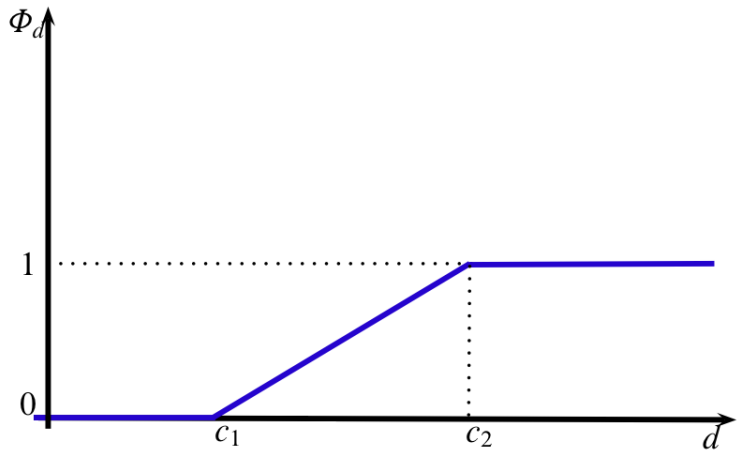

Figure 5. Performance gain

The parameters of the quarter-car model used in the simulations are given in Table 1. The control oriented qLPV model considers the nonlinearity of the generalized plant by selecting as scheduling parameters the measured outputs d and $\dot{d}$. Due to the structure of the dynamical equations the nonlinearities of the plant are cancelled out by a static term, i.e.,

$$u_c = k_s^{nl} d^3 - b_s^{sym} |\dot{d}| + b_s^{nl} \sqrt{|\dot{d}|} \mathrm{sgn}(\dot{d}) + \bar{u}_c.$$

Thus the generalized plant will contain only the nonlinearities introduced by the performance weights, with the control signal $\bar{u}_c$.

Table 1. Parameters of the quarter-car model

Symbols	Values	Unit	Description
m_s	290	kg	body mass
m_u	59	kg	unsprung mass
$b_{s,lin}$	700	N/m/s	lin. susp. damping
$b_{s,sym}$	100	N/m/s	nonlin. susp. damping
$b_{s,nl}$	200	$\mathrm{N/(m/s)^{1/2}}$	nonlin. susp. damping
$k_{s,lin}$	16182	N/m	lin. susp. stiffness
$k_{s,nl}$	235000	$\mathrm{N/m^3}$	nonlin. susp. damping
k_t	190000	N/m	tire stiffness

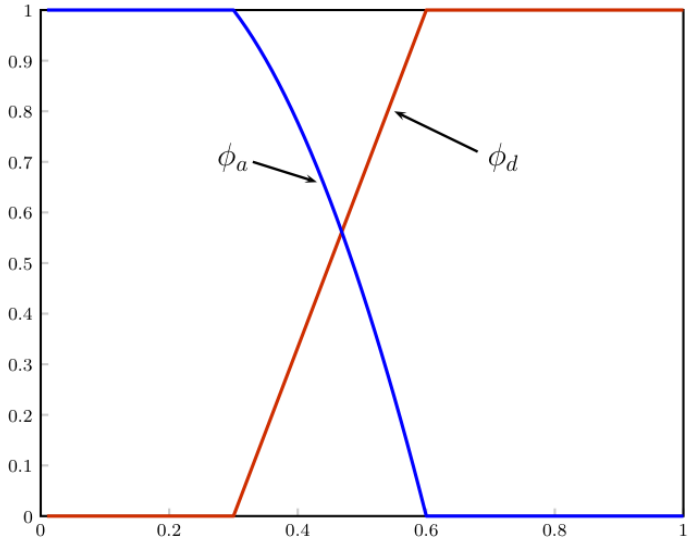

Figure 6. Gains of the performance weights: ϕ_a and ϕ_d

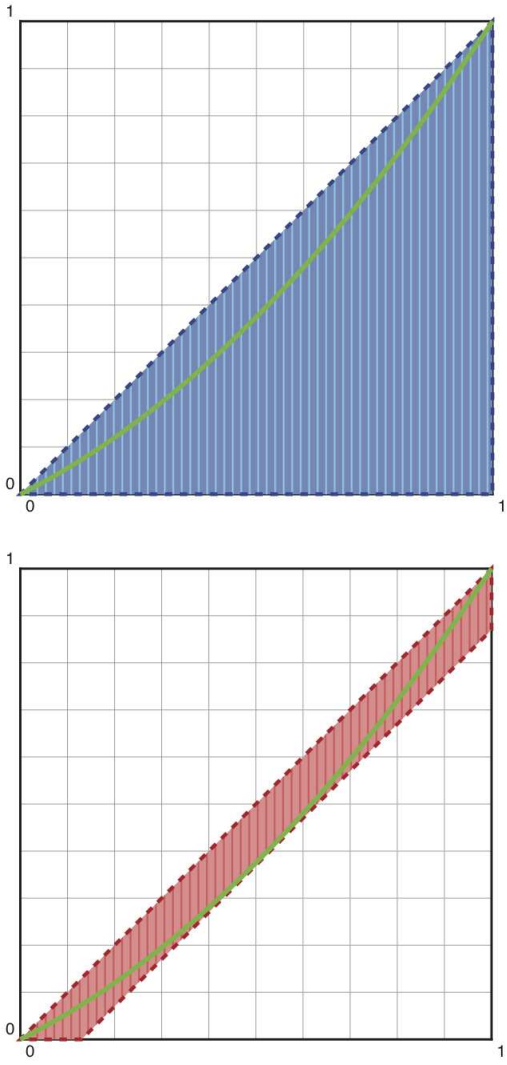

Figure 7. Convex relaxations for (ϕ_a, ϕ_d)

The weighting functions for heave acceleration, suspension deflection and control input are selected as

- $\mathrm{W_{p_a}} = (1 - 0.5\psi_\mathrm{d}(1 + \psi_\mathrm{d}))\mathrm{W_{p_a,0}(s)}$,
- $W_{p_d} = (1 - \psi_d)W_{p_d,0}(s)$,
- $W_{p_u} = 1e - 4$,

with $W_{pa,0}(s) = \frac{0.001s+0.3}{0.01s+1}$ and $W_{pa,0}(s) = \frac{0.02s+6}{0.05s+1}$. The function $\psi_d(d)$ has the shape as in Figure 5, thus the qualitative shapes of the performance weights ϕ_a and ϕ_d are depicted o Figure 6. Note that the design guarantees stability for a convex region, i.e., one can tune the position of c_1 and c_2 according to the engineering needs. In the simulations these values were fixed to $c_1 = 5$ mm and $c2 = 10$ mm. Moreover, the tuning can be done in operational time. For an example for an application where such a tuning was exploited in order to achieve a desired behavior see [4].

For reference purposes two H_∞ controllers were designed where controller $H_{\infty,a}$ concentrates only on the heave acceleration while controller $H_{\infty,d}$ concentrates only on the minimization of the suspension deflection.

The convex relaxations used for $\mathrm{diag}(\phi_a \phi_d)$ is depicted on Figure 7. Under the same conditions (weighting function, performance index) these tests have revealed that the value of the performance index that corresponds to the solution of the synthesis LMIs (15), (16) vary considerably depending on the choice made for the type of convex-hull. This result is in accordance with previous experiences obtained for stabilizing state feedback designs and indicates the influence of the convexification on the achievable performance in more complex settings, too.

Several qLPV controllers were design by using the tuning possibility of the LTI part of the controller. Two of them, qLPVa and qLPVb are included in the comparison in order to demonstrate the effects that can be achieved by such a tuning.

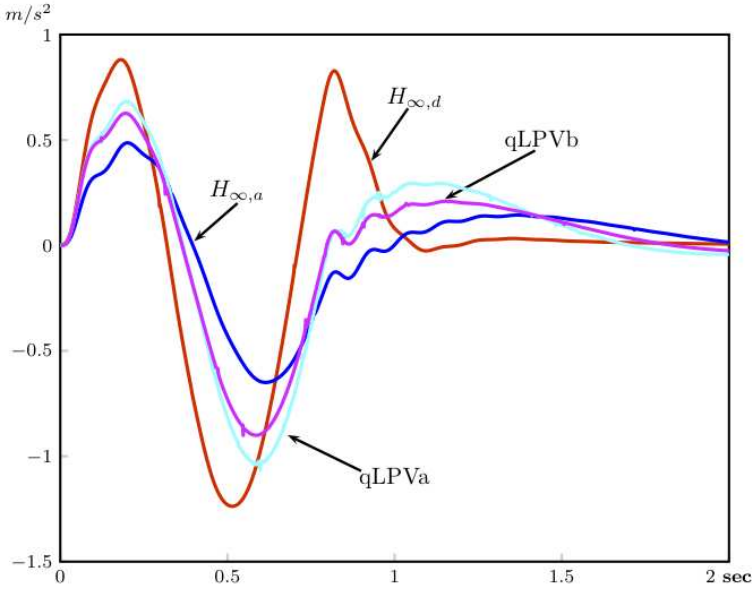

Figure 8. Achieved heave accelerations

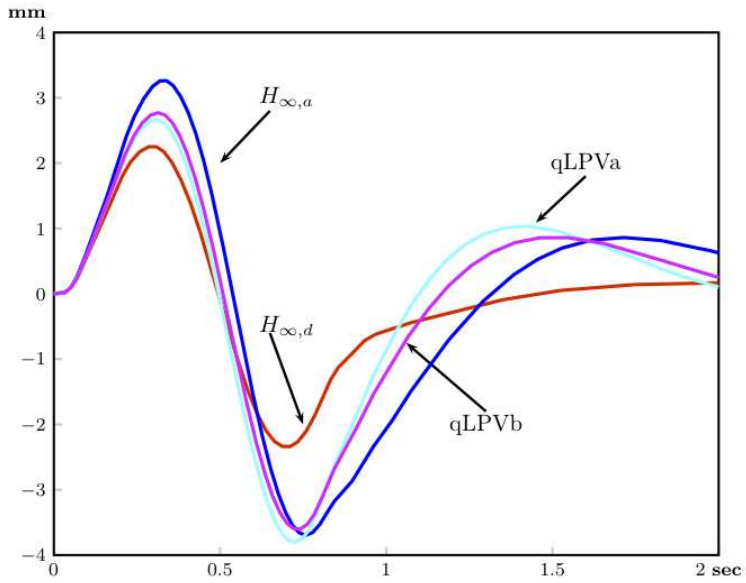

Figure 9. Achieved suspension deflections

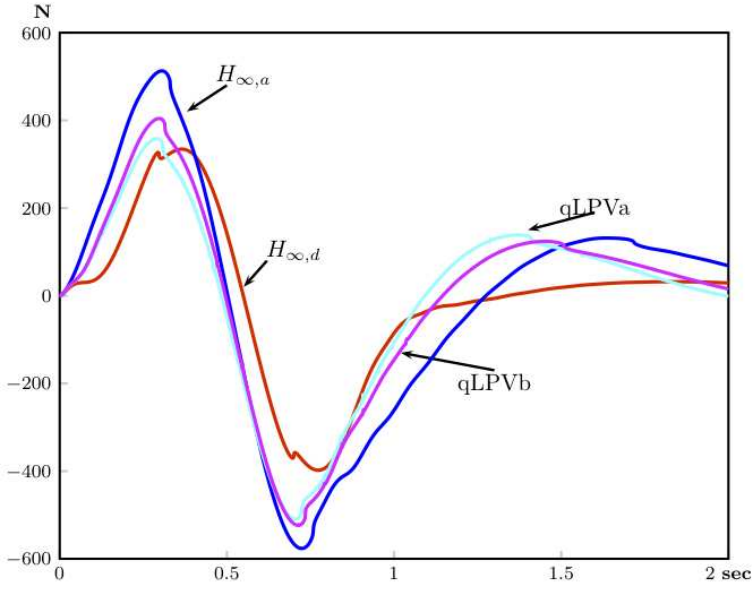

Figure 10. Control inputs of the designed controllers

The plots on Figure 8, 9 and 10 contain the achieved heave accelerations, the achieved suspension deflections and the applied control forces, respectively. The results reflects the achieved trade-off by the qLPV controllers between the conflicting multi-objective control criteria, i.e., road holding (suspension deflection) and passenger comfort (acceleration).

5. Conclusions

This paper has proposed methods to facilitate the design process of multi-objective qLPV robust control problems, often encountered in the design of vehicle systems, by efficient tuning possibilities. The proposed scheme is an iterative process in which a Tensor Product model transformation is applied to generate a finite element convex polytopic representation in order to obtain a quasi Linear Parameter Varying model. Then the LMI feasibility of a robust control objective is verified that is closely related by the original control task. This step provides a selection criterion that sorts out the suitable models from a finite set of model candidates generated by the TP method.

Since the choice of the most suitable convex relaxation has a great impact on the achievable performance, further research is done in order to provide algorithmic methods that facilitate the generation of different models by the TP technique. It is also a nontrivial question that for a given TP based model (9) how to derive the most suitable LFT description that fits the given control task.

Acknowledgment

The research has been conducted as part of the project TÁMOP-4.2.2.A-11/1/KONV-2012-0012: Basic research for the development of hybrid and electric vehicles. The Project is supported by the Hungarian Government and co-financed by the European Social Fund.

References

[1] Bokor, J.: *Robust adaptive control: the qLPV paradigm*, Proceedings of the European Control Conference, Kos, 2007

[2] Fekri, S., Athans, M., Pascoal, A.: *Issues, progress and new results in robust adaptive control*, Int. Journal of Adaptive Control and Signal Processing, vol. 20, pp. 519-579, 2006

[3] Gáspár, P., Szabó, Z., Bokor, J.: *An integrated vehicle control with actuator reconfiguration*, The 17th IFAC World Congress, Seoul, Korea, 2008

[4] Gáspár, P., Szabó, Z., Bokor, J.: *The design of a fault-tolerant vehicle control system*, Int. Jour. of Vehicle Autonomous Systems, vol. 37, pp. 36-55, 2009

[5] Iwasaki, T., Shibata, G.: *LPV system analysis via quadratic separator for uncertain implicit systems*, IEEE Transactions on Automatic Control, vol. 46, pp. 1195-1208, 2001

[6] Baranyi, P.: *TP model transformation as a way to LMI based controller design*, IEEE Transaction on Industrial Electronics, vol. 51, no. 2, pp. 387--400, April 2004

[7] Lathauwer, L. D., Moor, B. D., Vandewalle, J.: *A multilinear singular value decomposition*, SIAM Journal on Matrix Analysis and Applications, vol. 21, no. 4, pp. 1253-1278, 2000

[8] Szeidl, L., Várlaki, P.: *HOSVD based canonical form for polytopic models of dynamic systems*, Journal of Advanced Computational Intelligence, vol. 13, pp. 52-60, 2009
[9] Baranyi, P., Tikk, D., Yam, Y., Patton, R. J.: *From differential equations to PDC controller design via numerical transformation*, Computers in Industry, Elsevier Science, vol. 51, pp. 281-297, 2003
[10] Bokor, J., Baranyi, P., Michelberger, P., Várlaki, P.: *TP model transformation in non-linear system control*, The 3rd IEEE International Conference on Computational Cybernetics (ICCC), Mauritius, Greece, 13-16 April 2005, pp. 111-119
[11] Gahinet, P., Apkarian, P., Chilali, M.: *Affine parameter dependent Lyapunov functions and real parameter uncertainity*, IEEE Transactions on Automatic Control, vol. 41, pp. 436-442, 1996
[12] Wu, F., Yang, X. H., Packard, A., Becker, G.: *Induced* $\mathbb{L}^2$ *norm control for LPV systems with bounded parameter variation rates*, International Journal of Nonlinear and Robust Control, vol. 6, pp. 983-998, 1996
[13] Scherer, C.: *LMI relaxations in robust control*, European Journal of Control, vol. 12, pp. 3-29, 2006
[14] Dettori, M., Scherer, C.: *Robust stability analysis for parameter dependent systems using full block S-procedure*, Proc. Conference on Decision and Control, pp. 2798-2799, 1998
[15] Scherer, C.: *A full block S-procedure with applications*, Proc. Conference on Decision and Control, pp. 2602-2607, 1997
[16] Scherer, C.: *LPV control and full block multipliers*, Automatica, vol. 37, pp. 361-375, 2001
[17] Wu, F.: *A generalized LPV system analysis and control synthesis framework*, International Journal of Control, vol. 74, pp. 745-759, 2001
[18] Wu, F., Dong, K.: *Gain scheduling control of LFT systems using parameter dependent Lyapunov functions*, Automatica, vol. 42, pp. 39-50, 2006
[19] Arino, C., Sala, A.: *Relaxed LMI conditions for closed-loop fuzzy systems with tensor-product structure*, Engineering Applications of Artificial Intelligence, vol. 20, pp. 1036-1046, 2007
[20] Alleyne, A., Hedrick, J.: *Nonlinear control of a quarter car active suspension*, Proc. of the American Control Conference, vol. 1, pp. 21-25, 1992
[21] Packard, A., Balas, G.: *Theory and application of linear parameter varying control techniques*, American Control Conference, Workshop I, Albuquerque, New Mexico, 1997
[22] Saadaoui, H., Manamanni, N., Djema, M., Barbot, J. P., Floquet, T.: *Exact differentiation and sliding mode observers for switched Lagrangian systems*, Nonlinear Analysis: Theory, Methods & Applications, special issue: Hybrid Systems and Applications, Elsevier, vol. 65, no. 5, pp. 1050-1069, 2006

Modelling Cooperative Control Problems in the Cyber Environment: Introduction to Quasi Consensus Networks

A. Edelmayer[1,2], L. Virág[1], J. Kovács[1]

[1]Systems and Control Laboratory, Institute for Computer Science and Control, Hungarian Academy of Sciences
H-1111, Budapest, Kende u. 13-17, Hungary
e-mail: edelmayer@sztaki.mta.hu

[2]Multidisciplinary School of Technical Sciences
Research Group for Systems and Control Theory
Széchenyi István University, H-9026, Egyetem tér 1, Győr, Hungary

Abstract: The paper introduces the novel idea of the application of quasi consensus networks to modelling networked distributed systems. Quasi consensus networks operate alike standard consensus seeking ones without requesting the information state of the contributing systems to converge to a predetermined value. The quasi consensus-modelling paradigm can be used in modelling cooperative control problems in the cyber environment when the achievement of a common value of the information state is not the ultimate goal of the systems operation.

Keywords: consensus seeking, cooperative systems, detection and estimation of cyber physical systems, distributed systems modelling, networked systems

1. Introduction

An emerging trend in modern control theory that reflects the use of distributed and networked dynamical systems in the information age is called cyber physical systems (CPS). CPSs integrate data acquisition, computation and communication to interact with the physical world and with other systems in an attempt to acquire, distribute and share data around each other. The amount of literature dealing with various categories of cyber physical systems, spanning from distributed robotic microsystems to large-scale networked systems, is wide and varied.

A special operational policy of distributed systems, emerged quite lately in modern control theory, is based on the principle of cooperation. Cooperative systems consists of a set of interacting autonomous agents, interconnected over an information network to achieve a common desired task and enhance operational effectiveness through cooperative teamwork. The agents exchange information over a communication medium, either on wires or wireless. Examples include large-scale mass transport and power (energy, electricity) distribution networks, ad-hoc vehicle networks and others.

A particular policy of operation within cooperative behaviour is called coordination. Coordination is the organisation of the different elements of a complex distributed system so as to enable them to work together in a controlled and supervised way. Potential application of the coordination idea includes formation control of vehicles required to maintain a prescribed shape during travel, or rendezvous problems, where the movement trajectories of two or more autonomous vehicles are required to meet in space and time.

Hence, devices which acquire, process and transfer information from one agent to another are inherent part of the system, and are recognised as critical infrastructure of the distributed (control) systems based on interconnected information technology, which cannot be disregarded when modelling. Properties of the information exchange process, and so this communication infrastructure (which is frequently referred to cyber infrastructure), is inseparable part of systems operation.

Due to the largely fragmented nature of CPSs and the cyber infrastructure itself, this specific architecture is exposed to the possibility of being harmed by environmental effects or attacked maliciously. As most CPSs, especially those consisting of mobile autonomous agents, such as vehicle and robotic networks, are based on wireless communication, communication links have to be assumed insecure. Information coded radio waves are potentially subject of interception. By obtaining trustful network information the attackers are able to bypass intrusion prevention techniques. Fake and malicious nodes e.g., may be able to hacked into the network by eavesdropping on network traffic acquiring network information for launching attacks. Therefore, vulnerability of cyber physical systems has received increasing attention in the past years and security has to be addressed as a primary concern.

As vulnerability is an engineering principle that cannot be securely avoided CPSs have to use proper protection techniques as precautionary measure. First of all it is absolutely necessary to know at each time instant if the system is intact, i.e., it is complete and not damaged or impaired in any way. Therefore, timely detection and identification of intrusions and other malicious actions is of a primordial design goal.

Existing techniques of fault detection and identification may provide standard means for the implementation of this protection mechanism for CPSs as attacks can be thought as faults. One difficulty with this analogy is that faulty behaviours caused by malicious actions may be very difficult to detect as the attacker have knowledge on the system itself and thus could be able to use masking techniques to conceal the action. Model-based fault detection is one of the most powerful methods to the solution of this problem, as it possesses information on the system as well.

Using model-based detection, however, necessitates the availability of a system model. Due to the crucial role of distributed and networked systems, including CPSs, in advanced engineering systems modelling of these type of systems have received much attention lately. Recent modelling approaches are motivated by existing CPS use cases and attack experiences basically relying on representation of the complex CPS as a single, homogeneous entity of interconnected dynamical systems with special focus on the modelling of the interconnection scheme, while the behaviour of the cyber infrastructure is not explicitly treated by the theory.

This paper, instead of committing itself to the discussion of the detection problem as a whole, addresses the modelling issue only. A novel modelling paradigm i.e., the concept of quasi-consensus networks is introduced that can be useful in the description of the cyber infrastructure in cases when some conditions, posed by the standard consensus seeking operation, can be resolved. This specific system model, analogously to [9], allows the introduction of misbehaving agents for the modelling of faulty and/or changed behaviour of the system without taking particular restrictions on the way the consensus seeking is made.

The layout of the paper is as follows. In Section 2 the techniques that have been recently used for modelling CPSs are briefly reviewed. Based on this knowledge this is followed by the introduction of quasi consensus networks in Section 3. A brief section of conclusions on future works closes the paper.

2. Modelling Cyber Physical Systems

Living with the constructive assumption that cyber physical systems can be thought of like a set of interconnected dynamical systems, which are modelled by linear time invariant (LTI) dynamics the approach of [10] became quite common in the synthesis and analysis of large-scale CPSs. This approach considers the set of connected subsystems

$$\begin{aligned} x_i(t) &= A_i x_i(t) + B_i u_i(t), \\ y_i(t) &= C_i x_i(t) + D_i u_i(t) \end{aligned} \tag{1}$$

with the state $x_i(t) \in \mathbb{R}^n$, input $u_i(t) \in \mathbb{R}^m$ and measurement $y_i(t) \in \mathbb{R}^p$ vectors of the individual subsystems. The matrices A_i, B_i, C_i and D_i are given in the appropriate dimensions. These can be combined by taking interconnections among subsystems into consideration to produce the overall system equations by the time invariant descriptor system [5] in the form

$$\begin{aligned} E\dot{x}(t) &= Ax(t) + Bu(t), \\ \mathrm{y}(t) &= Cx(t) + Du(t), \end{aligned} \tag{2}$$

where $x(t) \in \mathbb{R}^n$, $u(t) \in \mathbb{R}^m$ and $y(t) \in \mathbb{R}^p$ are the state, input and measurement vectors of the combined system, respectively. $E \in \mathbb{R}^{n \times n}$ is called the connectivity matrix of the system, which encodes the interconnection structure of the networked subsystems. For practical reasons E is generally required to be singular. The input $u(t)$ can be thought quite generally, it can be composed and extended arbitrarily, representing unknown inputs, failures and other incipient effects depending on the purpose of modelling, which affect the plant in predetermined directions.

An obvious shortcoming of this modelling approach comes from the assertion that subsystems dynamics is viewed to be homogeneously LTI, which may prove to be a very strong assumption in modelling of complex, large-scale CPSs. For the difficulties of the use of nonlinear descriptor systems, see [6]. The use of heterogeneous or hybrid

system models (containing LTI and nonlinear subsystems jointly) is not a viable modelling option neither.

The classical modelling approach, which is based on the composition of the set of autonomous systems (2) that perform and are modelled individually then connected together as in (2), is useful in modelling large-scale CPSs. Examples can be cited from mass transport and power distribution networks.

A somewhat different approach is needed to CPSs, where compared to the previous approach, the emphasis of operation (and thus, modelling) is not on individual system dynamics but the quality of information acquisition and exchange, moreover, the devices which transmit and process information, i.e., the principles of communication and networking. This is a modelling approach where the performance of the cyber-infrastructure of the network gets in the forefront. Cyber-infrastructure is considered the enabling body of CPS functionality and viewed as the medium in which the input acquisition, processing and transmission of information occurs. Control and detection of cyber-infrastructure that must ensure that the global CPS are kept in an operating condition as expected is therefore of primary importance.

A particular class of advanced CPS applications is based on the principle of cooperation. In the modern theory of decentralised and distributed control, cooperative systems are thought to be as composed of multiple dynamic entities that share and exchange information or tasks among each other to support a common effort. The shared information among contributing parties of the overall system, which may take the form of common objectives, common control algorithms or common data is a necessary condition for cooperation [13]. Performing in the cyber environment in an attempt to align a common objective requires among coordinated systems to share a consistent view of the goals and other control specific data that is critical to the accomplishment of that objective. The instantaneous value of that information is called the information state [12].

Cooperative systems collect and exchange information by communication and sensing, and as such, are ultimately based on the quality and performance of the cyber-infrastructure. Coordinated control and filtering (targeting vehicle formation control, rendezvous and attitude alignment problems, flocking, foraging, payload transport and enhanced position estimation just to mention a few) are typical applications of the cooperating idea [1, 8, 14].

Consensus seeking cooperation algorithms are best known from coordinated control problems. In classical coordination systems, the goal is the zeroing of the difference of the value of the information states around all the contributing systems. To achieve a successful coordination, the contributing systems have to agree (i.e., have to have information consensus) over the objective value of the information state. In coordinated control scenarios, therefore, the goal is to design a control law so that the information states of the coordinated systems converge to a common value in time (*cf*. rendezvous problem) [2, 3].

This control law can be implemented by means of consensus iterations, where, at each iteration, the contributing actors get closer to the implementation of the common objective. In classical consensus iterations, at each time instant, a contributing system

update its state as a weighted combination of its own value and also those received from the partners. As a result of this procedure the information state may converge to the objective value in case stability can be ensured.

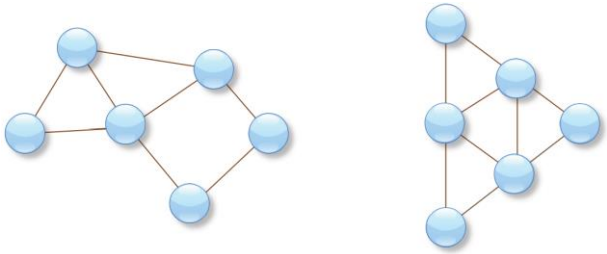

Figure 1. The initially unordered structure of vehicle topology (see Fig. 1/a) is made structured and ordered (Fig. 1/b) by selecting the distance between immediate neighbours as information state and applying a consensus algorithm to iteratively modify the value of this state as long as the desired formation is reached, i.e., until all the information states are equal

The most typical application of the consensus algorithm is in vehicle formation control, see Fig. 1, when onboard vehicle controllers manoeuver each vehicle to the equidistant locations which satisfy the geometric criteria of the formation. In the next section the consensus-based modelling is reviewed briefly and the idea of quasi-consensus networks is introduced.

3. Linear quasi-consensus networks

Standard consensus problems assume similar dynamics on the information state of each subsystems (*cf.* the assumption made in system models (2) for the system state dynamics). Apart from all the works which tend to model CPSs as linear descriptor systems it is a common approach to model information exchange among dynamical subsystems by means of graph theory. Team's communications topologies can be represented with directed or undirected graphs. This modelling technique became very popular as it fits to the description of complex networked system structures.

Consider the pair (N, E) denoting a directed graph with vertex set $N = \{1, \dots, n\}$ and edge set $E \subset N \times N$. The edge $(i, j) \in E$ indicates that the node (or agent) j can obtain information from node i. As the graph is directed, this is not necessarily vice versa and i is called the parent node and j is the child node. Undirected graphs are considered a special case of undirected ones where the edge (i, j) in the undirected graph corresponds to (j, i) in the directed one. The physical meaning of directed graph representation is that information flow is considered unidirectional between nodes, while undirected graph may represent bidirectional flow of information.

For the representation of the interconnection structures one needs to introduce the so called adjacency matrix that describes the structure of neighbourhood connections. The adjacency matrix $A = [a_{ij}] \in \mathbb{R}^n$ of the node set $N = \{1, \dots, n\}$ is defined such that a_{ij}

is a positive weight if $(j,i) \in E$, while $a_{ij} = 0$ if $(j,i) \notin E$. If weights are not relevant in the model, then $a_{ij} = 1, \forall\, (j,i) \in E$.

Based on the linear graph theoretic notions defined above the most common continuous time consensus seeking problem, similarly to [4] [11], can be represented by the linear system

$$\dot{x}_i(t) = -\sum_{j=1}^{n} a_{ij}(t)\big(x_i(t) - x_j(t)\big), \quad i = 1, \dots, n, \tag{3}$$

where $a_{ij}(t)$ is the (i,j) entry of the adjacency matrix of the associated communication graph at time t and x_i is the information state of the i^{th} subsystem (node). Setting $a_{ij} = 0$ means that subsystem i cannot receive information from subsystem j. Realize that the dynamics of system (3) is determined by the difference of the information state of the neighbouring subsystems.

Ensuring stability the information state $x_i(t)$ of subsystem i is driven toward the state of its immediate neighbours. Obviously, the critical question is, if under what conditions the information states of all nodes in the connected network converge to a common predetermined value and, in what time. This is the point when traditional consensus algorithms become problematic. Even in fixed, time invariant topologies, it is possible to guarantee only that the common value of the negotiated information state is a convex combination of the initial ones. However, topologies are more frequently dynamic and satisfying conditions under which the consensus is stable during random switching of the communication topologies is not trivial. As an additional difficulty, consensus making must satisfy certain requirements for performance criteria such as convergence time.

Now let the linear iteration over the adjacency matrix A be defined in terms of the matrix Laplacian. The Laplacian matrix $L = [\ell_{ii}] \in \mathbb{R}^{n\times n}$ of a directed graph, similarly to [7] is defined such that $\ell_{ij} = \sum_{j\neq i} a_{ij}$ and $\ell_{ij} = -a_{ij}$ for all $i \neq j$. If $(j,i) \notin E$ then $\ell_{ij} = -a_{ij} = 0$ to satisfy the conditions

$$\ell_{ij} \leq 0 \quad i \neq 1,$$

$$\sum_{j=1}^{n} \ell_{ij} = 0 \quad i = 1, \dots, n.$$

Based on the above the consensus algorithm [9] can be written in matrix form as

$$\dot{x}(t) = -L(t)x(t), \tag{4}$$

where $x = [x_1, \dots, x_n]^T$ is the information state and $L(t) = [\ell_{ij}(t)] \in \mathbb{R}^{n\times n}$ is the Laplacian of the interconnection graph that serves for the update rule of the information state $x(t)$. We say that (4) is consensus seeking if, for all initial information state $x_i(0)$ and all $i,j = 1, \dots, n$ the state difference $\tilde{x}_{ij} = |x_i(t) - x_j(t)|$ disappears i.e., it converges to zero as $t \to \infty$.

While the consensus paradigm discussed above is useful for many coordinated control applications, the assumptions might not be appropriate when each agent's information state evolves in an uncoordinated fashion and the objective of the control problem is different than zeroing out the state differences.

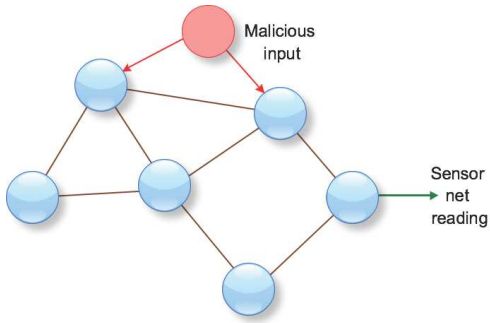

Figure 2. Sensor network under cyber attack

There are problems, however, when posing conditions for the information state convergence is overly restrictive and simply not necessary.

Consider, for example, the case of distributed sensor networks: the elements of the network provide measurement data at the output of the network which contain measurements slightly different from node to node, even in case we have a homogeneous set of redundant sensors in the network. If the measurement value is considered the information state of the network it is meaningless to require that this value converges to anything. However, the system model (4) still describes the connectivity of the network and provides useful means to model the information exchange around the network elements.

Proposition 1: The system representation (4) is thought quasi consensus network if, for all initial information state $x_i(0)$ and all $i,j = 1,\dots,n$ the state difference $\tilde{x}_{ij} = |x_i(t) - x_j(t)|$ is bounded as $t \to \infty$.

Note that the obvious extension of Proposition 1 includes systems permitting $\tilde{x}_{ij}$ to converge to a bounded constant value. Recall that traditional consensus systems like (3) ensures only that the information state converges to a common value but does not let the specification of a particular value of that state. Many cooperative problem setup in advanced control theory can be represented by quasi consensus system models. Examples are heterogeneous ad-hoc vehicle networks and sensor networks.

Quasi consensus models allow for some network elements to update their state differently than specified by the update matrix L. This is required for modelling faults and external disturbances or even malicious effects. By adding an exogenous input to the network to model (4) malicious inputs or other cyber attacks can be modelled as depicted in Fig. 2. A quasi consensus network with faulty behaviour can be represented as

$$\dot{x}(t) = -L(t)x(t) + B_v u_v(t), \tag{5}$$

where $u_v(t)$ is the malicious effect, which affects the network in the predetermined direction B_v. Now standard methods of fault detection can be used for the detection and isolation of the attack. This, however, is not in the scope of the paper.

4. Conclusions

This article provided a brief introduction to quasi consensus networks, a modelling paradigm applicable to networked decentralised systems. The approach fits to the description of heterogeneous cyber physical systems subject to faults and other external disturbances or malicious effects. Application of the quasi consensus seeking idea widens the possibility of the application of advanced methods of control and detection in the field of CPSs. More work will be needed to clarify the properties of the matrix Laplacian L in view of the application of particular detection and control problems, moreover, the construction and evaluation of malicious input models in the quasi consensus representation.

Acknowledgement

This work was supported by the project TÁMOP-4.2.2.C-11/1/KONV-2012-0012: *Smarter Transport – IT for cooperative transport systems,* which is supported by the Hungarian Government and co-financed by the European Social Fund. The financial support is gratefully acknowledged by the authors.

References

[1] Caughman, J.S., Lafferriere, G., Veerman, J.J.P., Williams, A.: *Decentralized control of vehicle formations*. Sys. Contr. Lttrs., vol. 54, no. 9, pp. 899-910, 2005

[2] Lin, J., Morse, A.S., Anderson, B.D.O.: *The multi-agent rendezvous problem*. In: Proceedings of 42nd IEEE Conference Decision and Control, vol. 2, pp. 1508-1513, 2003
DOI: 10.1109/CDC.2003.1272825

[3] Lin, J., Morse, A.S., Anderson, B.D.O.: *The multi-agent rendezvous problem - the asynchronous case.* In: Proceedings of 42nd IEEE Conference Decision and Control, vol. 2, pp. 1926-1931, 2003
DOI: 10.1109/CDC.2004.1430329

[4] Jadbabaie, A., Jin, J., Morse, A.S.: *Coordination of groups of mobile autonomous agents using nearest neighbour rules*. IEEE Transaction of Automatic Control, vol. 48, no. 6, pp. 988-1001, 2005

[5] Luenberger, D.G.: *Dynamic equations in descriptor form*. IEEE Transaction of Automatic Control, vol. 22, no. 3, pp. 312-321, 1977

[6] Luenberger, D.G.: *Non-linear descriptor systems.* Journal of. Economic Dynamics and Control, vol. 1, no. 4, pp. 219-242, 1979

[7] Merris, R.: *Laplacian matrices of graphs: a survey*. Linear Algebra and its Applications, no. vol. 197, no. 198, pp. 143-176, 1994

[8] Olfati-Saber, R., Jalalkamali, P.: *Coupled distributed estimation and control for mobile sensor networks.* IEEE Transaction of Automatic Control, vol. 57, no. 10, pp. 2609-2614, 2005

[9] Pasqualetti, F., Bicchi, A., Bullo, F.: *Consensus computation in unreliable networks: a system theoretic approach.* IEEE Transaction of Automatic Control, vol. 57, no. 1, pp. 90-104, 2012

[10] Pasqualetti, F., Dörfler, F. Bullo, F.: *Attack detection and identification in cyber-physical systems.* IEEE Transaction of Automatic Control, vol. 58, no. 11, pp. 2715-2729, 2013
DOI: 10.1109/TAC.2013.2266831

[11] Ren, W., Beard, R.W.: *Consensus seeking in multi agent systems under dynamically changing interaction topologies*. IEEE Transaction of Automatic Control, vol. 50, no. 5, pp. 655-661, 2005

[12] Ren, W., Beard, R.W., Atkins, E.M.: *Information consensus in multivehicle cooperative control.* IEEE Control Systems Magazine, vol. 27, no. 2, pp. 71-82, 2007

[13] Ren, W, Beard, R.W., McLain, T.W.: *Coordination variables and consensus building in multiple vehicle systems.* In V. Kumar, N. E. Leonard, and A. S. Morse, editors, Lecture Notes in Control and Information Sciences, pp. 171-188, 2004

[14] Veerman, J.J.P., Lafferriere, G., Caughman, J.S., Williams, A.: *Flocks and formations*. Journal of. Statistical Physics, vol. 121, no. 5-6, pp. 901-936, 2005

Robust Control for the 3 DoF Aeroelastic wing via TP Model Representation

B. Takarics[1], P. Baranyi[1], P. Várlaki[2]

[1]Research Center of Vehicle Industry, Széchenyi István University
H-9026 Egyetem tér 1. Győr, Hungary
Phone: +36 1 279 6111
E-mail: baranyi.peter@sztaki.mta.hu
[2] System Theory Research Group, Széchenyi István University
9026 Egyetem tér 1. Győr, Hungary

Abstract: Several control design approaches were utilized recently for actively stabilizing the 2 and 3 degrees-of-freedom (DoF) aeroelastic wind section, which have structural nonlinearities. The present paper focuses on the stabilization of the 3 DoF model. The proposed control design strategy takes into account the uncertainties of the trailing edge dynamics and robust output feedback control is designed where the only measurable state variable is the pitch angle. Beside robust asymptotic stability, the controller has to fulfill criteria related to the bound of the l_2 norm of the control signal. The control design is based on Tensor Product (TP) type convex polytopic representation of the 3 DoF aeroelastic wing section model and all of the control performance objectives are formulated via Linear Matrix Inequalities (LMIs). The convex TP type polytopic model is obtained via TP model transformation as the first step of the design and the feedback and observer gains are derived via LMI based convex optimization as the second step. The resulting controller and observer takes the polytopic structure of the TP type convex NATA model. The derived controller and observer structure is evaluated and validated via numerical simulations.

Keywords: *aeroelastic wing, robust LMI-based multi-objetive control, TP model transformation, qLPV systems*

Nomenclature

The variables related to the 3 degrees of freedom aeroelastic wing section are given bellow:

- a = non-dimensional distance from the mid-chord to the elastic axis

- b = semi-chord of the wing – m
- c_h = the plunge structural damping coefficients – Nms/rad
- c_{l_α} = aerofoil coefficient of lift about the elastic axis
- c_{l_β} = trailing-edge surface coefficient of lift about the elastic axis
- $c_{m_\alpha,eff.}$ = aerofoil moment coefficient about the elastic axis
- $c_{m_\beta,eff.}$ = trailing-edge moment coefficient about the elastic axis
- c_α = the pitch structural damping coefficient – Nms/rad
- h = plunging displacement – m
- I_α = the mass moment of inertia – kgm^2
- k_h = the plunge structural spring constant
- $k_\alpha(\alpha)$ = non-linear stiffness contribution
- L = aerodynamic force – N
- M = aerodynamic moment – Nm
- m = the mass of the wing – kg
- U = free stream velocity – m/s
- x_α = the non-dimensional distance between elastic axis and the center of mass
- α = pitching displacement – rad
- β = control surface deflection – rad
- ρ = air density – kg/m^3

1. Introduction

Active stabilization of aeroelastic wing sections has been in focus of aerospace and control engineers for several decades [13]. [6, 8] derived the unsteady aerodynamics of the 3 degrees of freeeddom (DoF) Nonlinear Aeroelastic Test Apparatus (NATA) model. A very broad range of control solutions were examined in [20, 11, 14, 25, 19, 17, 12, 24, 15], which include adaptive control, neural network based control, mixed H_∞/H_2 scheduling control etc. An improved model of the NATA is proposed in [16].

Tensor Product (TP) model transformation and LMI based approach is applied in [5, 4, 10, 21, 22]. [5] proposes state feedback control for the 2 DoF version of the NATA model and [4] improves the control solution with an observer and [10] adds further improvement via convex hull manipulation based optimization. [21] extends the TP model

based approach by adding nonlinear friction to the 2 DoF NATA based on [7] and output feedbeck control design for the 3 DoF NATA model based on [16] is given in [22] for both linear and nonlinear friction models.

The current research aims to extend the TP model type based control approaches listed above with robustness properties and limits on the l_2 norm of the control signal. The model used in the paper is the same 3 DoF NATA model presented in [16]. The control design framework is formulated with the assumption that not all states can be measured, thus output feedback design is proposed.

The control design process is executed in two steps. First, we obtain the TP type convex polytopic form of the NATA model via TP model transformation, which can derive various types of convex representations of the same model. The quasi Linear Parameter Varying (qLPV) model can be given by analytical equations based in the system dynamics, via soft-computing or black-box identification. The second step is to design the controller and observer via LMI based convex optimization, where the control performance criteria are formulated in terms of LMIs and the resulting control solution is defined by the same polytopic form as the qLPV model.

It is shown that various structures of the same uncertainty can highly influence the feasibility of the LMIs and the control performance of the resulting solutions.

The paper is structured as follows: the following section presents the dynamic equations and the qLPV model of the 3 DoF NATA, Section 3 introduces the proposed control design strategy, Section 4 gives the results of the control design. Section 5 shows the results of the numerical simulations with detailed evaluation and at the end of the paper are the conclusions.

2. Dynamic Equations and qLPV Model of the Aeroelastic Wing Section

The following section presents the basic dynamic equations related to the 3 DoF NATA model based on [15, 16]. The degrees of freedom of the model are related to the plunge h, pitch α and trailing-edge surface deflection β. The equations of motion are given as:

$$\begin{pmatrix} m_h + m_\alpha + m_\beta & m_a x_a b + m_\beta r_\beta + m_\beta x_\beta & m_\beta r_\beta \\ m_a x_a b + m_\beta r_\beta + m_\beta x_\beta & \hat{I}_\alpha + \hat{I}_\beta + m_\beta r_\beta^2 + 2 x_\beta m_\beta r_\beta & \hat{I}_\beta + x_\beta m_\beta r_\beta \\ m_\beta r_\beta & \hat{I}_\beta + x_\beta m_\beta r_\beta \hat{I}_\beta m x_\alpha b & I_\alpha \end{pmatrix} \begin{pmatrix} \ddot{h} \\ \ddot{\alpha} \\ \ddot{\beta} \end{pmatrix} + \quad (1)$$

$$\begin{pmatrix} c_h & 0 & 0 \\ 0 & c_\alpha & 0 \\ 0 & 0 & c_{\beta_{servo}} \end{pmatrix} \begin{pmatrix} \dot{h} \\ \dot{\alpha} \\ \dot{\beta} \end{pmatrix} + \begin{pmatrix} k_h & 0 & 0 \\ 0 & k_\alpha(\alpha) & 0 \\ 0 & 0 & k_{\beta_{servo}} \end{pmatrix} \begin{pmatrix} h \\ \alpha \\ \beta \end{pmatrix} = \begin{pmatrix} -L \\ M \\ k_{\beta_{servo}}\beta_{des} \end{pmatrix}.$$

The non-linear stiffness $k_\alpha(\alpha)$ is defined as $k_\alpha(\alpha) = 25.55 - 103.19\alpha + 543.24\alpha^2$ ([16]) and the quasi-steady aerodynamic force and moment are defined by:

$$L = \rho U^2 b C_{l_\alpha} \left(\alpha + \frac{\dot{h}}{U} + \left(\frac{1}{2} - a \right) b \frac{\dot{\alpha}}{U} \right) + \rho U^2 b c_{l_\beta} \beta \tag{2}$$

$$M = \rho U^2 b^2 C_{m_{\alpha,eff.}} \left(\alpha + \frac{\dot{h}}{U} + \left(\frac{1}{2} - a \right) b \frac{\dot{\alpha}}{U} \right) + \rho U^2 b C_{m_{\beta,eff.}} \beta.$$

Both the quasi-steady aerodynamic force L and the quasi-steady aerodynamic moment M defined for the low-velocity regime only. The trailing-edge servo-motor dynamics are taken form [16] as:

$$\hat{I}_\beta \ddot{\beta} + c_{\beta_{servo}} \dot{\beta} + k_{\beta_{servo}} \beta = k_{\beta_{servo}} \mathbf{u}_\beta. \tag{3}$$

Let us combine equations (1), (3) and (2) in order to obtain:

$$\underbrace{\begin{pmatrix} m_h + m_\alpha + m_\beta & m_a x_a b + m_\beta r_\beta + m_\beta x_\beta & m_\beta r_\beta \\ m_a x_a b + m_\beta r_\beta + m_\beta x_\beta & \hat{I}_\alpha + \hat{I}_\beta + m_\beta r_\beta^2 + 2 x_\beta m_\beta r_\beta & \hat{I}_\beta + x_\beta m_\beta r_\beta \\ m_\beta r_\beta & \hat{I}_\beta + x_\beta m_\beta r_\beta \hat{I}_\beta m x_\alpha b & I_\alpha \end{pmatrix}}_{\mathbf{M}_{eom}} \begin{pmatrix} \ddot{h} \\ \ddot{\alpha} \\ \ddot{\beta} \end{pmatrix} + \tag{4}$$

$$+ \underbrace{\begin{pmatrix} c_h + \rho b S C_{l_\alpha} U & \left(\frac{1}{2} - a\right) b \rho b S C_{l_\alpha} U & 0 \\ -\rho b^2 S C_{m_{\alpha,eff}} U & c_\alpha - \left(\frac{1}{2} - a\right) b \rho b^2 S C_{m_{\alpha,eff}} U & 0 \\ 0 & 0 & c_{\beta_{servo}} \end{pmatrix}}_{\mathbf{C}_{eom}} \begin{pmatrix} \dot{h} \\ \dot{\alpha} \\ \dot{\beta} \end{pmatrix} +$$

$$+ \underbrace{\begin{pmatrix} k_h & \rho b S C_{l_\alpha} U^2 & \rho b S C_{l_\beta} U^2 \\ 0 & k_\alpha(\alpha) - \rho b^2 S C_{m_{\alpha,eff}} U^2 & -\rho b^2 S C_{m_{\beta,eff}} U^2 \\ 0 & 0 & k_{\beta_{servo}} \end{pmatrix}}_{\mathbf{K}_{eom}} \begin{pmatrix} h \\ \alpha \\ \beta \end{pmatrix} = \underbrace{\begin{pmatrix} 0 \\ 0 \\ k_{\beta_{servo}} \end{pmatrix}}_{\mathbf{F}_{eom}} \mathbf{u}.$$

where: $\mathbf{M}_{eom}$ is the mass matrix of the equation of motion, $\mathbf{C}_{eom}$ is the damping matrix of the equation of motion, $\mathbf{K}_{eom}$ is the stiffness matrix of the equation of motion, $\mathbf{F}_{eom}$ is the forcing matrix of the equation of motion.

The qLPV state-space representation can be defined as:

$$\mathbf{x}(t) = \begin{pmatrix} x_1(t) \\ x_2(t) \\ x_3(t) \\ x_4(t) \\ x_5(t) \\ x_6(t) \end{pmatrix} = \begin{pmatrix} \dot{h} \\ \dot{\alpha} \\ \dot{\beta} \\ h \\ \alpha \\ \beta \end{pmatrix} \quad \text{and} \quad \mathbf{u}(t) = u_\beta .$$

The state matrix and the input matrix are:

$$\mathbf{A}(\mathbf{p}(t)) = \begin{pmatrix} -\mathbf{M}_{eom}^{-1}\mathbf{C}_{eom}(\mathbf{p}(t)) & -\mathbf{M}_{eom}^{-1}\mathbf{K}_{eom}(\mathbf{p}(t)) \\ -\mathbf{I} & 0 \end{pmatrix}, \quad \mathbf{B} = \begin{pmatrix} \mathbf{M}_{eom}^{-1}\mathbf{F}_{eom} \\ 0 \end{pmatrix}. \tag{5}$$

Let u assume that the only measurable state is $x_5(t) = \alpha$, thus the output and feed-through matrices are:

$$\mathbf{C} = \begin{pmatrix} 0 & 0 & 0 & 0 & 1 & 0 \end{pmatrix}, \quad \mathbf{D} = 0. \tag{6}$$

We can construct the system matrix as:

$$\mathbf{S}(\mathbf{p}(t)) = \begin{pmatrix} \mathbf{A}(\mathbf{p}(t)) & \mathbf{B} \\ \mathbf{C} & \mathbf{D} \end{pmatrix} \tag{7}$$

The parameters of the aeroelastic wing section are defined in [16] as:

$m_h = 6.516\ kg$; $m_\alpha = 6.7\ kg$; $m_\beta = 0.537\ kg$; $x_\alpha = 0.21$; $x_\beta = 0.233$; $r_\beta = 0\ m$; $a = -0.673\ m$; $b = 0.1905\ m$; $\hat{I}_\alpha = 0.126\ kgm^2$; $\hat{I}_\beta = 10^{-5}$; $c_h = 27.43\ Nms/rad$; $c_\alpha = 0.215\ Nms/rad$; $c_{\beta_{servo}} = 4.182 \times 10^{-4}\ Nms/rad$; $k_h = 2844$; $k_{\beta_{servo}} = 7.6608 \times 10^{-3}$; $\rho = 1.225\ kg/m^3$; $C_{l_\alpha} = 6.757$; $C_{m_{\alpha,eff}} = -1.17$; $C_{l_\beta} = 3.774$; $C_{m_{\beta,eff}} = -2.1$; $S = 0.5945\ m$.

3. The Proposed Control Design Methodology

3.1. TP model transformation based polytopic models

TP model transformation is a numerical method able to uniformly transform qLPV dynamic models into Higher Order Singular Value Decomposition (HOSVD) basec canonical form or various convex polytopic representation. The main concepts of the mathematical background of TP model transformation is given in [2, 1, 3] and some of the recent applications for TP model type LMI based control design can be found in [9, 22]. Let us list the main definitions related to TP model transformation and TP type convex polytopic representation:

Definition 1. *(Finite element TP type convex polytopic model - TP model [2, 1, 3]):* $\mathbf{S}(\mathbf{p}(t))$ *in (7) for any parameter is given as the parameter-varying convex combination of LTI system matrices* $\mathbf{S} \in \mathbb{R}^{O \times I}$.

$$\mathbf{S}(\mathbf{p}(t)) = \sum_{i_1=1}^{I_1} \sum_{i_2=1}^{I_2} .. \sum_{i_N=1}^{I_N} w_{n,i_n}(p_n(t)) \mathbf{S}_{i_1,i_2,..,i_N} = \mathscr{S} \overset{N}{\underset{n=1}{\boxtimes}} \mathbf{w}_n(p_n(t)), \tag{8}$$

where $\mathbf{p}(t) \in \Omega$. *The coefficient tensor* $\mathscr{S} \in \mathbb{R}^{I_1 \times I_2 \times \cdots \times I_n \times O \times I}$ *has* $N+2$ *dimensions, it is constructed from the LTI vertex systems* $\mathbf{S}_{i_1,i_2,\ldots,i_N}$ *(8) and the row vector* $\mathbf{w}_n(p_n(t))$ *contains one variable and continuous weighting functions* $w_{n,i_n}(p_n(t))$, $i_n = 1 \ldots I_N$. *In order to get convex representation the weighting functions satisfy the following criteria:*

$$\forall n,i,p_n(t) : w_{n,i}(p_n(t)) \in [0,1]; \tag{9}$$

$$\forall n,p_n(t) : \sum_{i=1}^{I_n} w_{n,i}(p_n(t)) = 1. \tag{10}$$

Definition 2. *(NO/CNO, NOrmal type TP model [2, 1, 3]): The TP model is NO (normal) type model if its weighting functions are Normal, that is if it satisfies (9), (10), and the largest value of all weighting functions is 1. The convex TP model is CNO (close to normal) if it satisfies (9), (10) and the largest value of all weighting functions is 1 or close to 1.*

The TP type polytopic convex model given in (8) can be immediately applied for LMI based control design. Since TP model transformation is based on HOSVD it can give an upper bound of the approximation error in case nonzero singular values are discarded during the process. TP model transformation can be applied for qLPV models based on analytical dynamic equations, soft-computing based or black-box identification.

3.2. The structure of the uncertainty

We take the uncertainty structure presented in [23], which can be given as:

$$\begin{aligned}\dot{x}(t) =&(\mathbf{A}(\mathbf{p}(t)) + \mathbf{D}_a(\mathbf{p}(t))\Delta_a(t)\mathbf{E}_a(\mathbf{p}(t)))x(t)\\ &(\mathbf{B}(\mathbf{p}(t)) + \mathbf{D}_b(\mathbf{p}(t))\Delta_b(t)\mathbf{E}_b(\mathbf{p}(t)))u(t),\end{aligned} \tag{11}$$

where $\Delta_a(t)$ and $\Delta_b(t)$ are the uncertain blocks that satisfy

$$\|\Delta_a(t)\| \leq \frac{1}{\gamma_a}, \quad \Delta_a(t) = \Delta_a^T(t), \tag{12}$$

$$\|\Delta_b(t)\| \leq \frac{1}{\gamma_b}, \quad \Delta_b(t) = \Delta_b^T(t) \tag{13}$$

and $\mathbf{D}_a(\mathbf{p}(t))$, $\mathbf{E}_a(\mathbf{p}(t))$, $\mathbf{D}_b(\mathbf{p}(t))$ and $\mathbf{E}_b(\mathbf{p}(t))$ are known scaling matrices.

3.3. LMI based control for TP type polytopic models

The paper presents an output feedback control structure as it is assumed that only the pitch angle α of the NATA model is measurable. The observer has to satisfy $\mathbf{x}(t) - \hat{\mathbf{x}}(t) \to 0 \quad \text{as} \quad t \to \infty$, where $\hat{\mathbf{x}}(t)$ is the observed state vector. Parameter vector $\mathbf{p}(t)$ does not include any observed parameters, therefore the design strategy that was presented in [18, 23] can be applied:

$$\begin{aligned}\dot{\hat{\mathbf{x}}}(t) &= \mathbf{A}(\mathbf{p}(t))\hat{\mathbf{x}}(t) + \mathbf{B}(\mathbf{p}(t))\mathbf{u}(t) + \mathbf{K}(\mathbf{p}(t))(\mathbf{y}(t) - \hat{\mathbf{y}}(t))\\ \hat{\mathbf{y}}(t) &= \mathbf{C}(\mathbf{p}(t))\hat{\mathbf{x}}(t),\end{aligned}$$

where $\mathbf{u}(t) = -\mathbf{F}(\mathbf{p}(t))\mathbf{x}(t)$.

The resulting controller and observer of the proposed control design strategy and the TP type polytopic model have a common polytopic structure:

$$\begin{aligned}
\dot{\hat{\mathbf{x}}}(t) &= \mathscr{A} \bigboxtimes_{n=1}^{N} \mathbf{w}_n(p_n(t))\hat{\mathbf{x}}(t) + \mathscr{B} \bigboxtimes_{n=1}^{N} \mathbf{w}_n(p_n(t))\mathbf{u}(t) + \mathscr{K} \bigboxtimes_{n=1}^{N} \mathbf{w}_n(p_n(t))(\mathbf{y}(t) - \hat{\mathbf{y}}(t)) \\
\hat{\mathbf{y}}(t) &= \mathscr{C} \bigboxtimes_{n=1}^{N} \mathbf{w}_n(p_n(t))\hat{\mathbf{x}}(t) \\
\mathbf{u}(t) &= -\left(\mathscr{F} \bigboxtimes_{n=1}^{N} \mathbf{w}_n(p_n(t)) \right) \mathbf{x}(t).
\end{aligned} \tag{14}$$

The resulting tensors of the vertex feedback and observer gains $\mathscr{F}$ and $\mathscr{K}$ contain the LTI feedback gains $\mathbf{F}_{i_1,i_2,\ldots,i_N}$ and LTI observer gains $\mathbf{K}_{i_1,i_2,\ldots,i_N}$. The control design has to satisfy the following control performance objectives:

- Asymptotically stable controller and observer;
- Robust stability of the controller for parameter uncertainties.
- Constrain on the control value.

There is a large number of LMIs already developed for polytopic systems guaranteeing various control performance specifications and in the present case we select the LMIs derived and given in [23].

Theorem 1. *(Globally and asymptotically stable controller for uncertain qLPV systems [23]) A controller stabilising the uncertain qLPV system (11) can be obtained by solving the following LMIs for* $\mathbf{P} > \mathbf{0}$ *and* $\mathbf{M}_r$ $(r = 1, \ldots, R)$

$$\mathbf{S}_{rr} < \mathbf{0},$$

$$\mathbf{T}_{rs} < \mathbf{0},$$

where

$$\mathbf{S}_{rr} = \begin{pmatrix} \left(\mathbf{P}\mathbf{A}_r^T + \mathbf{A}_r\mathbf{P} - \mathbf{B}_r\mathbf{M}_r - \mathbf{M}_r^T\mathbf{B}_r^T\right) & \mathbf{D}_{ar} & \mathbf{D}_{br} & \mathbf{P}\mathbf{E}_{ar}^T & -\mathbf{M}_r^T\mathbf{E}_{br}^T \\ \mathbf{D}_{ar}^T & -\mathbf{I} & 0 & 0 & 0 \\ \mathbf{D}_{br}^T & 0 & -\mathbf{I} & 0 & 0 \\ \mathbf{E}_{ar}\mathbf{P} & 0 & 0 & -\gamma_a^2\mathbf{I} & 0 \\ -\mathbf{E}_{br}\mathbf{M}_r & 0 & 0 & 0 & -\gamma_b^2\mathbf{I} \end{pmatrix},$$

and

$$\mathbf{T}_{rs} = \begin{pmatrix} \begin{pmatrix} \mathbf{P}\mathbf{A}_r^T \\ +\mathbf{A}_r\mathbf{P} \\ -\mathbf{B}_r\mathbf{M}_s \\ -\mathbf{M}_s^T\mathbf{B}_r^T \\ +\mathbf{P}\mathbf{A}_s^T \\ +\mathbf{A}_s\mathbf{P} \\ -\mathbf{B}_s\mathbf{M}_r \\ -\mathbf{M}_r^T\mathbf{B}_s^T \end{pmatrix} & \mathbf{D}_{ar} & \mathbf{D}_{br} & \mathbf{D}_{as} & \mathbf{D}_{bs} & \mathbf{P}\mathbf{E}_{ar}^T & -\mathbf{M}_s^T\mathbf{E}_{br}^T & \mathbf{P}\mathbf{E}_{as}^T & -\mathbf{M}_r^T\mathbf{E}_{bs}^T \\ \mathbf{D}_{ar}^T & -\mathbf{I} & 0 & 0 & 0 & 0 & 0 & 0 & 0 \\ \mathbf{D}_{br}^T & 0 & -\mathbf{I} & 0 & 0 & 0 & 0 & 0 & 0 \\ \mathbf{D}_{as}^T & 0 & 0 & -\mathbf{I} & 0 & 0 & 0 & 0 & 0 \\ \mathbf{D}_{bs}^T & 0 & 0 & 0 & -\mathbf{I} & 0 & 0 & 0 & 0 \\ \mathbf{E}_{ar}\mathbf{P} & 0 & 0 & 0 & 0 & -\gamma_a^2\mathbf{I} & 0 & 0 & 0 \\ -\mathbf{E}_{br}\mathbf{M}_r & 0 & 0 & 0 & 0 & 0 & -\gamma_b^2\mathbf{I} & 0 & 0 \\ \mathbf{E}_{as}\mathbf{P} & 0 & 0 & 0 & 0 & 0 & 0 & -\gamma_a^2\mathbf{I} & 0 \\ -\mathbf{E}_{bs}\mathbf{A}_r & 0 & 0 & 0 & 0 & 0 & 0 & 0 & -\gamma_b^2\mathbf{I} \end{pmatrix}$$

for $r < s \leq R$, except the pairs (r,s) such that $\forall \mathbf{p}(t) : w_r(\mathbf{p}(t))w_s(\mathbf{p}(t)) = 0$ and where $\mathbf{M}_r = \mathbf{F}_r\mathbf{P}$.

The feedback gains can be obtained from the solution of the above LMIs as $\mathbf{F}_r = \mathbf{M}_r\mathbf{P}^{-1}$.

Theorem 2. *(Globally and asymptotically stable controller with constraint on the control value [23]) The simultaneous solution of the LMIs of Theorem 1 and Theorem 2 in the form of:*

$$\phi^2\mathbf{I} \leq \mathbf{P}$$
$$\begin{pmatrix} \mathbf{P} & \mathbf{M}_r{}^T \\ \mathbf{M}_r & \mu^2\mathbf{I} \end{pmatrix} \geq 0$$

yields an asymptotically stable controller, where $\|\mathbf{u}(t)\|_2 \leq \mu$ is enforced at all time and $\|\mathbf{x}(0)\|_2 \leq \phi$.

Theorem 3. *(Globally and asymptotically stable observer [23]) Assume the polytopic model (8) and a control structure as given by (14). An asymptotically stable observer can be obtained by solving the following LMIs for $\mathbf{P} > \mathbf{0}$ and $\mathbf{N}_r$ $(r = 1,\ldots,R)$:*

$$\begin{aligned} \mathbf{A}_r^T\mathbf{P} - \mathbf{C}_r^T\mathbf{N}_r^T + \mathbf{P}\mathbf{A}_r - \mathbf{N}_r\mathbf{C}_r &< \mathbf{0}, \\ \mathbf{A}_r^T\mathbf{P} - \mathbf{C}_s^T\mathbf{N}_r^T + \mathbf{P}\mathbf{A}_r - \mathbf{N}_r\mathbf{C}_s + \mathbf{A}_s^T\mathbf{P} - \mathbf{C}_r^T\mathbf{N}_2^T + \mathbf{P}\mathbf{A}_s - \mathbf{N}_s\mathbf{C}_r &< \mathbf{0} \end{aligned}$$

for $r < s \leq R$, except the pairs (r,s) such that $\forall \mathbf{p}(t) : w_r(\mathbf{p}(t))w_s(\mathbf{p}(t)) = 0$, and where $\mathbf{N}_r = \mathbf{P}\mathbf{K}_r$. The observer gains can derived from the solution of the above LMIs as $\mathbf{K}_r = \mathbf{P}^{-1}\mathbf{N}_r$.

4. Control Design Results

4.1. Results of TP model transformation

Executing TP model transformation on the qLPV model (5) of the NATA systems leads us to TP type convex representation of the system. The transformation space Ω and the discretization grid M are defined as: $\Omega : U \in [8,20](m/s)$ and $\alpha \in [-0.3,0.3](rad)$ and $M = M_1 \times M_2 = 137 \times 137$. HOSVD on the discretized tensor $\mathcal{S}^D \in \mathbb{R}^{M_1 \times M_2 \times 7 \times 7}$ results

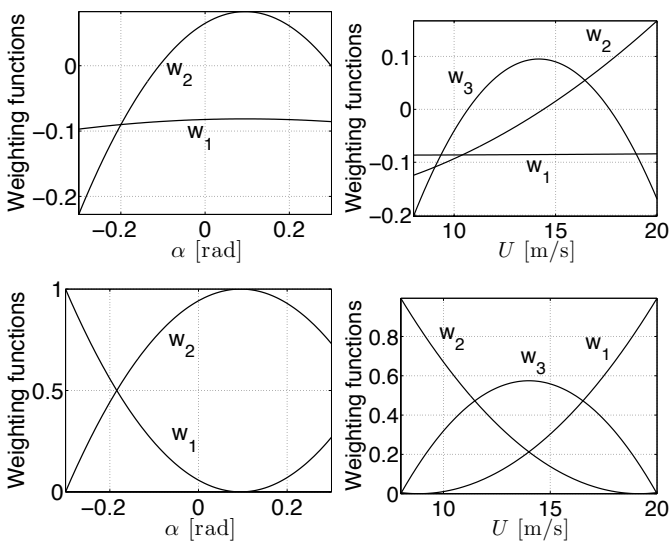

Figure 1. Weighting functions: (above) HOSVD-based canonical form (bellow) CNO type convex form

in rank 2 and 3 in the fist and second dimension respectively, which means that the exact HOSVD based canonical form of the NATA model can be defined with 6 LTI vertex systems. The CNO type convex representation can also be given by 6 LTI vertex systems. Figure 1 shows the weighting functions $w_{1,i}(U)$, $i = 1..2$ and $w_{2,j}(\alpha)$, $j = 1..3$ for the HOSVD-based canonical form and the CNO type convex representation.

4.2. Output feedback control design based on LMIs

4.2.1 Uncertainty in the dynamics of the trailing-edge servo-motor

The dynamics of the trailing-edge servo motor (3) was derived in [16]. The dynamics have two parameters, $k_{\beta_{servo}}$ and $c_{\beta_{servo}}$. The aim of this paper is to design a controller that shows robustness properties regarding these two parameters, therefore the first step is to define the uncertainty structure of the NATA model based on the methodology given as (11) in [23]. Element groups A_{13}, A_{23}, A_{33} and $A_{16}(\mathbf{p}(t)), A_{26}(\mathbf{p}(t)), A_{36}(\mathbf{p}(t))$ of the state matrix $\mathbf{A}(\mathbf{p}(t))$ contain parameters $c_{\beta_{servo}}$ and $k_{\beta_{servo}}$, respectively. B_{11}, B_{21} and B_{31} of input matrix $\mathbf{B}$ include $k_{\beta_{servo}}$ as well. Based on the considerations above one can define the uncertain blocks $\Delta_a(t)$ and $\Delta_b(t)$ as:

$$\Delta_a(t) = \begin{pmatrix} \Delta_{k_{\beta_{servo}}}(t) & 0 \\ 0 & \Delta_{c_{\beta_{servo}}}(t) \end{pmatrix} \tag{15}$$

and

$$\Delta_b(t) = \left(\Delta_{k_{\beta_{servo}}}(t) \right), \tag{16}$$

where bounded functions $\Delta_{k_{\beta_{servo}}}(t)$ and $\Delta_{c_{\beta_{servo}}}(t)$ stand for the difference of the actual and nominal values of parameters $k_{\beta_{servo}}$ and $c_{\beta_{servo}}$. Scaling matrices $\mathbf{D}_a(\mathbf{p}(t))$, $\mathbf{E}_a(\mathbf{p}(t))$, $\mathbf{D}_b(\mathbf{p}(t))$ and $\mathbf{E}_b(\mathbf{p}(t))$ are defined with the aim to match the system matrix elements with the related uncertainties.

Uncertainty structure (11) gives two possibilities to construct the scaling matrices:

Case 1 of uncertainty

$$\mathbf{D}_a = \begin{pmatrix} -\mathbf{M}_{eom_{13}}^{-1} c_{\beta_{servo}} & -\mathbf{M}_{eom_{13}}^{-1} k_{\beta_{servo}} \\ -\mathbf{M}_{eom_{23}}^{-1} c_{\beta_{servo}} & -\mathbf{M}_{eom_{23}}^{-1} k_{\beta_{servo}} \\ -\mathbf{M}_{eom_{33}}^{-1} c_{\beta_{servo}} & -\mathbf{M}_{eom_{33}}^{-1} k_{\beta_{servo}} \\ 0 & 0 \\ 0 & 0 \\ 0 & 0 \end{pmatrix}, \quad \mathbf{E}_a = \begin{pmatrix} 0 & 0 & 1 & 0 & 0 & 0 \\ 0 & 0 & 0 & 0 & 0 & 1 \end{pmatrix} \tag{17}$$

and

$$\mathbf{D}_b^T = \begin{pmatrix} \mathbf{M}_{eom_{13}}^{-1} k_{\beta_{servo}} & \mathbf{M}_{eom_{23}}^{-1} k_{\beta_{servo}} & \mathbf{M}_{eom_{33}}^{-1} k_{\beta_{servo}} & 0 & 0 & 0 \end{pmatrix}, \quad \mathbf{E}_b = 1. \tag{18}$$

Case 2 of uncertainty

$$\mathbf{D}_a = \begin{pmatrix} -\mathbf{M}_{eom_{13}}^{-1} & -\mathbf{M}_{eom_{13}}^{-1} \\ -\mathbf{M}_{eom_{23}}^{-1} & -\mathbf{M}_{eom_{23}}^{-1} \\ -\mathbf{M}_{eom_{33}}^{-1} & -\mathbf{M}_{eom_{33}}^{-1} \\ 0 & 0 \\ 0 & 0 \\ 0 & 0 \end{pmatrix}, \quad \mathbf{E}_a = \begin{pmatrix} 0 & 0 & c_{\beta_{servo}} & 0 & 0 & 0 \\ 0 & 0 & 0 & 0 & 0 & k_{\beta_{servo}} \end{pmatrix} \tag{19}$$

and

$$\mathbf{D}_b^T = \begin{pmatrix} \mathbf{M}_{eom_{13}}^{-1} & \mathbf{M}_{eom_{23}}^{-1} & \mathbf{M}_{eom_{33}}^{-1} & 0 & 0 & 0 \end{pmatrix}, \quad \mathbf{E}_b = k_{\beta_{servo}}. \tag{20}$$

4.2.2 Resulting control solutions

In order to derive controller and observer feedback gains we applied the CNO type TP model of the NATA system for LMI based design. The various control design specifications are based on the requirements given in the previous section and both uncertainty structure cases were considered in the control design process.

In the first step of the control design we define the maximal allowable uncertainty of $k_{\beta_{servo}}$ and $c_{\beta_{servo}}$. The uncertain blocks $\Delta_a(t)$ and $\Delta_b(t)$ are given as (15) and (16), which

satisfy criteria given in (12) and (13). Matrix $\Delta_a(t)$ being diagonal has a norm equal to the absolute value of its largest element and the norm of the scalar $\Delta_b(t)$ is equal to its absolute value. The minimal value of γ_b is set to equal the minimal value of γ_a since $\Delta_b(t)$ is part of $\Delta_a(t)$. The maximal difference between the nominal and actual values of the two parameters are then given as:

$$\Delta_{k_{\beta_{servo}}}^{max} = \frac{1}{\gamma_a} \geq |\Delta_{k_{\beta_{servo}}}(t)|;$$

$$\Delta_{c_{\beta_{servo}}}^{max} = \frac{1}{\gamma_a} \geq |\Delta_{c_{\beta_{servo}}}(t)|.$$

Controller 1.1 and 1.2

The specification for designing Controller 1.1 and 1.2 was to find $\gamma_{a_{min}} = \gamma_{b_{min}}$, which leads maximal allowable uncertainty in $k_{\beta_{servo}}$ and $c_{\beta_{servo}}$. LMIs from Theorem 1 were applied to design the feedback gains. Uncertainty structure case 1 resulted in $\gamma_{a_{min}} = \gamma_{b_{min}} = 1.44$ while structure 2 resulted in $\gamma_{a_{min}} = \gamma_{b_{min}} = 1.77$.

Controller 2.1 and 2.2

Controllers 2.1, 2.2, 3.1, 3.2, 4.1 and 4.2 were designed with the aim to set a trade-off between the maximal allowable uncertainty and maximal control signal amplitude. In these cases LMIs from Theorems 1 and 2 were applied. The initial state condition is bounded as $\phi = 0.002$. The maximal uncertainty was set as 50%, thus the aim is to find the minimal l_2 norm of the control signal defined by μ_{min} in Theorem 2 that lead to stable controller when $\gamma_{a_{min}} = \gamma_{b_{min}} = 2$. Controller 2.1 resulted in $\mu_{min} = 44$ and Controller 2.2 in $\mu_{min} = 13286$.

Controller 3.1 and 3.2

Controllers 3.1 and 3.2 were designed based on the same principle as controller 2.1 and 2.2 with $\gamma_{a_{min}} = \gamma_{b_{min}} = 5$. Controller 3.1 resulted in $\mu_{min} = 26$ and Controller 3.2 in $\mu_{min} = 3672$.

Controller 4.1 and 4.2

Table 1. Simulation environment 1 and 2

Description	Environment 1	Environment 2
Parameter uncertainty	$\Delta_{k_{\beta_{servo}}}(t) = \frac{1}{\gamma_{a_{min}}} sin\left(6\pi t + \frac{\pi}{2}\right)$	$\Delta_{k_{\beta_{servo}}}(t) = \frac{1}{\gamma_{a_{min}}} sin\left(6\pi t + \frac{\pi}{2}\right)$
Parameter uncertainty	$\Delta_{c_{\beta_{servo}}}(t) = \frac{1}{\gamma_{a_{min}}} sin(10\pi t)$	$\Delta_{c_{\beta_{servo}}}(t) = \frac{1}{\gamma_{a_{min}}} sin(10\pi t)$
Computation delay	–	1 *ms* constant time delay
Control signal saturation	–	$\pm 2[rad/s]$
Sensor noise	–	normally distributed random noise, 10% variance
Free stream velocity	$U(t) = 14.1$	$U(t) = 14.1 + 5sin(2\pi t)$
Input disturbance	–	$u_d(t) = \frac{30}{180}\pi$ from $t = 1$ *s*

The maximal uncertainty was set as 10% with $\gamma_{a_{min}} = \gamma_{b_{min}} = 10$ and the control design achieved $\mu_{min} = 22$ and $\mu_{min} = 3595$ for controllers 4.1 and 4.2 respectively.

Observer

The observer gains for every controller were designed by applying LMIs from Theorem 3.

5. Numerical Simulation Results

5.1. Simulation environment setup and results

Simulations were executed at $U = 14.1 m/s$, which falls in the critical free stream velocity range in which the uncontrolled aeroelastic model develops limit cycle oscillations. The figures bellow show only that part of the simulations where the controller is turned on and the open loop part where the oscillations develop are not depicted. Two simulation environments were examined, in the first case there were no perturbations and the second case contained some perturbations, which may occur in case of a physical implementation of the control solution. The characteristics of the two environments are given in Table 1.

Table 2. Evaluation of the controllers and the observer

Controller	Evaluation
Controller 1.1 & 1.2	– maximal parameter uncertainty (70% and 56.5%) – very high control signal ($u_{max} \approx 10^5$) – settling time approximately 1s in environment 1 – environment 2 leads to limit cycle oscillations – high gains – *Practical implementation is difficult due to high control signals*
Controller 2.1 & 2.2	– 50% allowable parameter uncertainty – high control signal ($u_{max_{2.1}} = 150$, $u_{max_{2.2}} = 250$) – settling time approximately 1s in environment 1 – settling time approximately 1.5s in environment 2 – *Acceptable solution for high uncertainty*
Controller 3.1 & 3.2	– 20% allowable parameter uncertainty – low control signal ($u_{max_{2.1}} = 35$, $u_{max_{2.2}} = 7.8$) – settling time approximately 1s in environment 1 – settling time approximately 1.5s in environment 2 – *Advantageous control signal magnitude*
Controller 4.1 & 4.2	– 10% allowable parameter uncertainty – lowest control signal ($u_{max_{2.1}} = 15$, $u_{max_{2.2}} = 7$) – settling time approximately 1s in environment 1 – settling time approximately 1.5s in environment 2 – *Decreasing the uncertainty does not decrease the control signal magnitude significantly*

Figures 2 and 3 show the closed loop responses of controllers 2.1 and 2.2 with observer in simulation environments 1 and 2; and controllers 3.1 and 3.2 with observer in simulation environments 1 and 2.

5.2. Evaluation of the results

All of the designed controllers and the observer is able to asymptotically stabilize the 3 DoF aeroelastic model with parametric uncertainties in domain Ω. The performance of each controller is evaluated regarding to the settling time, control signal magnitude and maximal parameter uncertainty. The main characteristics of the control solutions are given in Table 2.

The general conclusion based on the time responses of the closed loop systems is that

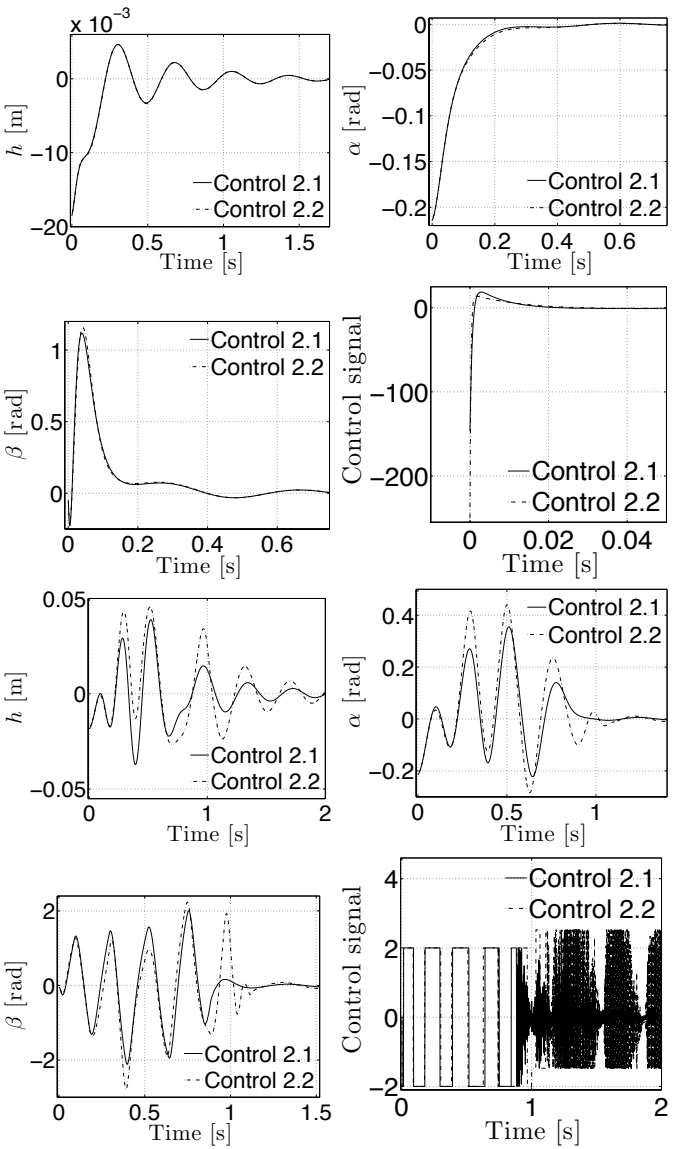

Figure 2. Time responses of controller 2.1 and 2.2 for environment 1 (top) and environment 2 (bottom)

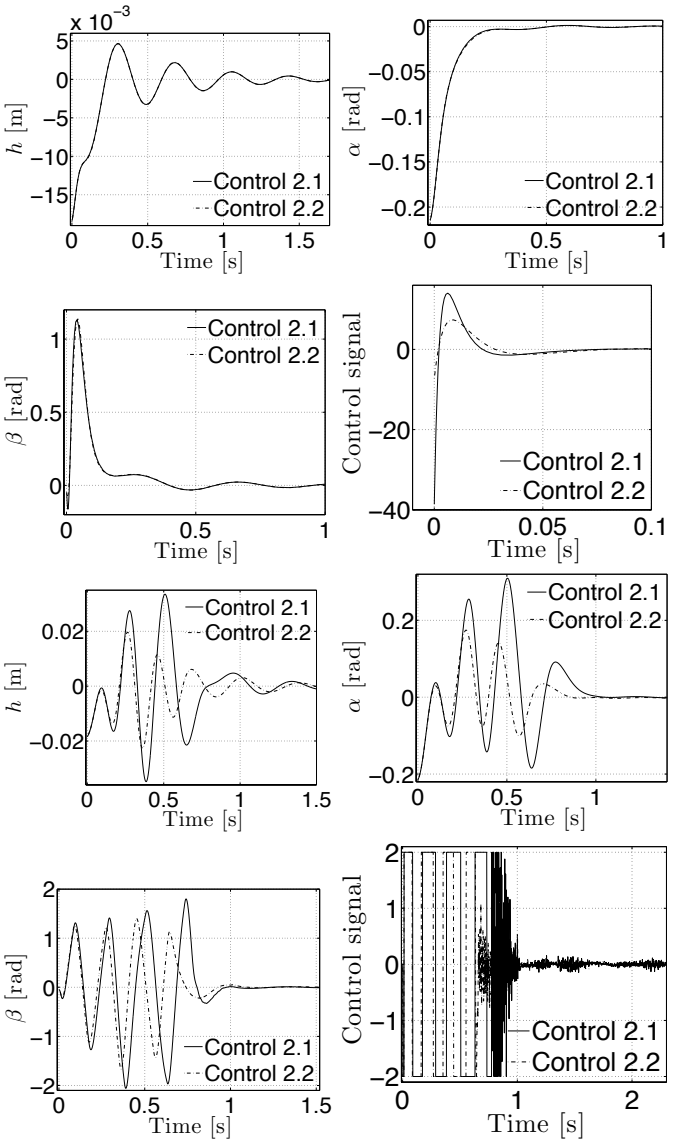

Figure 3. Time responses of controller 3.1 and 3.2 for environment 1 (top) and environment 2 (bottom)

it is possible to find an acceptable trade-off between the allowable uncertainty and the control signal magnitude. Increasing the allowable uncertainty leads to very high control signals, which make the physical implementation difficult, on the other hand, there is a lower limit of the uncertainty bellow which there is no significant gain in the decrease of the control signal magnitude. It is also worth to note that the structure of the uncertainties can highly influence the feasibility of the LMIs, in the present case structure 1 gave better control performance at high allowable uncertainties and structure had better performance in the lower uncertainty range.

Regarding the settling time, there is no significant difference between the controllers, except for controller 1.1 and 1.2 in environment 2, which are not able to stabilize the perturbed system due to very high feedback gains and the effect of the time delay.

6. Conclusions

The paper proposes output feedback control design strategy to robustly stabilize the degrees-of-freedom Nonlinear Aeroelastic Test Apparatus, which can have parameter uncertainties in the trailing edge dynamics. It was shown that it is possible to find an optimal trade-off between the bound of control signal magnitude and the magnitude of the acceptable parameter uncertainties by carrying out the numerical control design systematically in a straightforward manner. The various structures of the same uncertainties are highly influencing the Linear Matrix Inequalities feasibilities and also have a high influence on the control performance. In the present system it was possible to derive two different uncertainty structures and both of the structures have their own advantages and disadvantages, thus the investigation of the uncertainty structures is not neglect-able. The Tensor Model transformation and Linear Matrix Inequalities based multi objective control design for quasi Linear Parameter Varying models can be executes in a routine-like fashion.

Acknowledgements

The research was supported by the Hungarian National Development Agency, (ERC-HU-09-1-2009-0004, MTASZTAK) (OMFB-01677/2009).

The research was part of the Zoltán Magyary Postdoctoral Scholarship.

This research was supported by the European Union and the State of Hungary, co-financed by the European Social Fund in the framework of TÁMOP 4.2.4. A/1-11-1-2012-0001 'National Excellence Program'.

References

[1] P. Baranyi. TP model transformation as a way to LMI based controller design. *IEEE Transaction on Industrial Electronics*, 51(2):387–400, April 2004.

[2] P. Baranyi, L. Szeidl, P. Várlaki, and Y. Yam. Definition of the HOSVD-based canonical form of polytopic dynamic models. In *3rd International Conference on Mechatronics (ICM 2006)*, pages 660–665, Budapest, Hungary, July 3-5 2006.

[3] P. Baranyi, L. Szeidl, P. Várlaki, and Y. Yam. Numerical reconstruction of the HOSVD-based canonical form of polytopic dynamic models. In *10th International Conference on Intelligent Engineering Systems*, pages 196–201, London, UK, June 26-28 2006.

[4] Peter Baranyi. Output feedback control of Two-Dimensional aeroelastic system. *Journal of Guidance, Control, and Dynamics*, 29:762–767, May 2006.

[5] Peter Baranyi. Tensor product Model-Based control of Two-Dimensional aeroelastic system. *Journal of Guidance, Control, and Dynamics*, 29:391–400, March 2006.

[6] J. J. Block. *Active control of an aeroelastic structure*. Texas A&M University, 1996.

[7] J. J. Block and Heather Gilliat. Active control of an aeroelastic structure. In *AIAA Meeting Papers on Disc*, pages 1–11, Reno, NV, January 1997. American Institute of Aeronautics and Astronautics, Inc.

[8] Jeffry J. Block and Thomas W. Strganac. Applied active control for a nonlinear aeroelastic structure. *Journal of Guidance, Control, and Dynamics*, 21:838–845, November 1998.

[9] Pr Galambos and Pr Baranyi. Trepresenting the model of impedance controlled robot interaction with feedback delay in polytopic lpv form: Tp model transformation based approach. *Acta Polytechnica Hungarica*, 10(1):139–157, January 2013.

[10] P. Grof, P. Baranyi, and P. Korondi. Convex hull manipulation based control performance optimisation. *WSEAS Transactions on Systems and Control*, 5(8):691–700, August 2010. Stevens Point, Wisconsin, USA.

[11] Jeonghwan Ko, Thomas W. Strganac, and Andrew J. Kurdila. Adaptive feedback linearization for the control of a typical wing section with structural nonlinearity. *Nonlinear Dynamics*, 18(3):289–301, 1999. 10.1023/A:1008323629064.

[12] Keum W. Lee and Sahjendra N. Singh. Multi-Input Noncertainty-Equivalent adaptive control of an aeroelastic system. *Journal of Guidance, Control, and Dynamics*, 33:1451–1460, September 2010.

[13] Vivek Mukhopadhyay. Historical perspective on analysis and control of aeroelastic responses. *Journal of Guidance, Control, and Dynamics*, 26:673–684, September 2003.

[14] George Platanitis and Thomas Strganac. Control of a nonlinear wing section using leading- and Trailing-Edge surfaces. *Journal of Guidance, Control, and Dynamics*, 27:52–58, January 2004.

[15] Zebb Prime, Ben Cazzolato, and Con Doolan. A mixed H2/Hx scheduling control scheme for a two degree-of-freedom aeroelastic system under varying airspeed and gust conditions. In *Proceedings of the AIAA Guidance, Navigation and Control Conference and Exhibit*, pages 1–16, Honolulu, Hawaii, 2008.

[16] Zebb Prime, Ben Cazzolato, Con Doolan, and Thomas Strganac. Linear-Parameter-Varying control of an improved Three-Degree-of-Freedom aeroelastic model. *Journal of Guidance, Control, and Dynamics*, 33, March 2010.

[17] K. K. Reddy, J. Chen, A. Behal, and P. Marzocca. Multi-Input/Multi-Output adaptive output feedback control design for aeroelastic vibration suppression. *Journal of Guidance, Control, and Dynamics*, 30:1040–1048, July 2007.

[18] C. W. Scherer and S. Weiland. *Linear Matrix Inequalities in Control*. DISC course lecture notes, 2000. http://w3.ele.tue.nl/fileadmin/ele/MBS/CS/Files/Courses/DISClmi/lmis1.pdf, retrieved on 05.02.2012.

[19] S Singh. State feedback control of an aeroelastic system with structural nonlinearity. *Aerospace Science and Technology*, 7:23–31, January 2003.

[20] Thomas W. Strganac, Jeonghwan Ko, and David E. Thompson. Identification and control of limit cycle oscillations in aeroelastic systems. *Journal of Guidance, Control, and Dynamics*, 23:1127–1133, November 2000.

[21] Bela Takarics, Patricia Grof, Peter Baranyi, and Peter Korondi. Friction compensation of an aeroelastic wing - a TP model transformation based approach. pages 527–533. IEEE, September 2010.

[22] B Takarics and Pr Baranyi. Tensor-product-model-based control of a three degrees-of-freedom aeroelastic model. *Journal of Guidance, Control, and Dynamics*, 36(5):1527–1533, September 2013.

[23] K. Tanaka and H. O. Wang. *Fuzzy Control Systems Design and Analysis: A Linear Matrix Inequality Approach*. John Wiley & Sons, Inc., 2001.

[24] Z. Wang, A. Behal, and P. Marzocca. Model-Free control design for Multi-Input Multi-Output aeroelastic system subject to external disturbance. *Journal of Guidance, Control, and Dynamics*, 34:446–458, March 2011.

[25] Wenhong Xing and Sahjendra N. Singh. Adaptive output feedback control of a nonlinear aeroelastic structure. *Journal of Guidance, Control, and Dynamics*, 23:1109–1116, November 2000.